การตรวจวัดรังสีคอสมิกด้วยเครื่องตรวจวัดนิวตรอนเคลื่อนที่ “ช้างแวน” ไปยังทวีปแอนตาร์กติกา

The 3rd Neutron Monitor Bootcamp (2020)

Waraporn Nuntiyakul

ภาควิชาฟิสิกส์และวัสดุศาสตร์ คณะวิทยาศาสตร์ มหาวิทยาลัยเชียงใหม่

OUTLINE

- Introduction
  - Cosmic Rays
  - Standard-Neutron Monitor
  - Semi-leaded Neutron Detector
- Cosmic Ray Spectra
- Latitude Surveys
  - 1994-2007 (13 survey years)
  - 1995
  - 2009
  - 2018-Present
- Outreach

INTRODUCTION: COSMIC RAYS

- Energetic particles or γ-rays from space
- Discovered by Hess in 1912 (Nobel Prize in 1936)
- Ordinary matter accelerated to high energies
  - p, ^{4}He, ^{12}C, ^{16}O, heavy nuclei and γ, e^{+}, e^{-}, μ, ν, …
- Key sources of cosmic rays for Earth's radiation environment:
  - From solar storms (solar energetic particles)
  - From supernova explosions inside the Milky-Way Galaxy (Galactic cosmic rays)
  - From intense events/objects GRB, AGN outside the Galaxy (Extra Galactic cosmic rays)
- Key cause of biological mutation

Hajo Drescher, Frankfurt U.

Hajo Drescher, Frankfurt U.

Hajo Drescher, Frankfurt U.

Hajo Drescher, Frankfurt U.

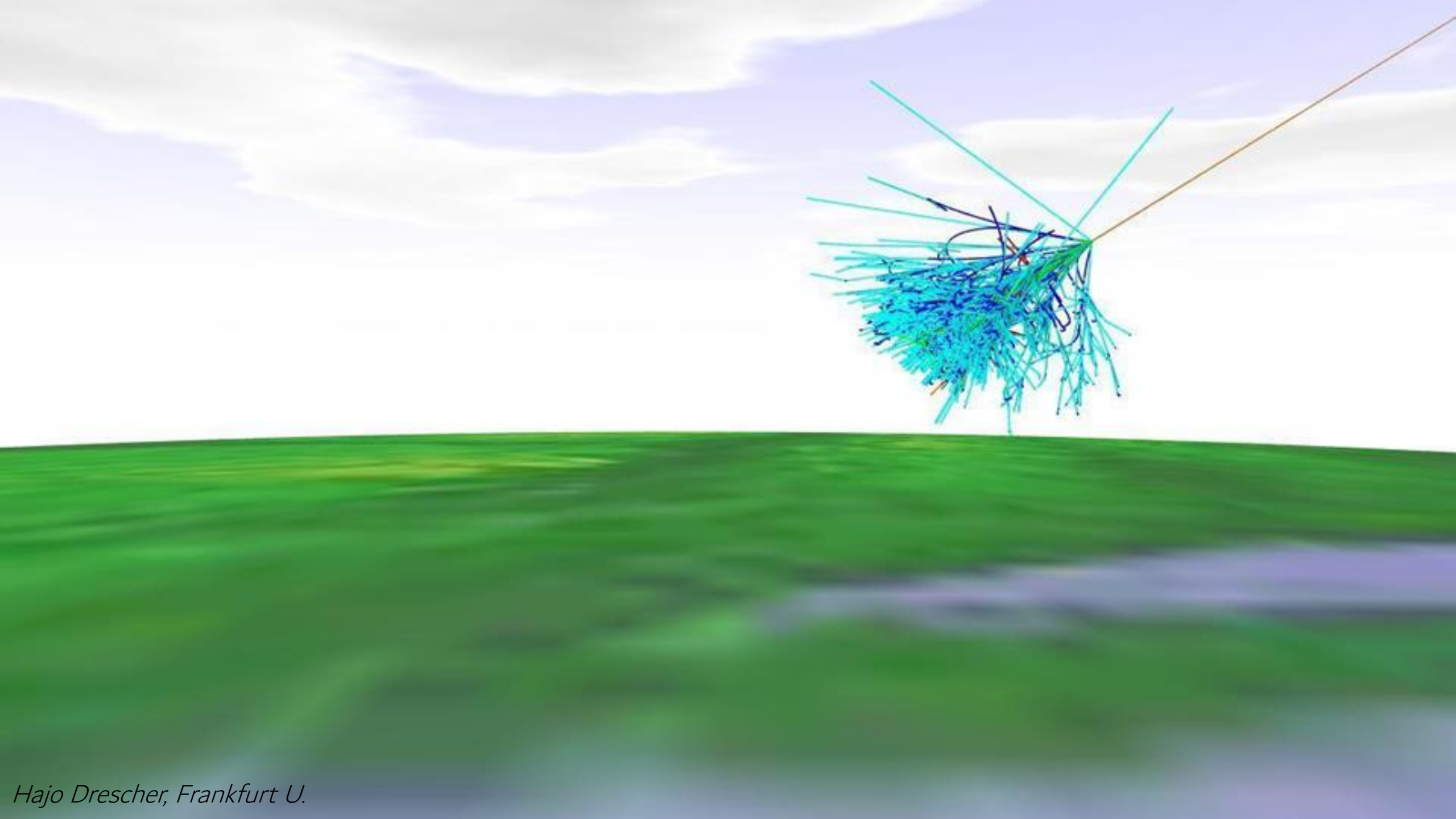

Hajo Drescher, Frankfurt U.

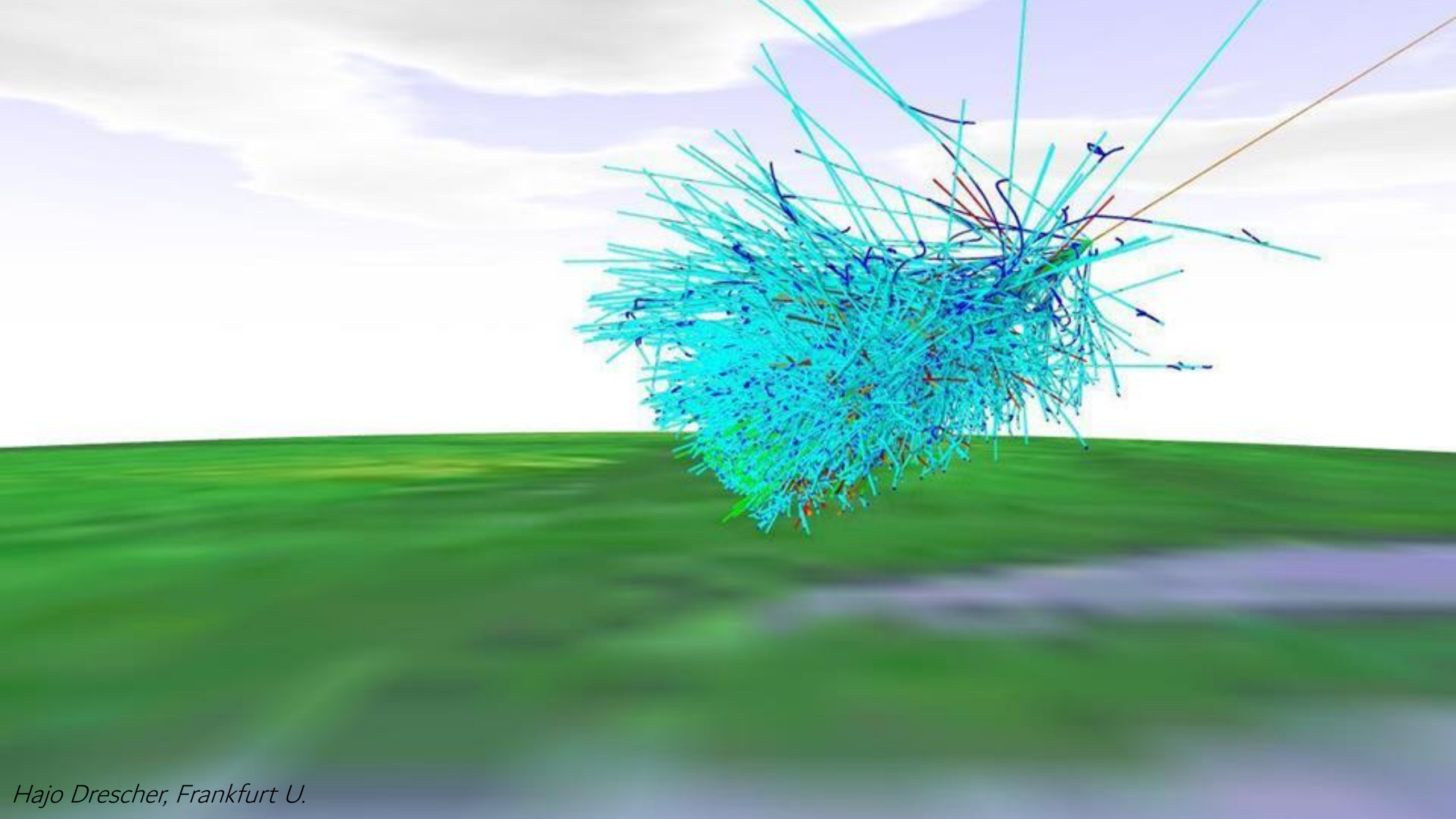

Hajo Drescher, Frankfurt U.

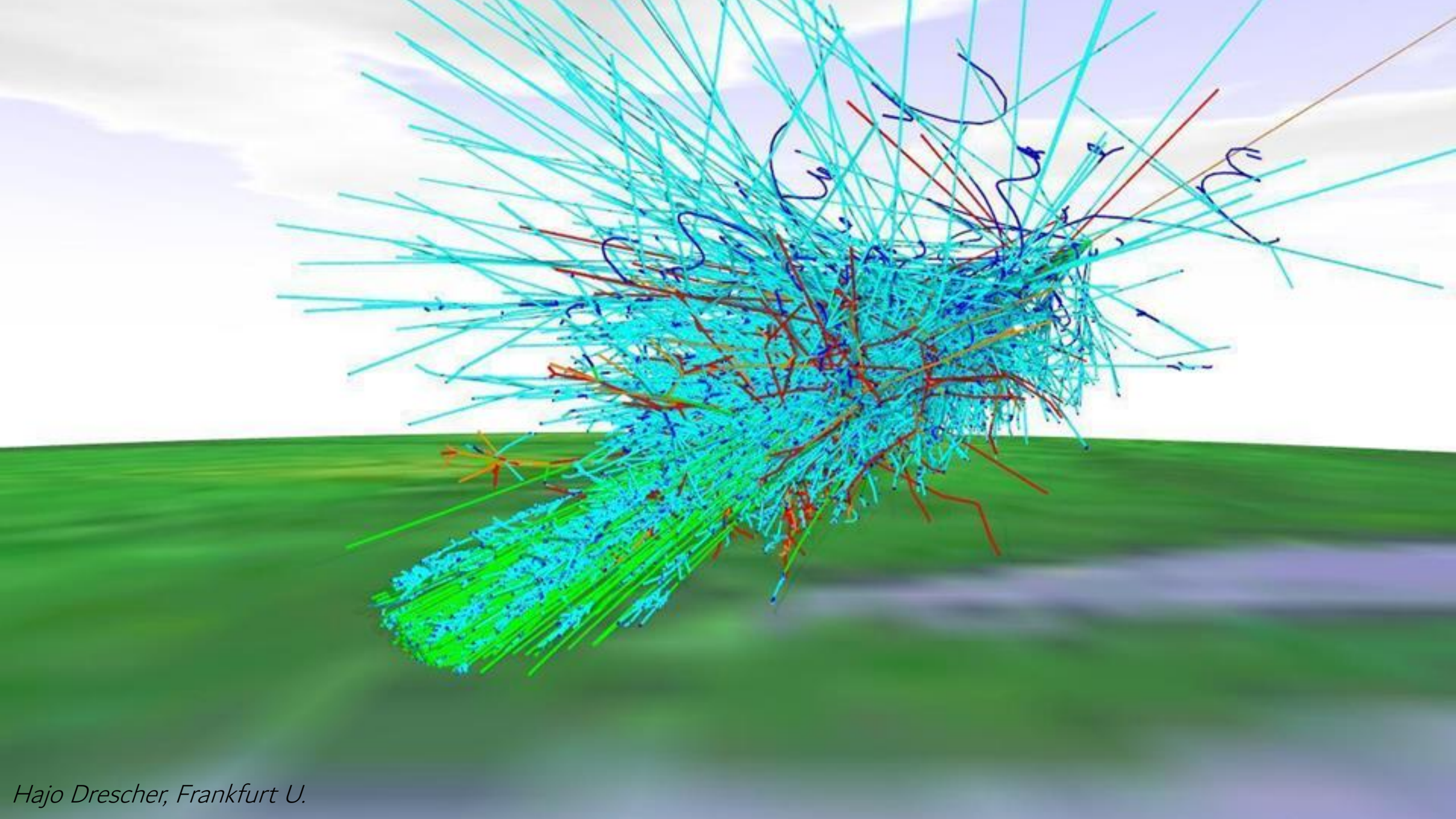

Hajo Drescher, Frankfurt U.

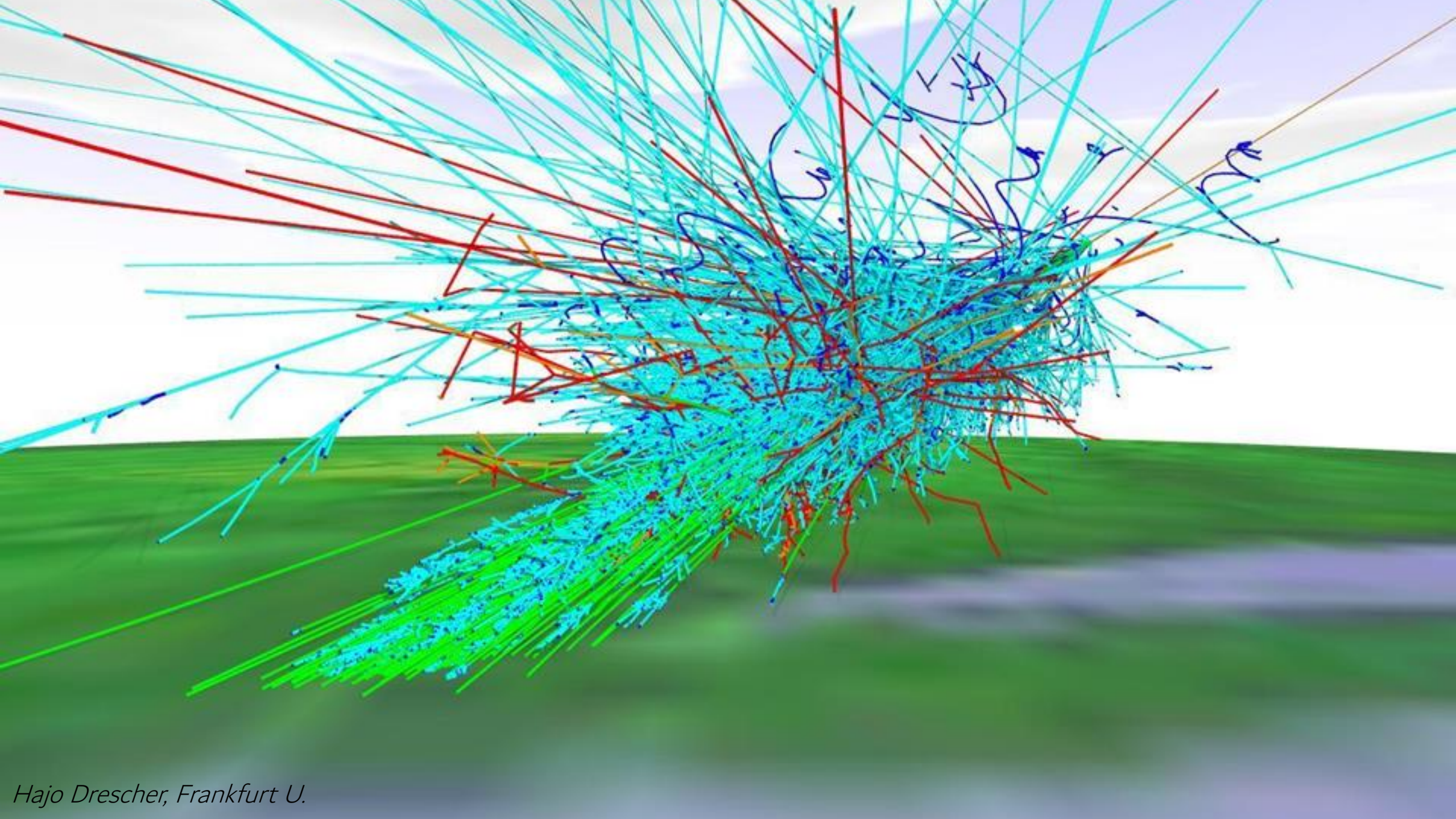

Hajo Drescher, Frankfurt U.

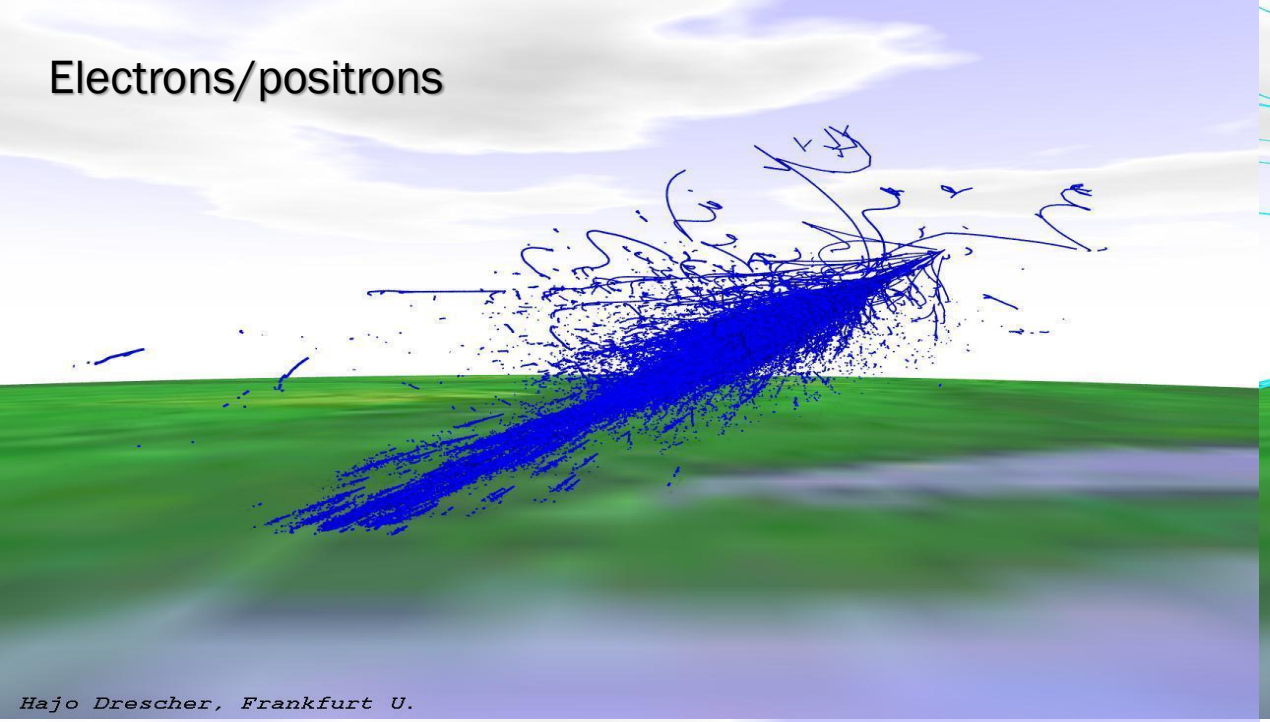
Electrons/positrons
Hajo Drescher, Frankfurt U.

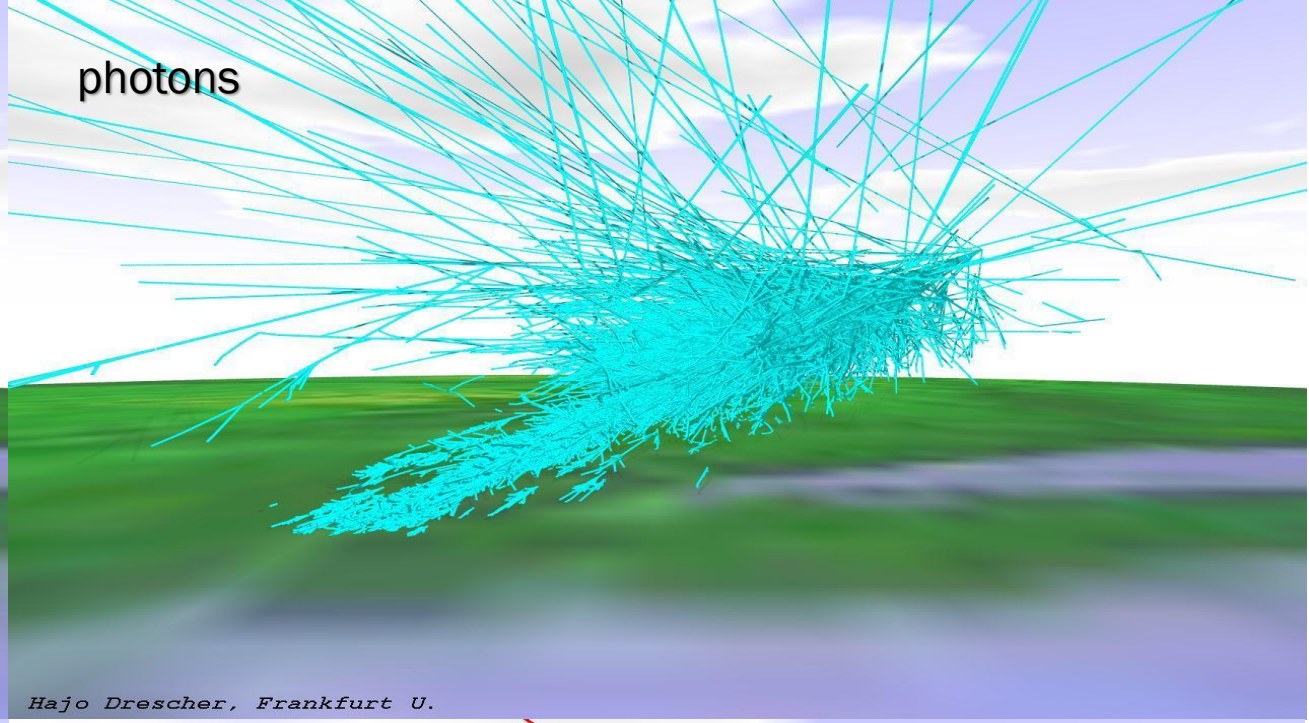
photons
Hajo Drescher, Frankfurt U.

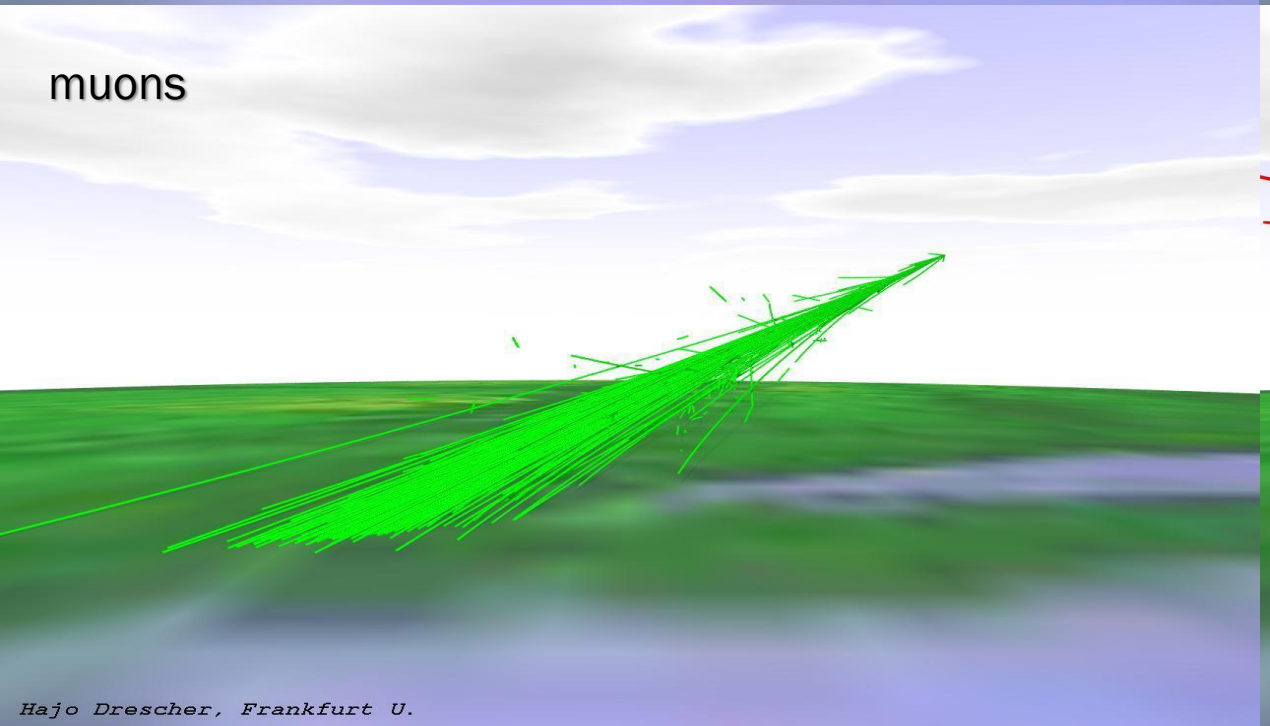
muons
Hajo Drescher, Frankfurt U.

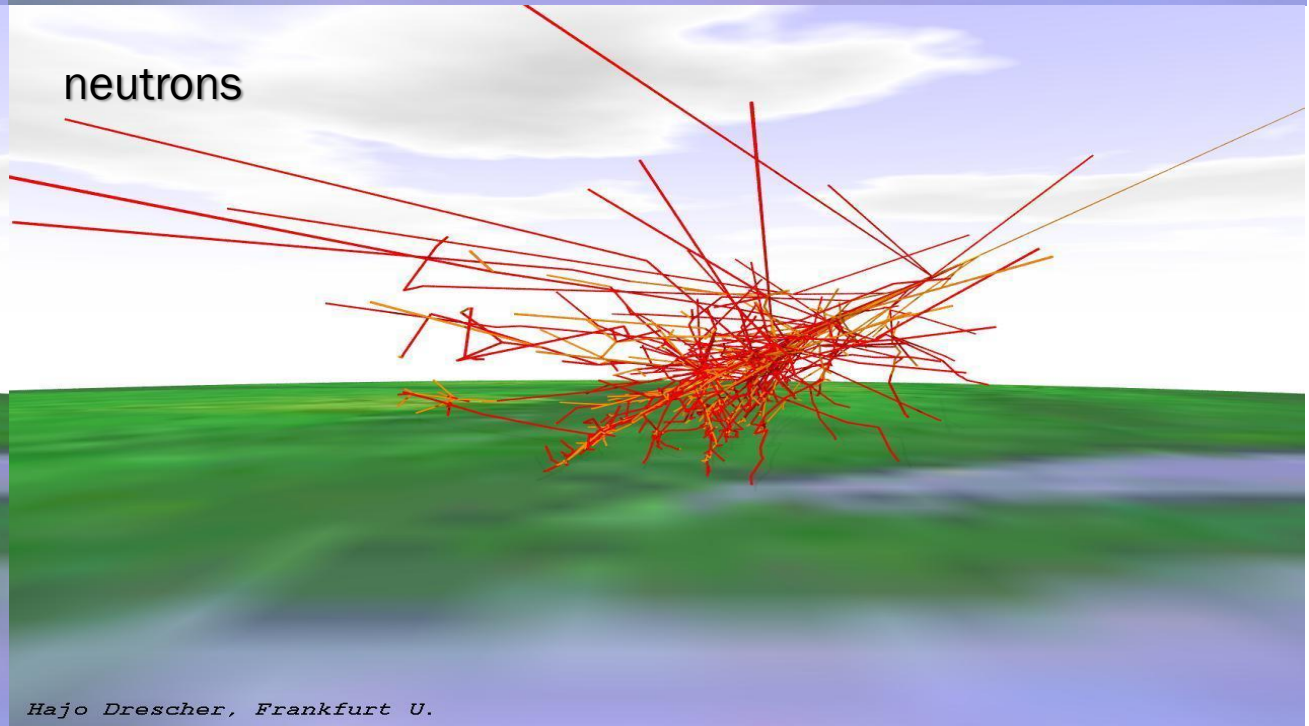
neutrons
Hajo Drescher, Frankfurt U.

INTRODUCTION: STANDARD NEUTRON MONITOR (NM64)

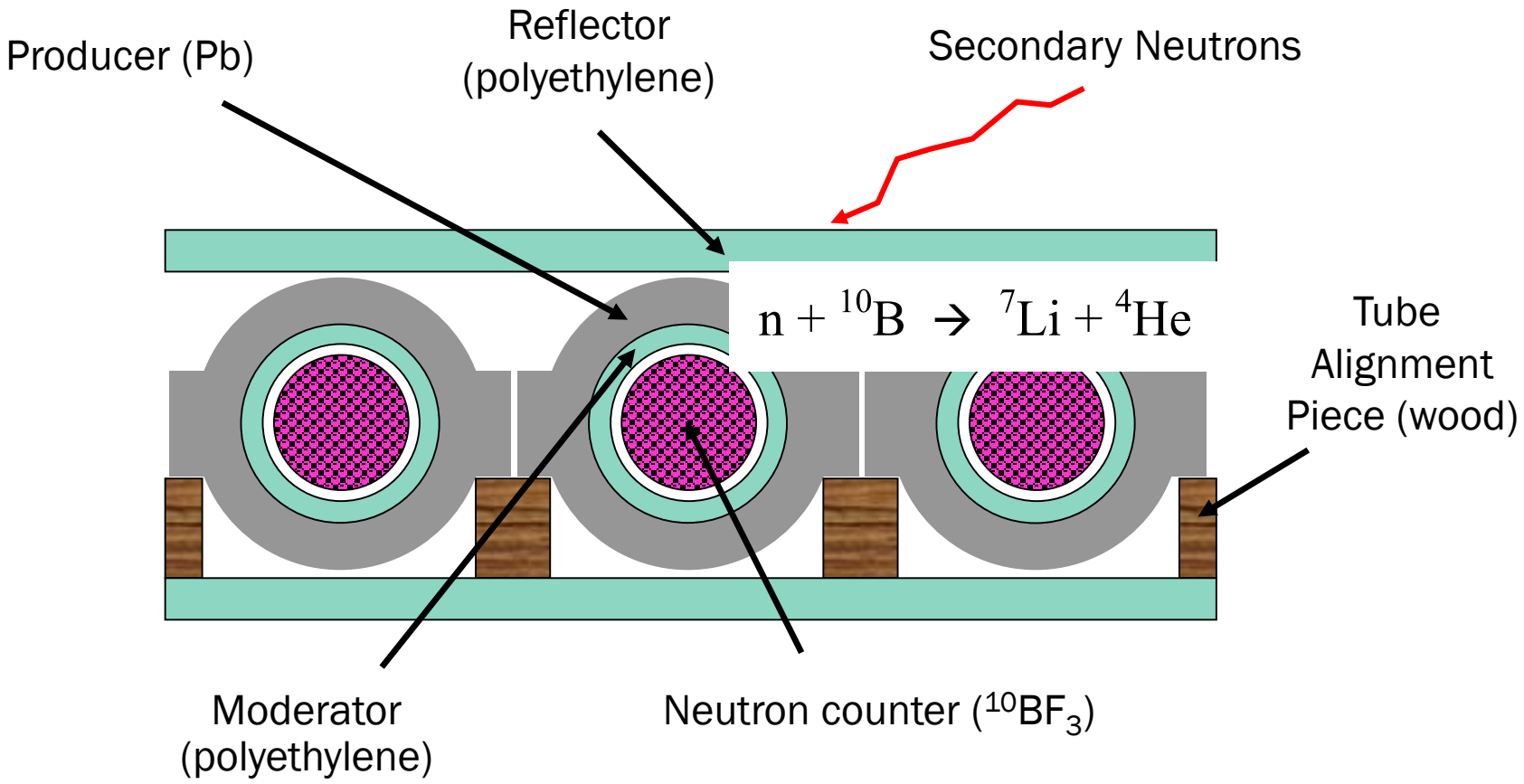

FIGURE 1 3NM64

INTRODUCTION: SEMI LEADED COUNTER

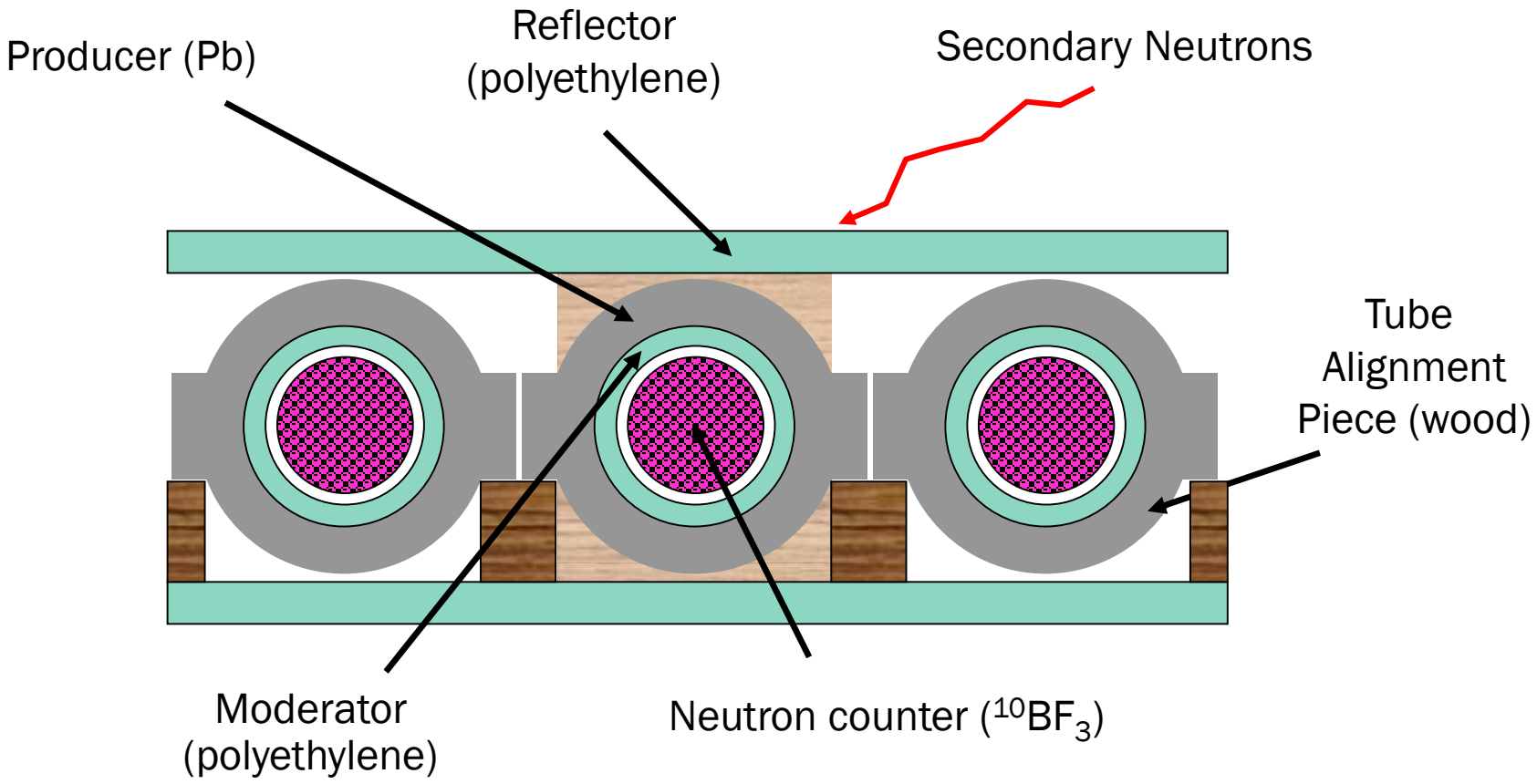

FIGURE 2 Semi leaded neutron detector

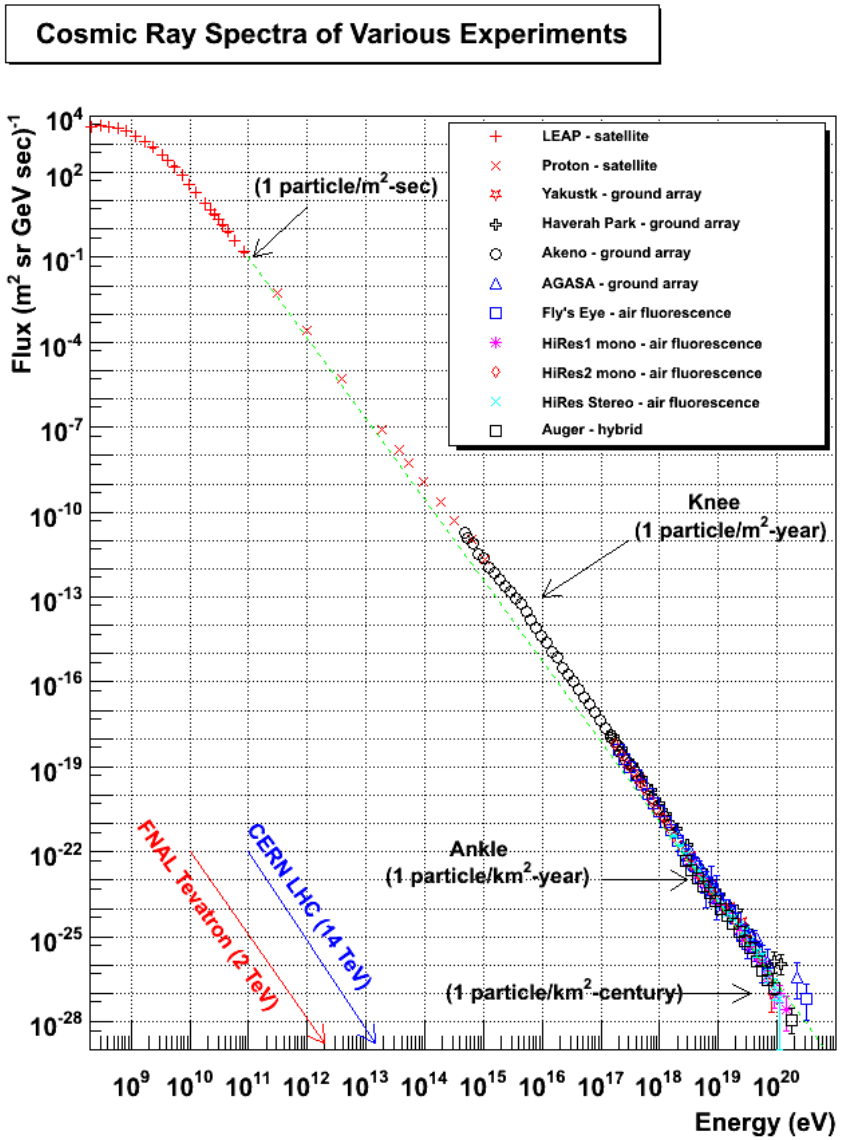

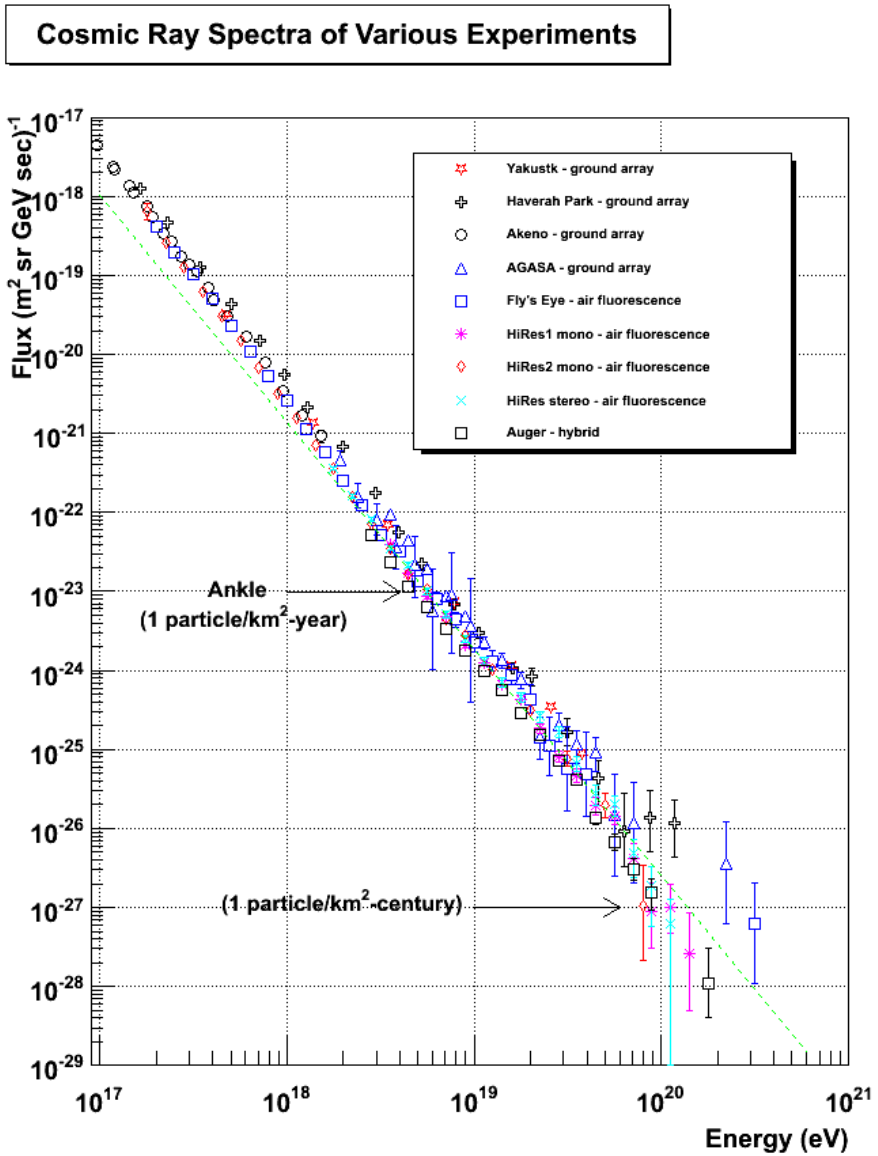

Figure 3

https://www.physics.utah.edu/~whanlon/spectrum.html

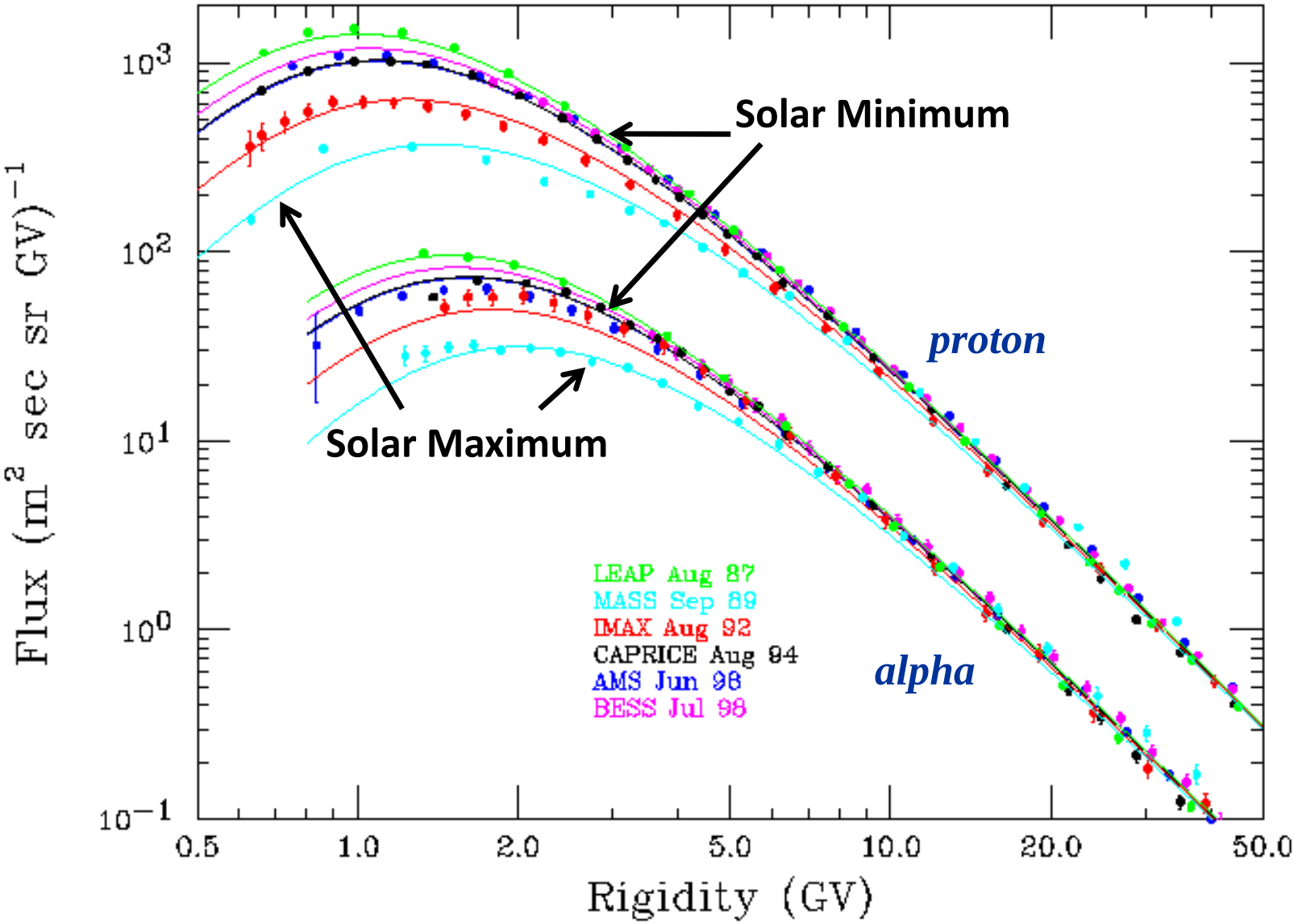
Solar Minimum
Solar Maximum
proton
alpha
LEAP Aug 87
MASS Sep 89
IMAX Aug 92
CAPRICE Aug 94
AMS Jun 98
BESS Jul 98
Flux (m^2 sec sr GV)$^{-1}$
Rigidity (GV)
10^3
10^2
10^1
10^0
10^{-1}
0.5
1.0
2.0
5.0
10.0
20.0
50.0

Figure 4

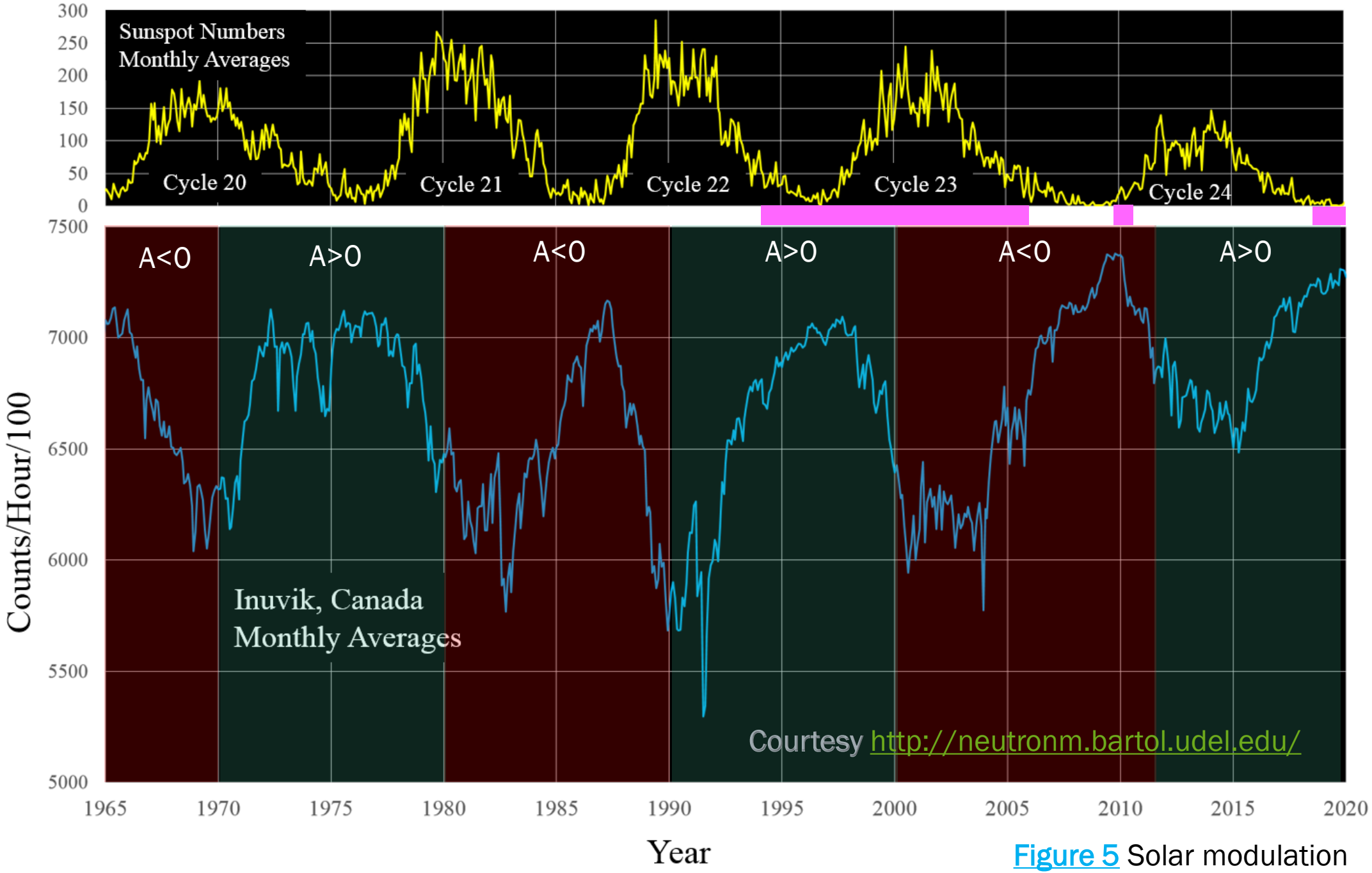

Figure 5 Solar modulation

Chinese Icebreaker XueLong

survey years:

- 2018-2019
- 2019-2020

GCR spectrum — heliospheric Modulation — Yield function — geomagnetic Transmission

Count Rate

$$N(\Theta,\Phi,h,t)=\int_0^{\infty}\left[\sum_i G_i(P)M_i(P,t)Y_i(P,h)\right]T(P,\Theta,\Phi,t)\mathrm{d}P \qquad \text{---------(1)}$$

$$N(P_c,h,t)=\int_{P_c}^{P_L}\sum_i G_i(P)M_i(P,t)Y_i(P,h)\mathrm{d}P \qquad \text{---------(2)}$$

Differential Response function

$$DRF(P)=-\left[\frac{dN}{dP_c}\right]_p=\sum_i G_i(P)M_i(P,t)Y_i(P,h)$$

LATITUDE SURVEY: VOYAGE IN 1994-2007 SURVEY YEAR

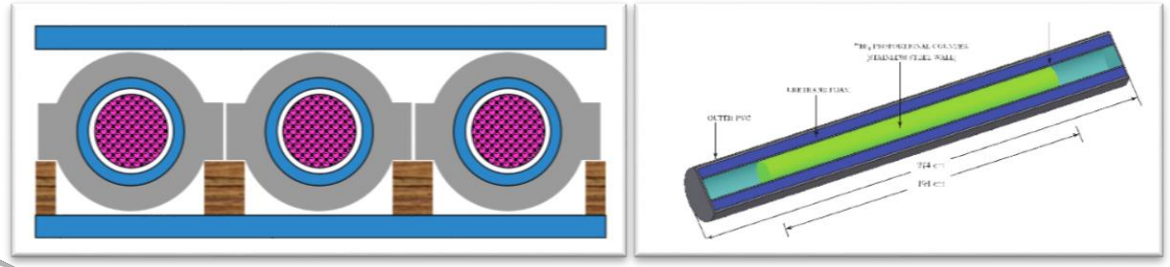

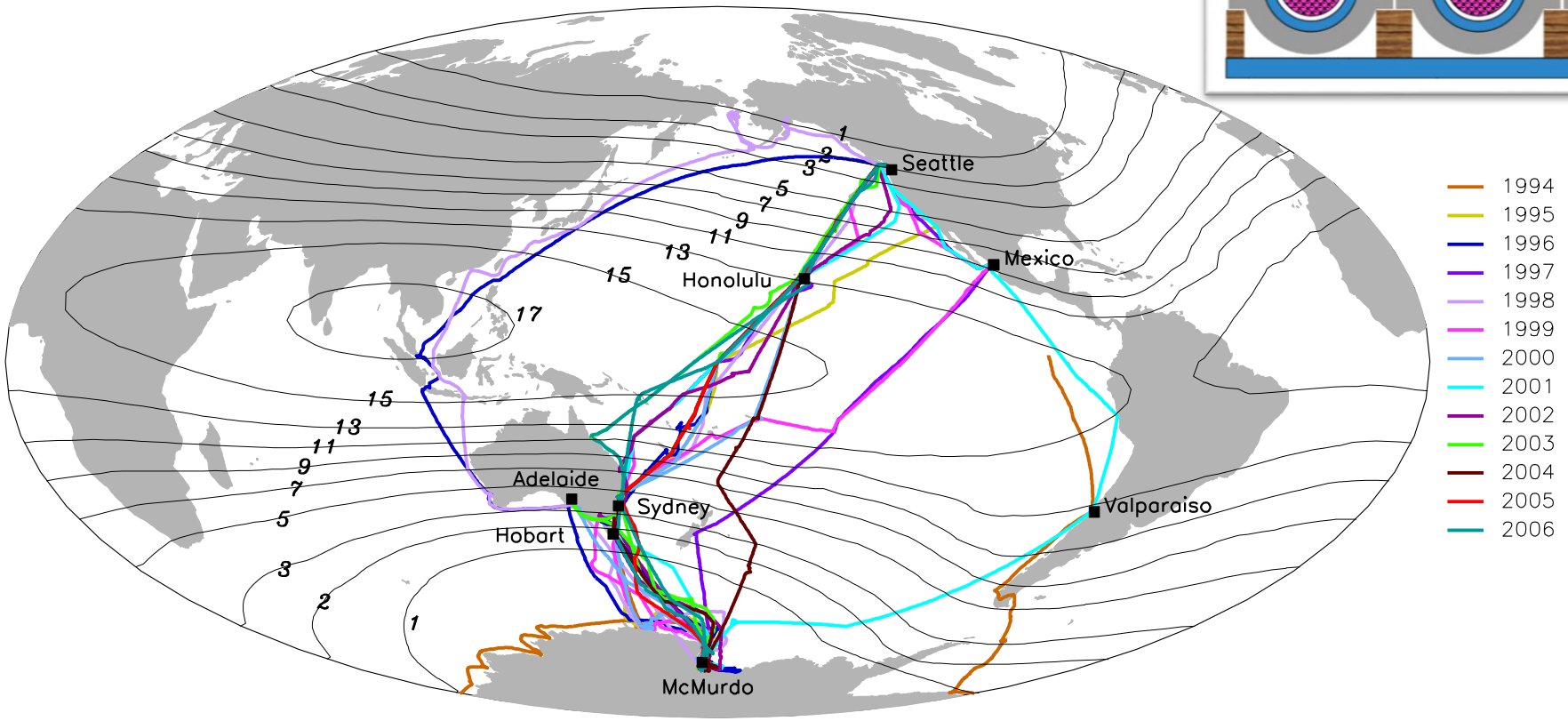

Figure 6 The track of the ship-borne neutron monitor latitude surveys for 1994-2007, superimposed on contours of the vertical cutoff rigidity indicated by black solid lines. Italic numbers at each contour indicate the vertical cutoff rigidity in GV.

DIFFERENTIAL RESPONSE FUNCTION (DRF)

1995 SURVEY YEAR

$$N(P_c) = N_0\left(1 - e^{-\alpha P_c^{-\kappa}}\right),$$

$$N(P_c) = \int_{P_c}^{\infty} DRF(P)dP,$$

$$DRF(P) = N_0 \alpha P^{-\kappa-1} \kappa e^{-\alpha P^{-\kappa}}.$$

$$DRF(P) = -\left[\frac{dN}{dP_c}\right]_p = \sum_i J_i(P,t)Y_i(P,h)$$

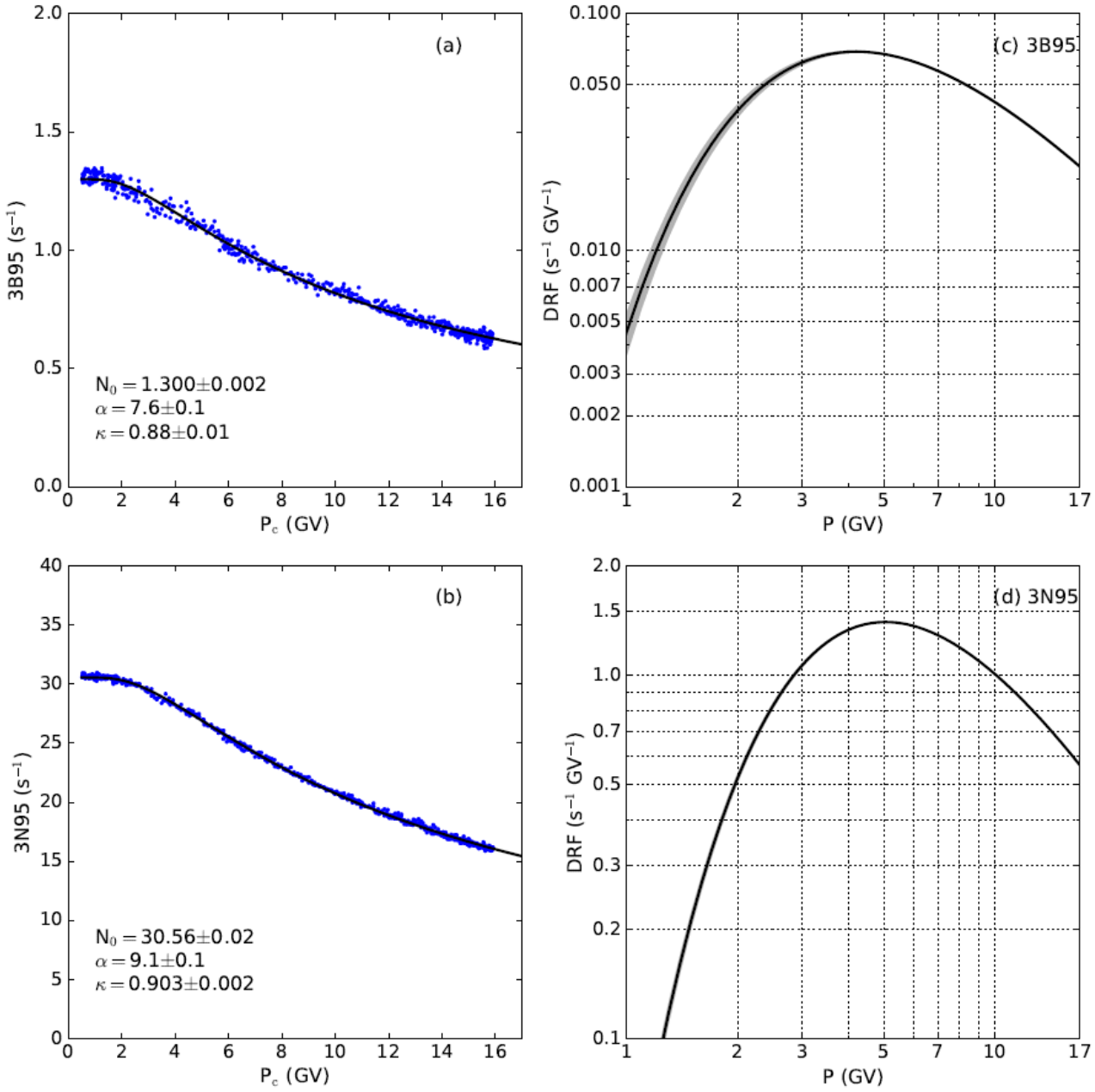

FIGURE 7 Dorman function fits to (a) bare and (b) neutron monitor data separately; (c) and (d) show the resulting differential response functions (DRFs).

Integral Response function

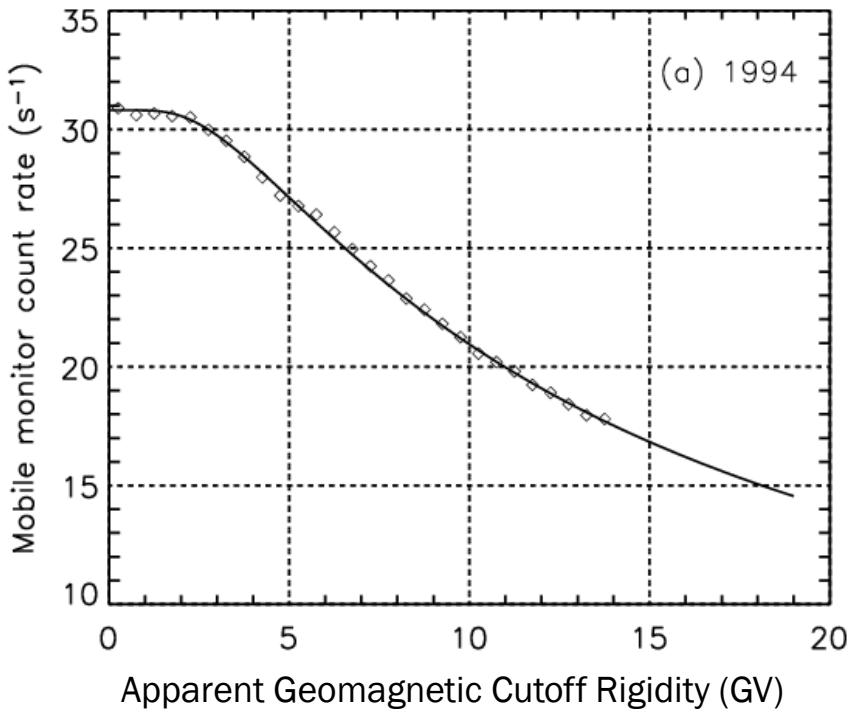

Differential Response function

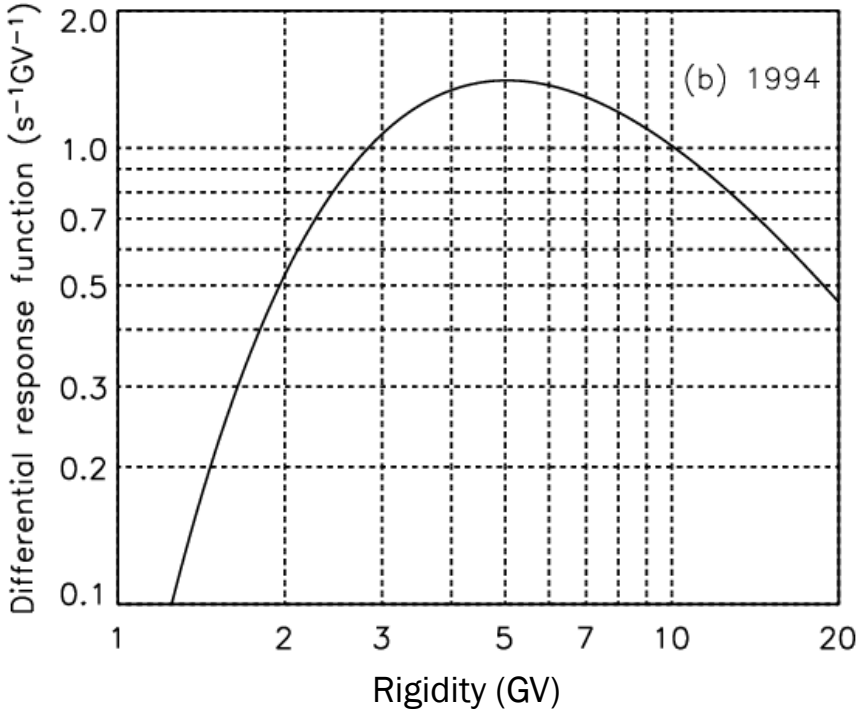

Integral Response function

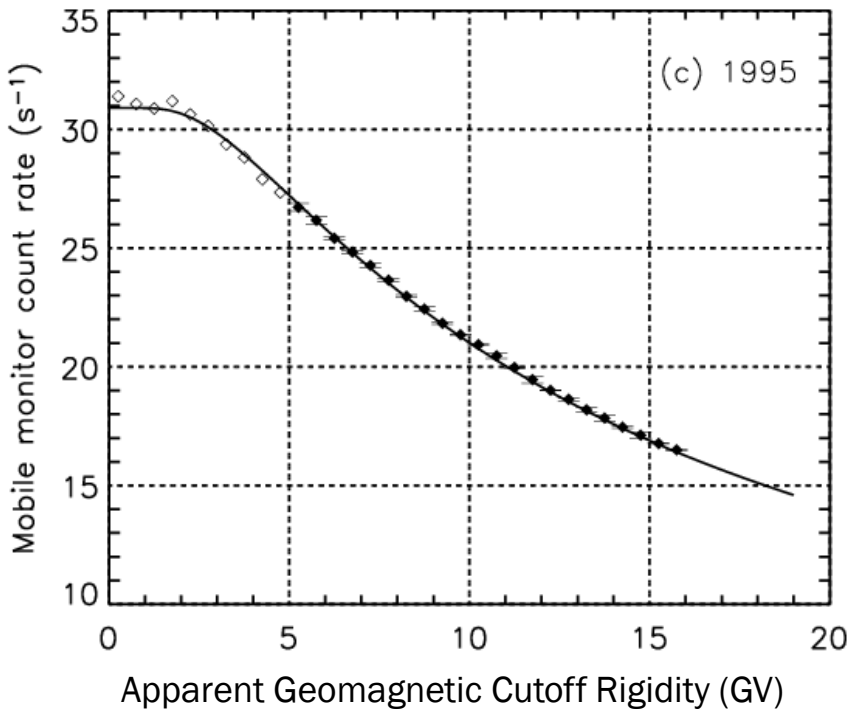

Differential Response function

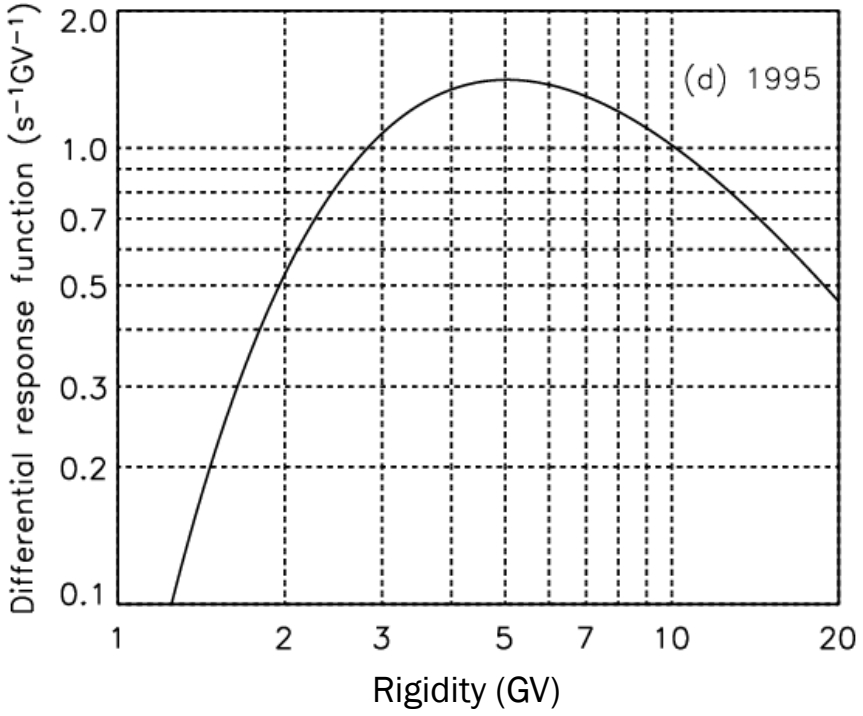

Integral Response function

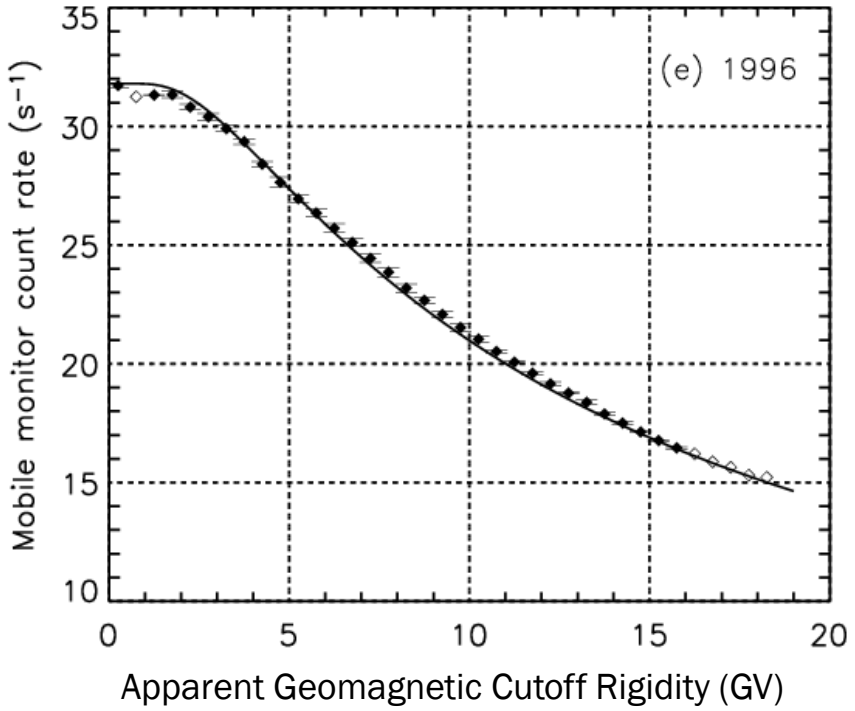

Differential Response function

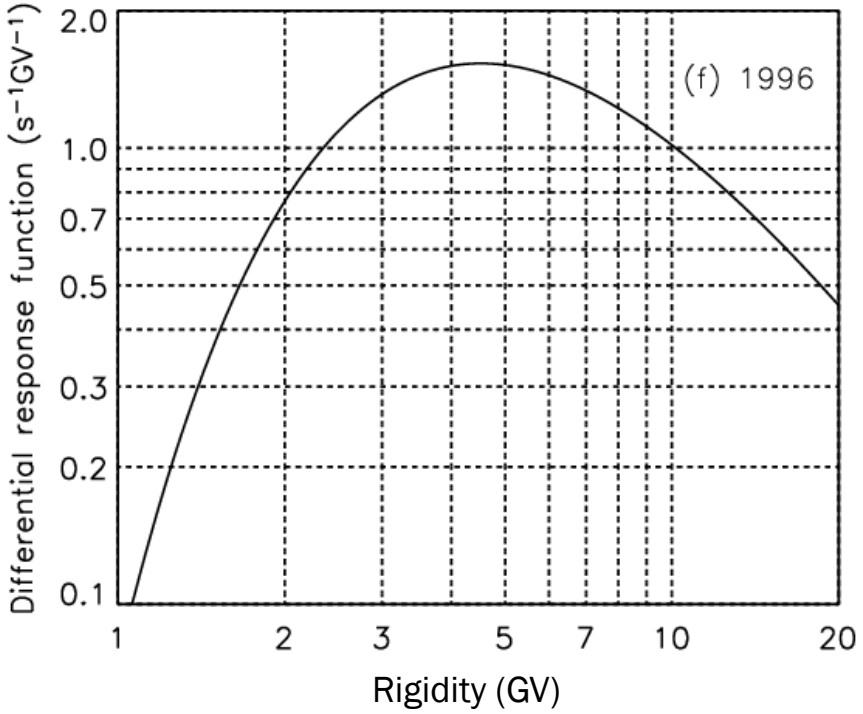

Integral Response function

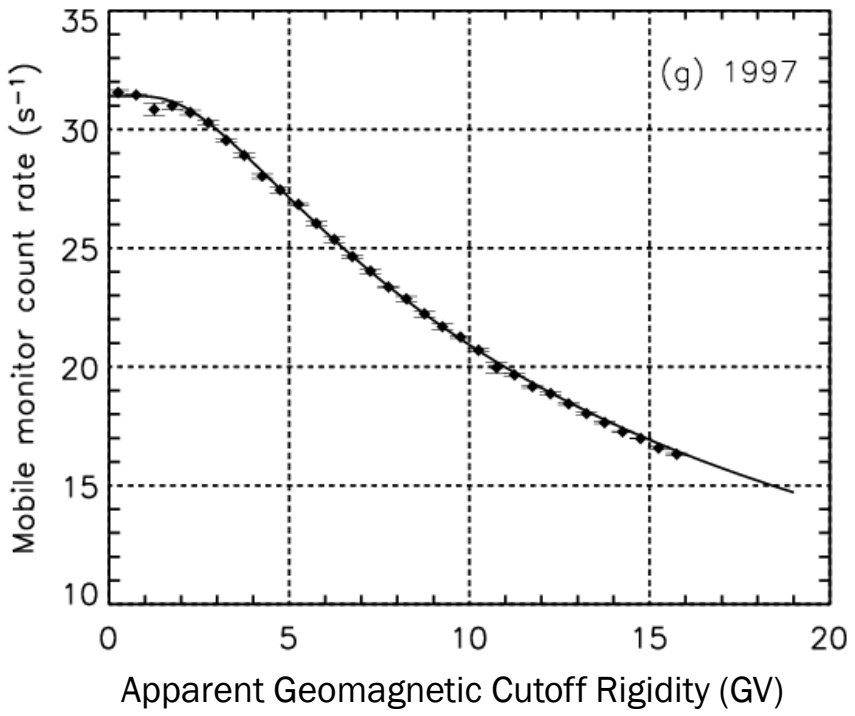

Differential Response function

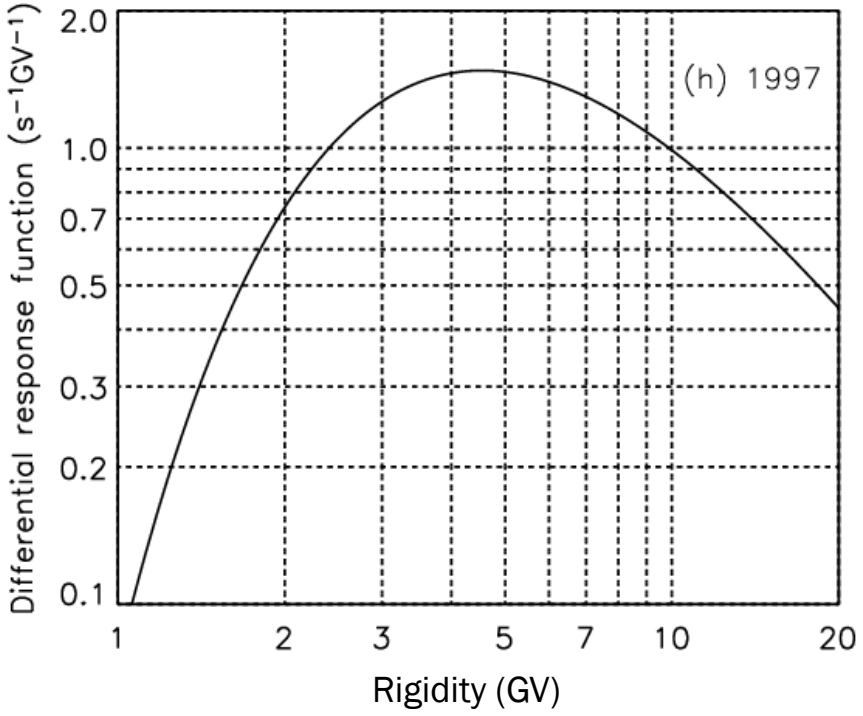

Integral Response function

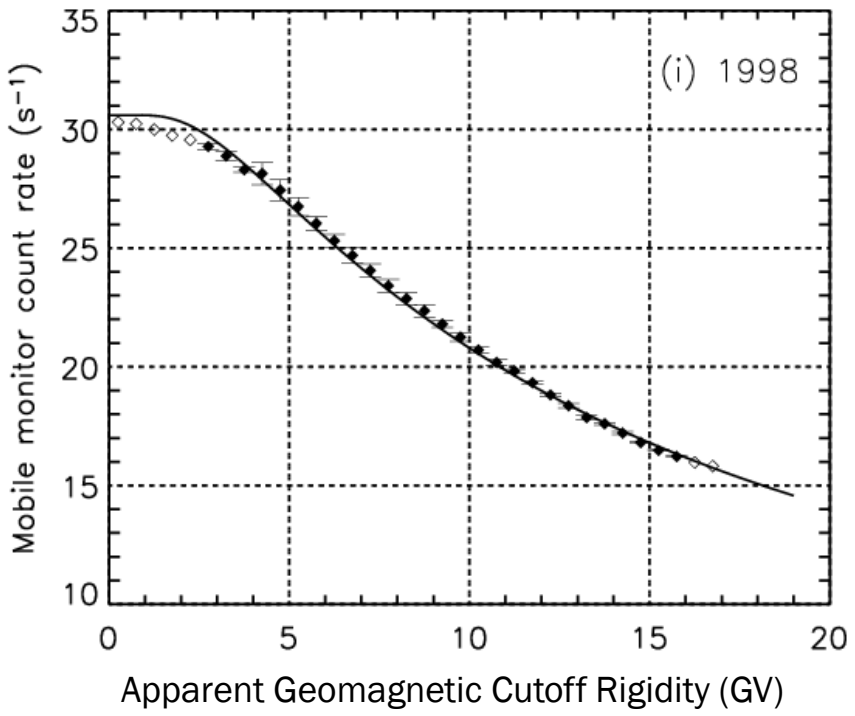

Differential Response function

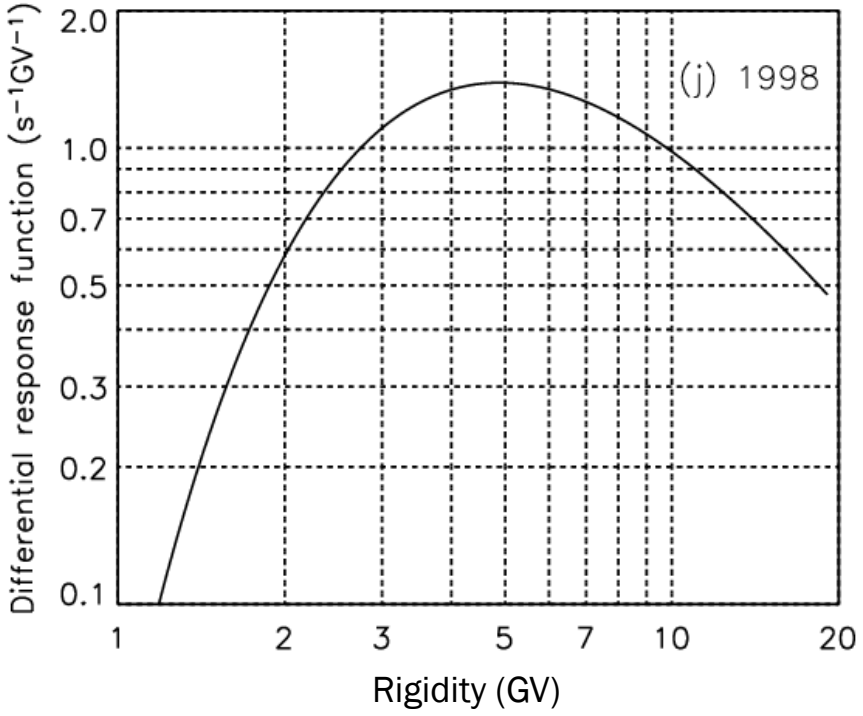

Integral Response function

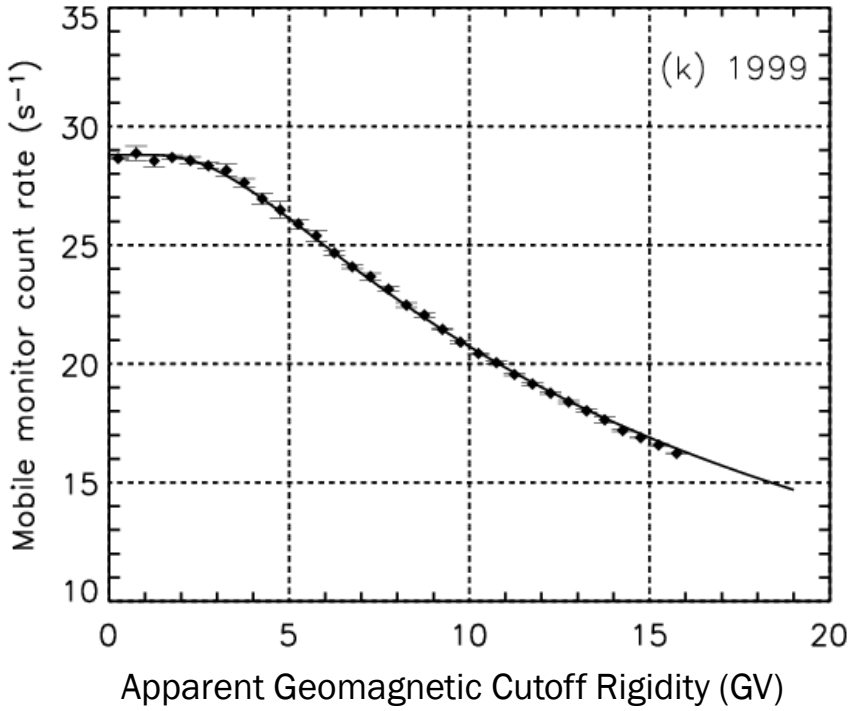

Differential Response function

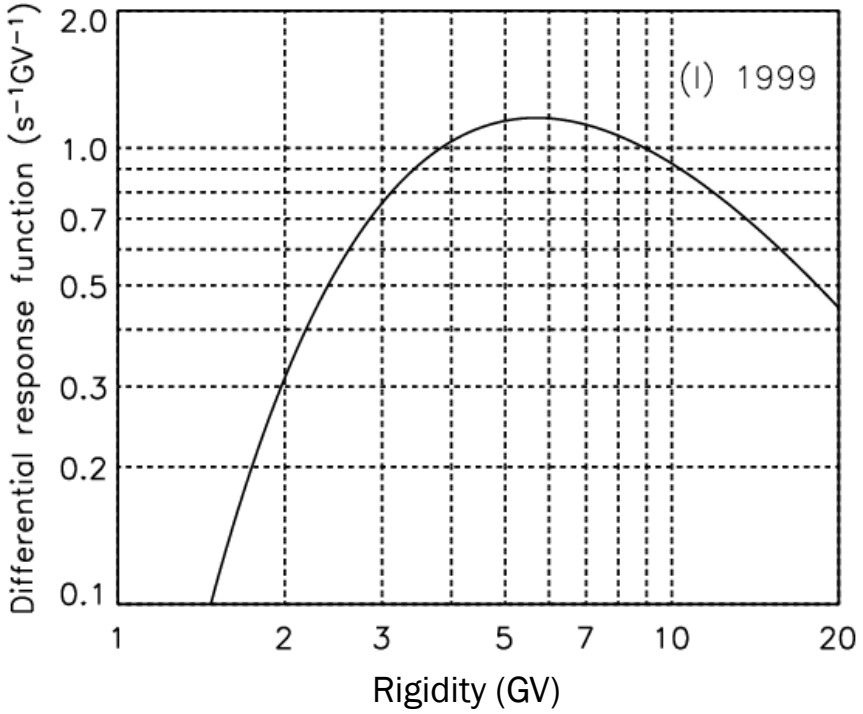

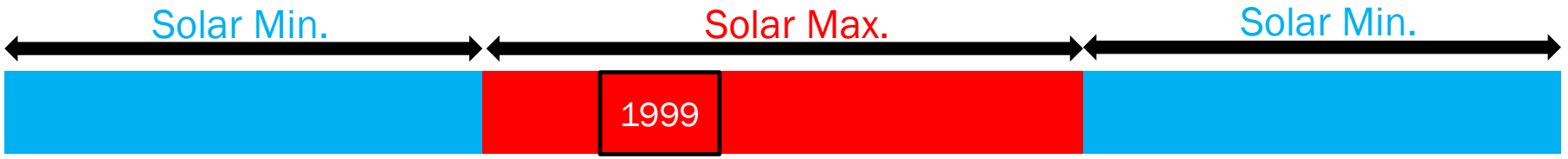

Integral Response function

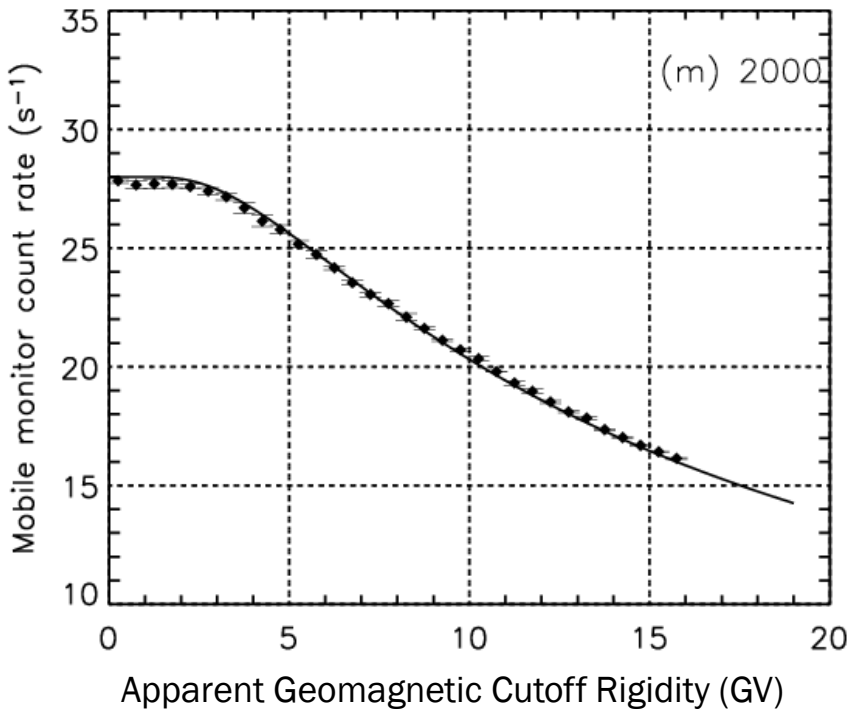

Differential Response function

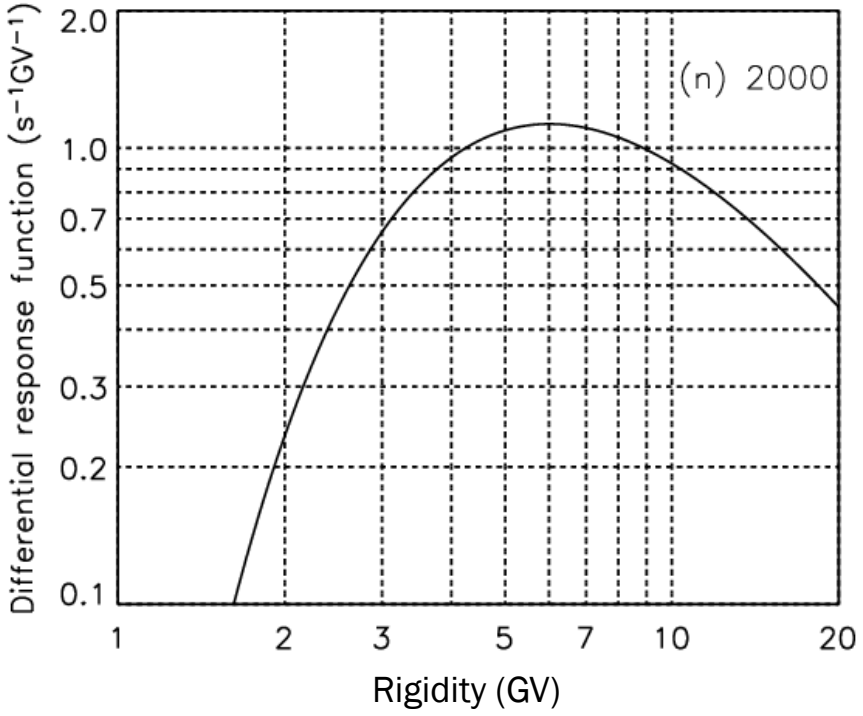

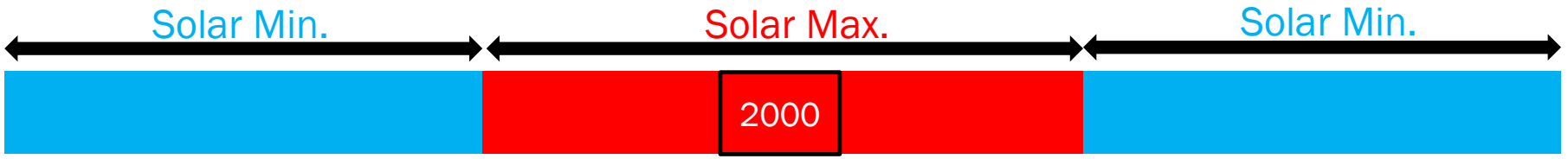

Integral Response function

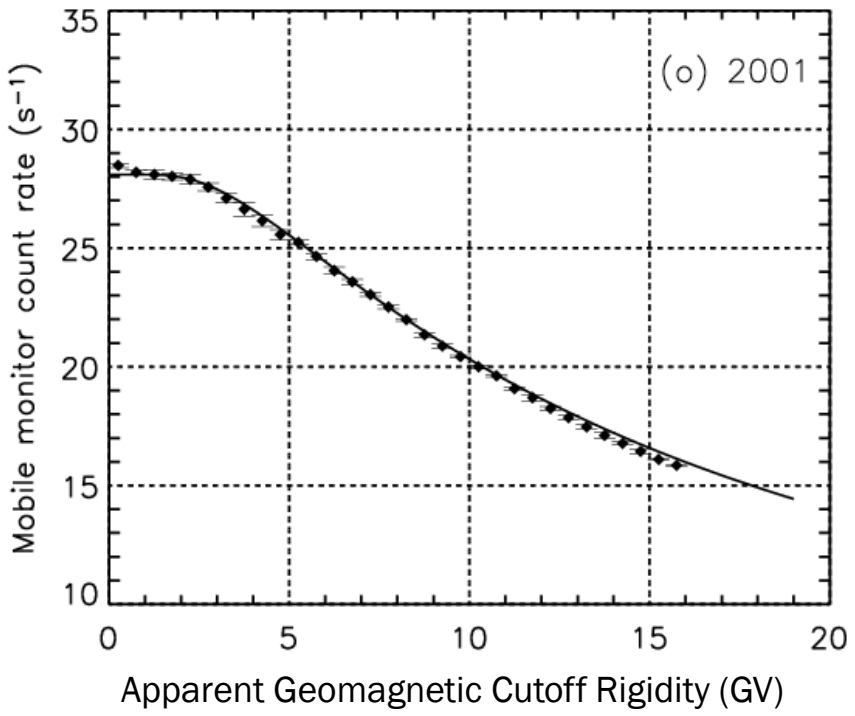

Differential Response function

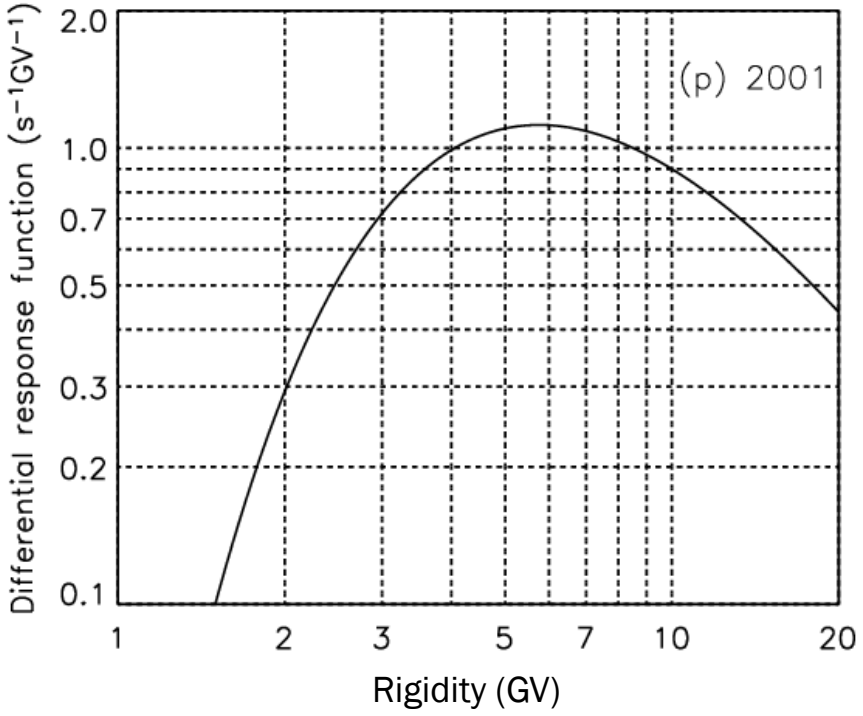

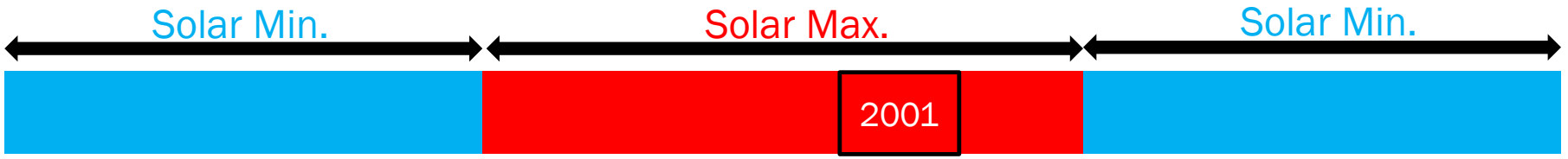

Integral Response function

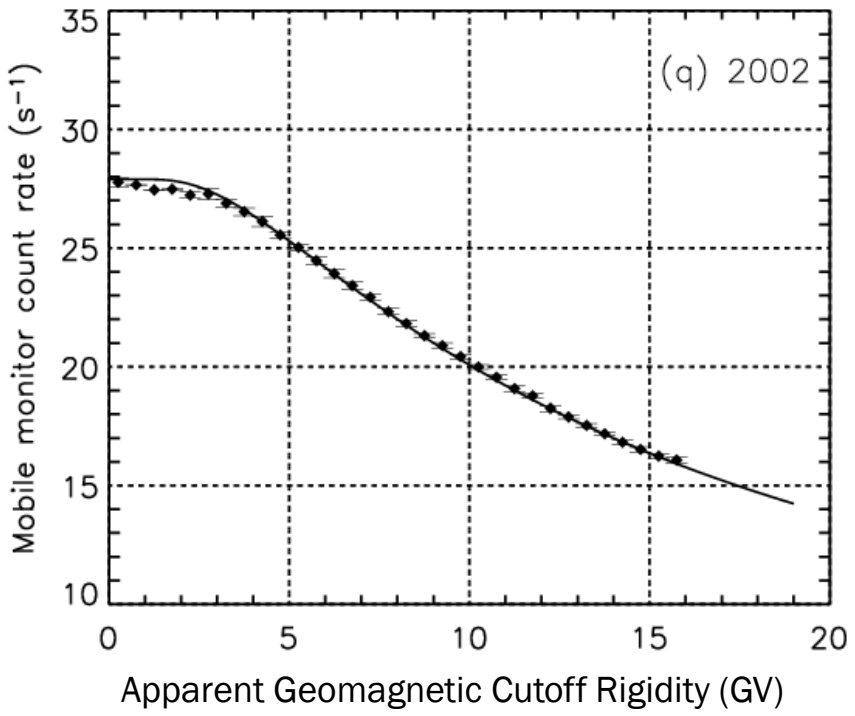

Differential Response function

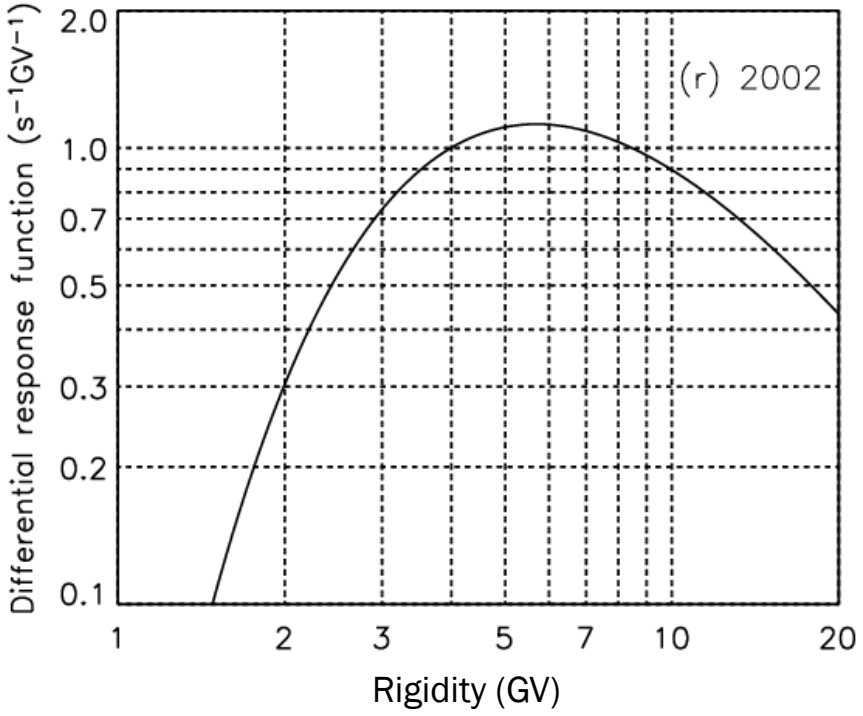

Integral Response function

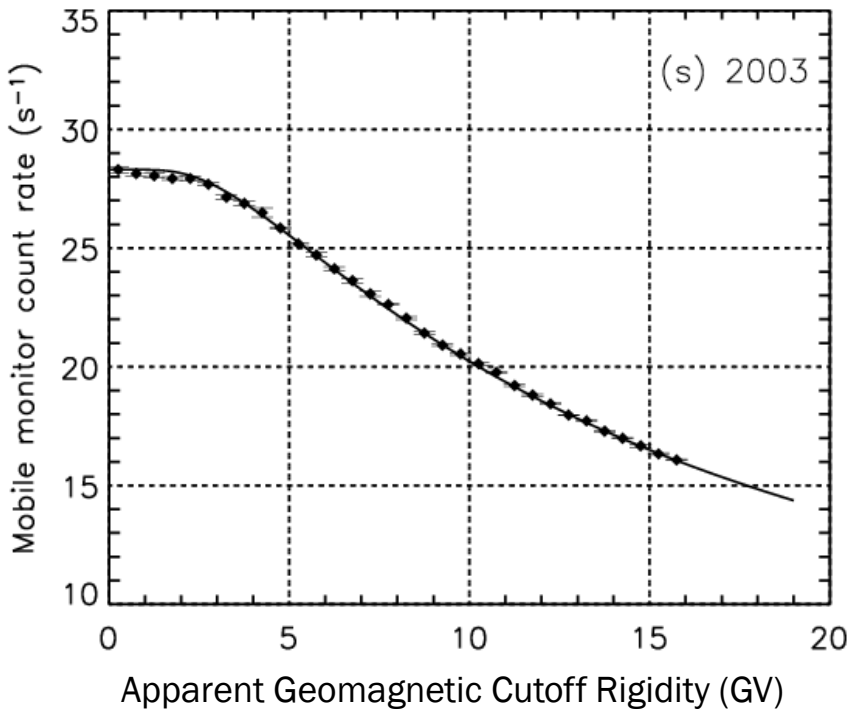

Differential Response function

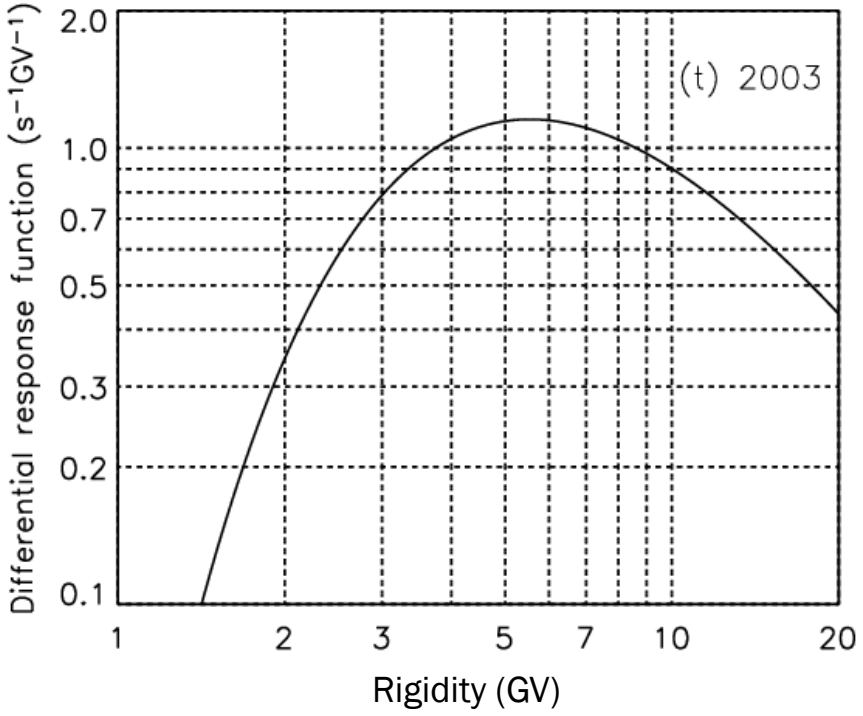

Integral Response function

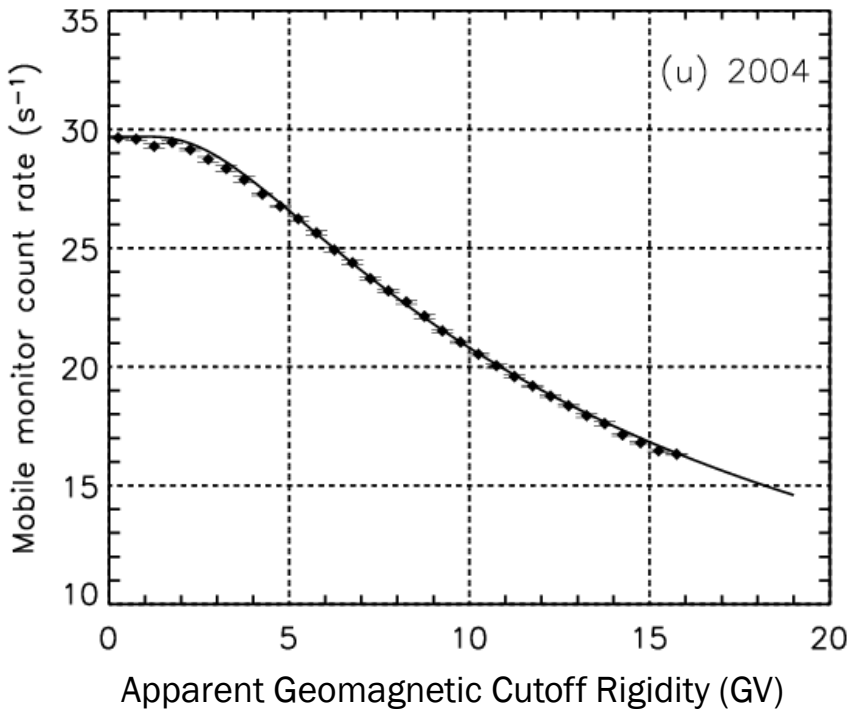

Differential Response function

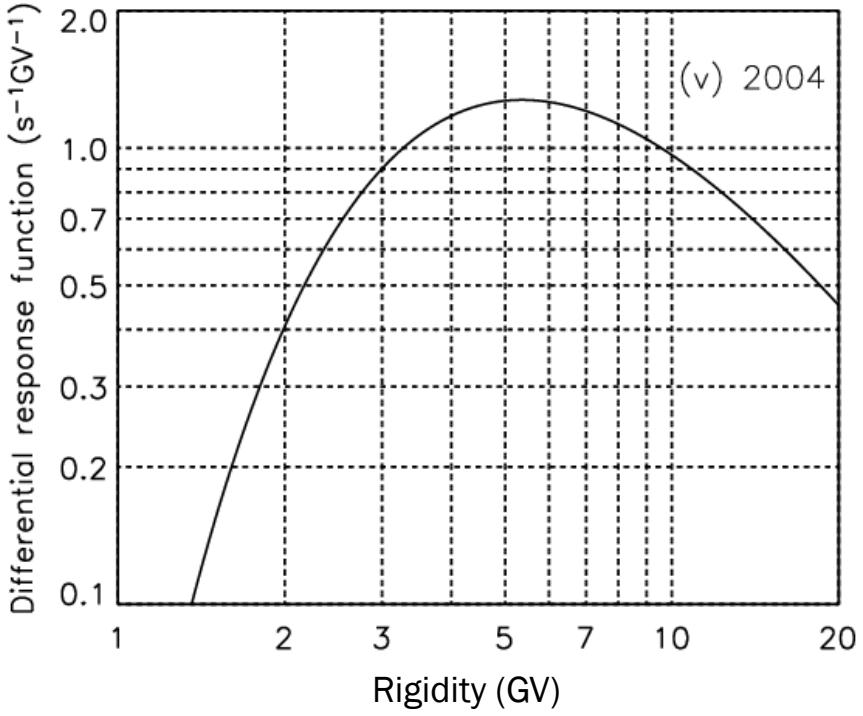

Integral Response function

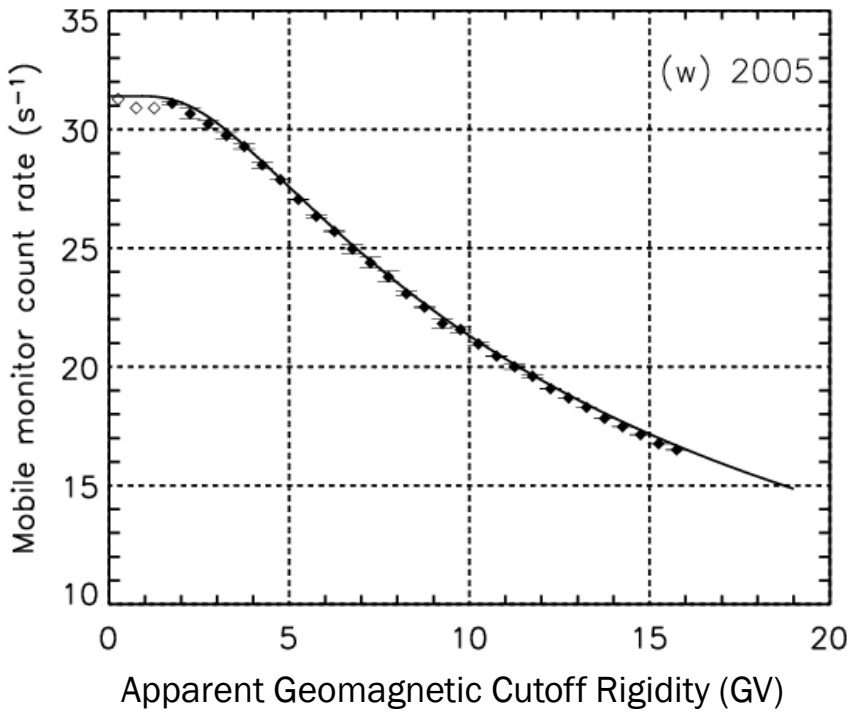

Differential Response function

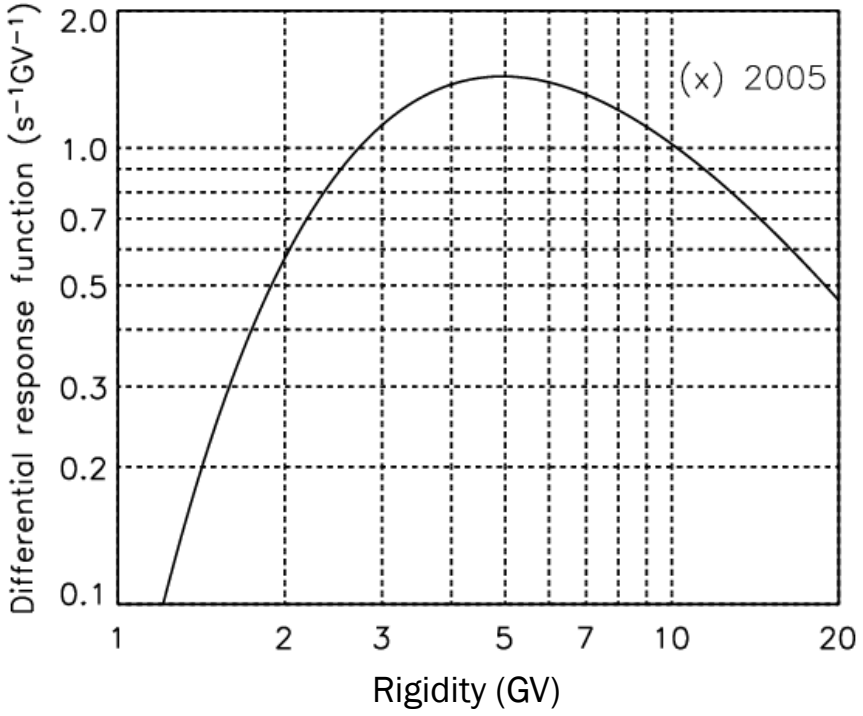

Integral Response function

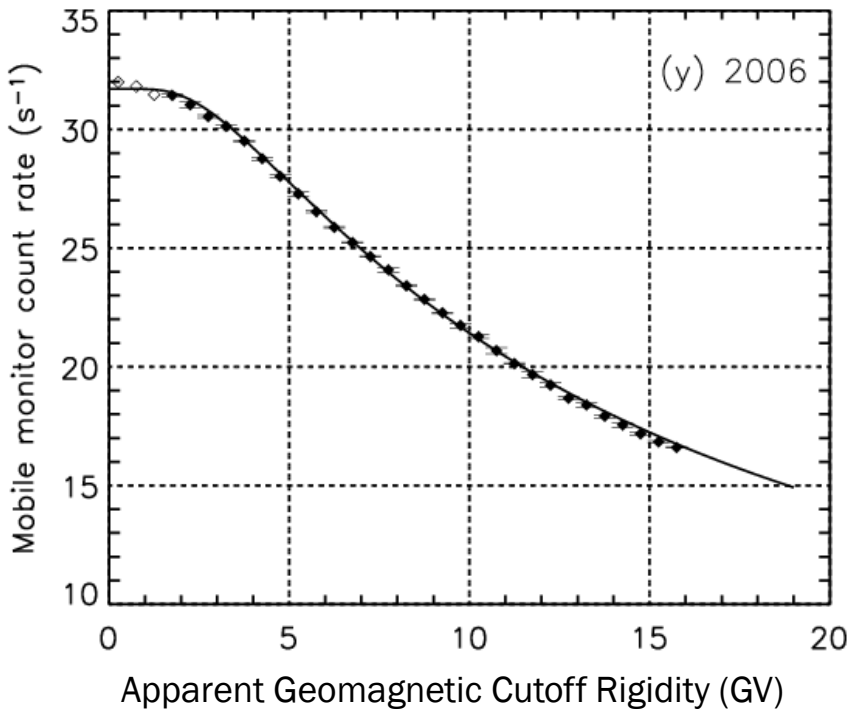

Differential Response function

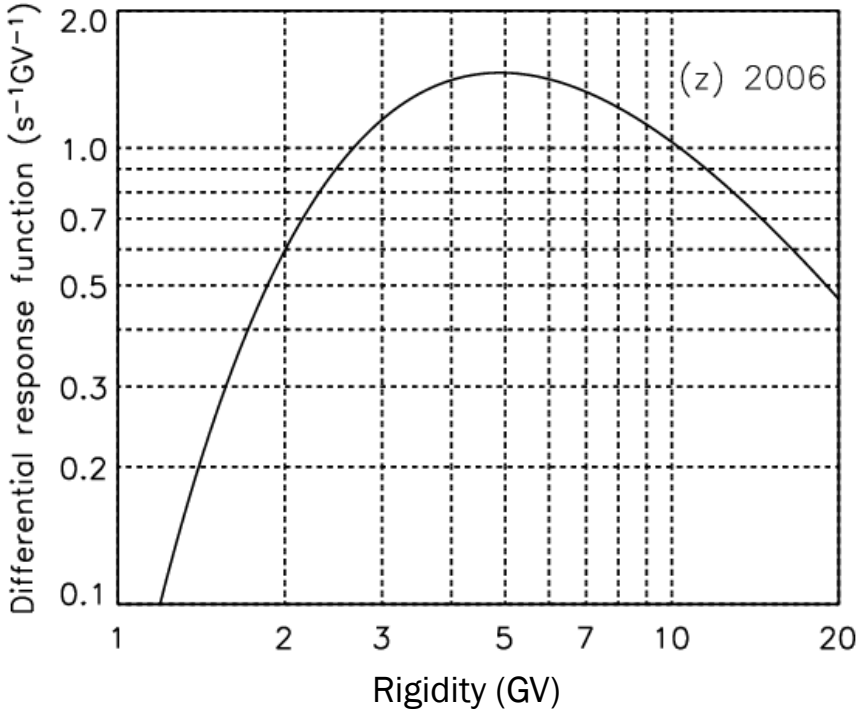

Left: Moraal et al. 1989
Below: Nuntiyakul et al. 2014

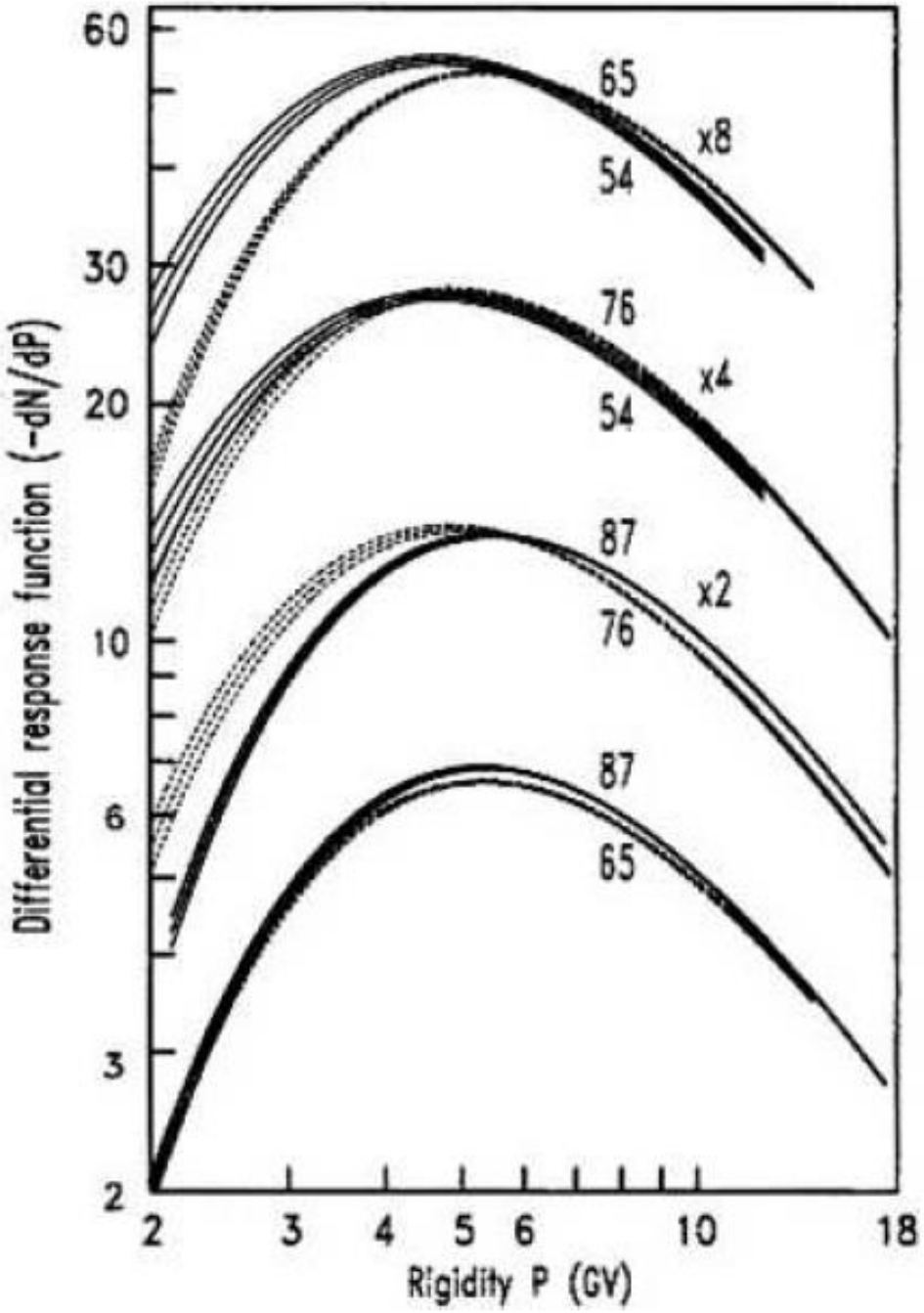

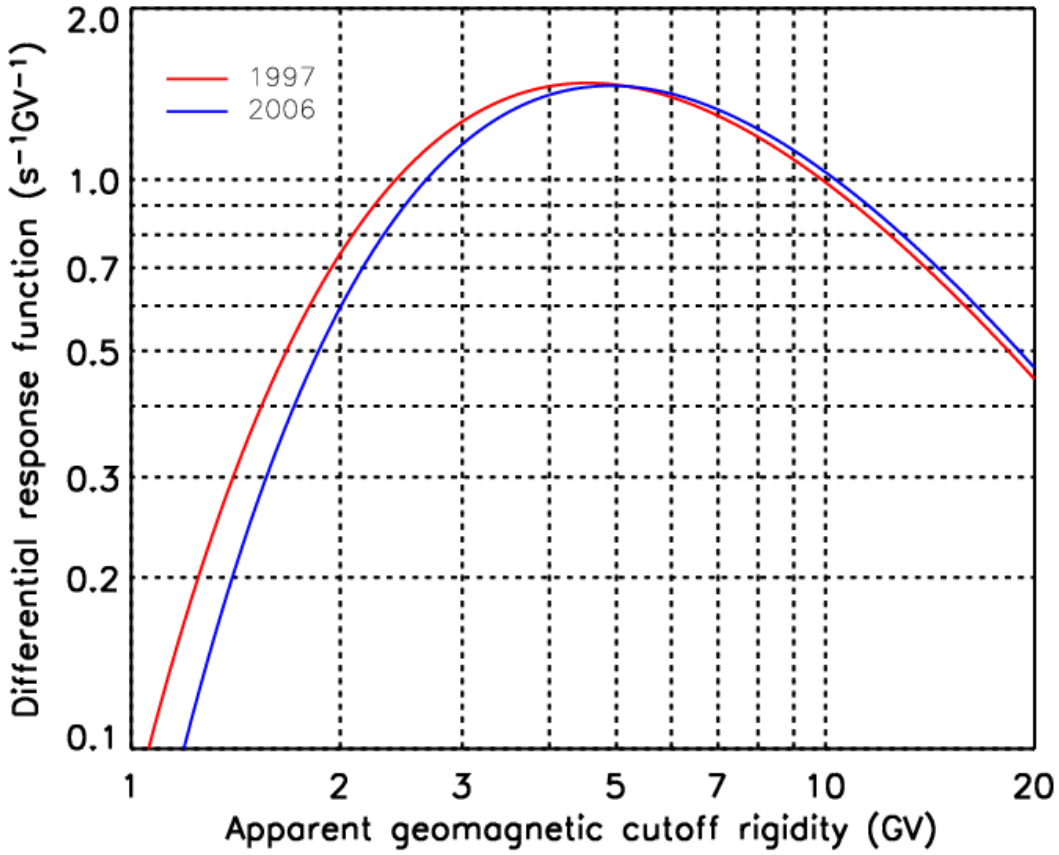

Figure 8 Differential response functions for two survey years, near solar minimum, of opposite polarity and similar modulation level. A crossover is apparent at 4.9 GV.

Straight-Line Fits of 3-NM64 (Uncorrected for McMurdo) Vs. McMurdo Rate for All Cutoff Rigidity Bins (BEFORE 2000)

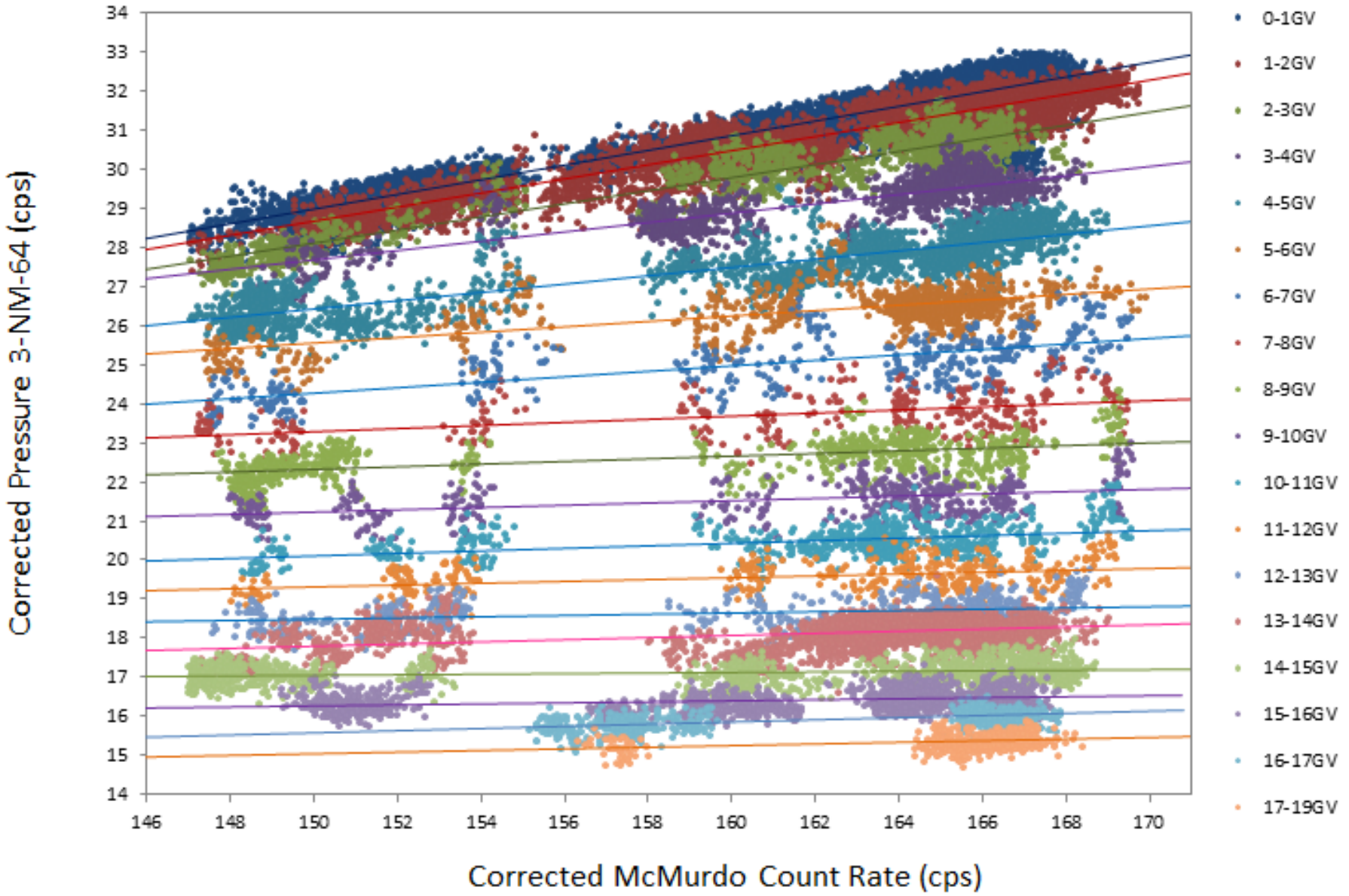

Figure 9 Straight-line fits of 3NM64 Vs. McMurdo count rate (before 2000)

Straight-Line Fits of 3-NM64 (Uncorrected for McMurdo) Vs. McMurdo Rate for All Cutoff Rigidity Bins (AFTER 2000)

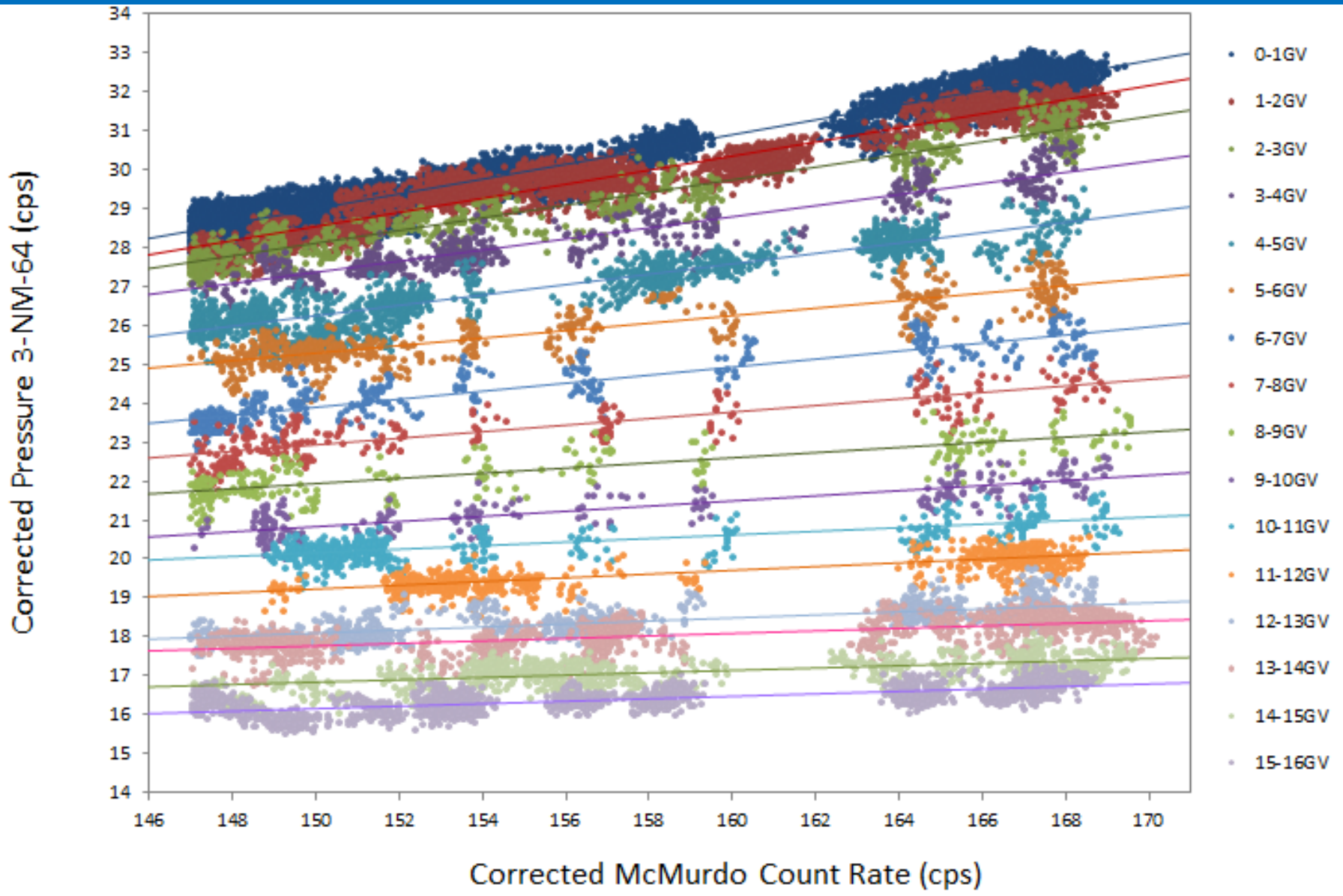

Figure 10 Straight-line fits of 3NM64 Vs. McMurdo count rate (after 2000)

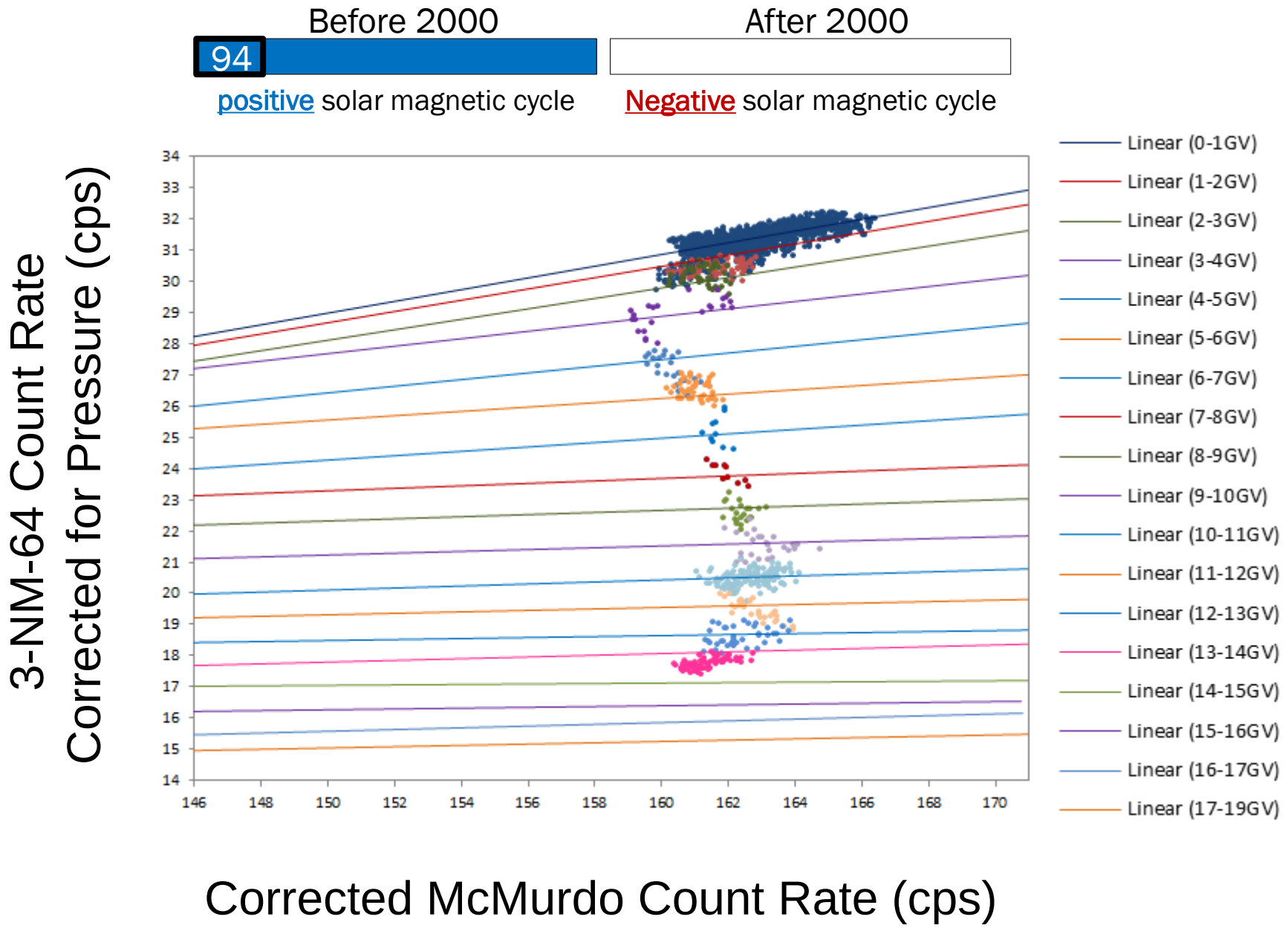
Before 2000
After 2000
94
positive solar magnetic cycle
Negative solar magnetic cycle
3-NM-64 Count Rate
Corrected for Pressure (cps)
Corrected McMurdo Count Rate (cps)
Linear (0-1GV)
Linear (1-2GV)
Linear (2-3GV)
Linear (3-4GV)
Linear (4-5GV)
Linear (5-6GV)
Linear (6-7GV)
Linear (7-8GV)
Linear (8-9GV)
Linear (9-10GV)
Linear (10-11GV)
Linear (11-12GV)
Linear (12-13GV)
Linear (13-14GV)
Linear (14-15GV)
Linear (15-16GV)
Linear (16-17GV)
Linear (17-19GV)

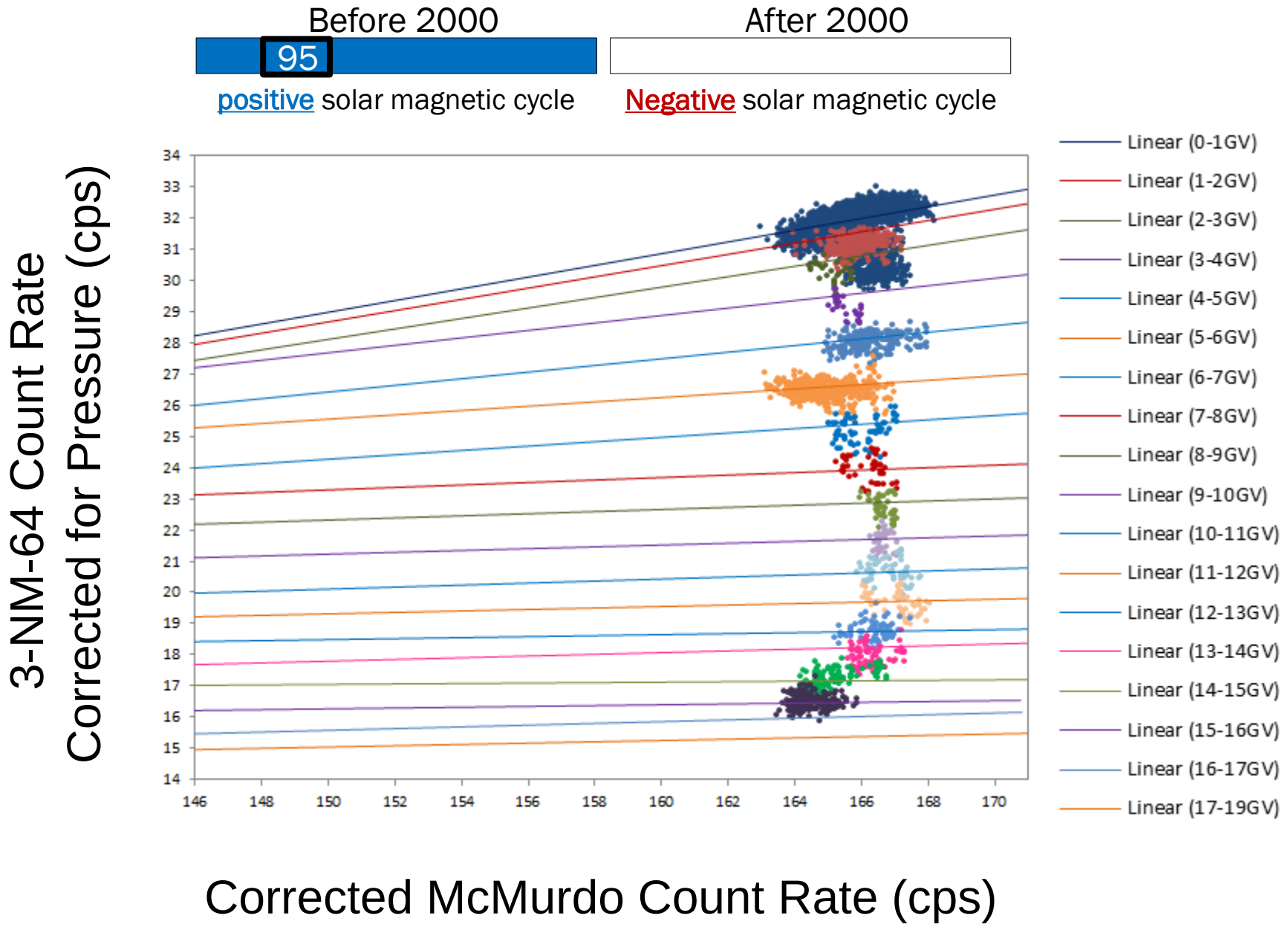
Before 2000
After 2000
95
positive solar magnetic cycle
Negative solar magnetic cycle
3-NM-64 Count Rate
Corrected for Pressure (cps)
Corrected McMurdo Count Rate (cps)
Linear (0-1GV)
Linear (1-2GV)
Linear (2-3GV)
Linear (3-4GV)
Linear (4-5GV)
Linear (5-6GV)
Linear (6-7GV)
Linear (7-8GV)
Linear (8-9GV)
Linear (9-10GV)
Linear (10-11GV)
Linear (11-12GV)
Linear (12-13GV)
Linear (13-14GV)
Linear (14-15GV)
Linear (15-16GV)
Linear (16-17GV)
Linear (17-19GV)

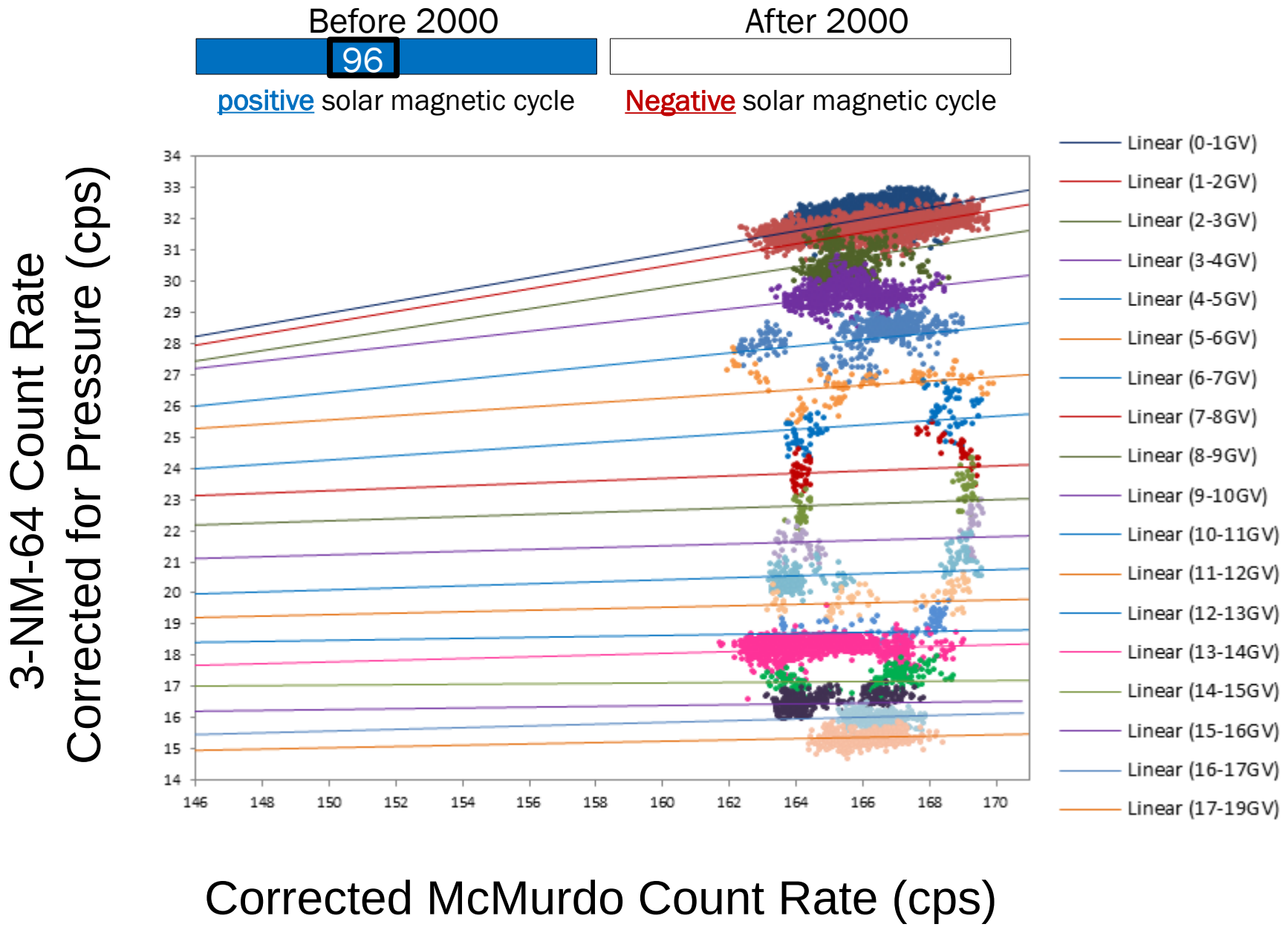
Before 2000
96
After 2000
positive solar magnetic cycle
Negative solar magnetic cycle
3-NM-64 Count Rate
Corrected for Pressure (cps)
34
33
32
31
30
29
28
27
26
25
24
23
22
21
20
19
18
17
16
15
14
146
148
150
152
154
156
158
160
162
164
166
168
170
Linear (0-1GV)
Linear (1-2GV)
Linear (2-3GV)
Linear (3-4GV)
Linear (4-5GV)
Linear (5-6GV)
Linear (6-7GV)
Linear (7-8GV)
Linear (8-9GV)
Linear (9-10GV)
Linear (10-11GV)
Linear (11-12GV)
Linear (12-13GV)
Linear (13-14GV)
Linear (14-15GV)
Linear (15-16GV)
Linear (16-17GV)
Linear (17-19GV)
Corrected McMurdo Count Rate (cps)

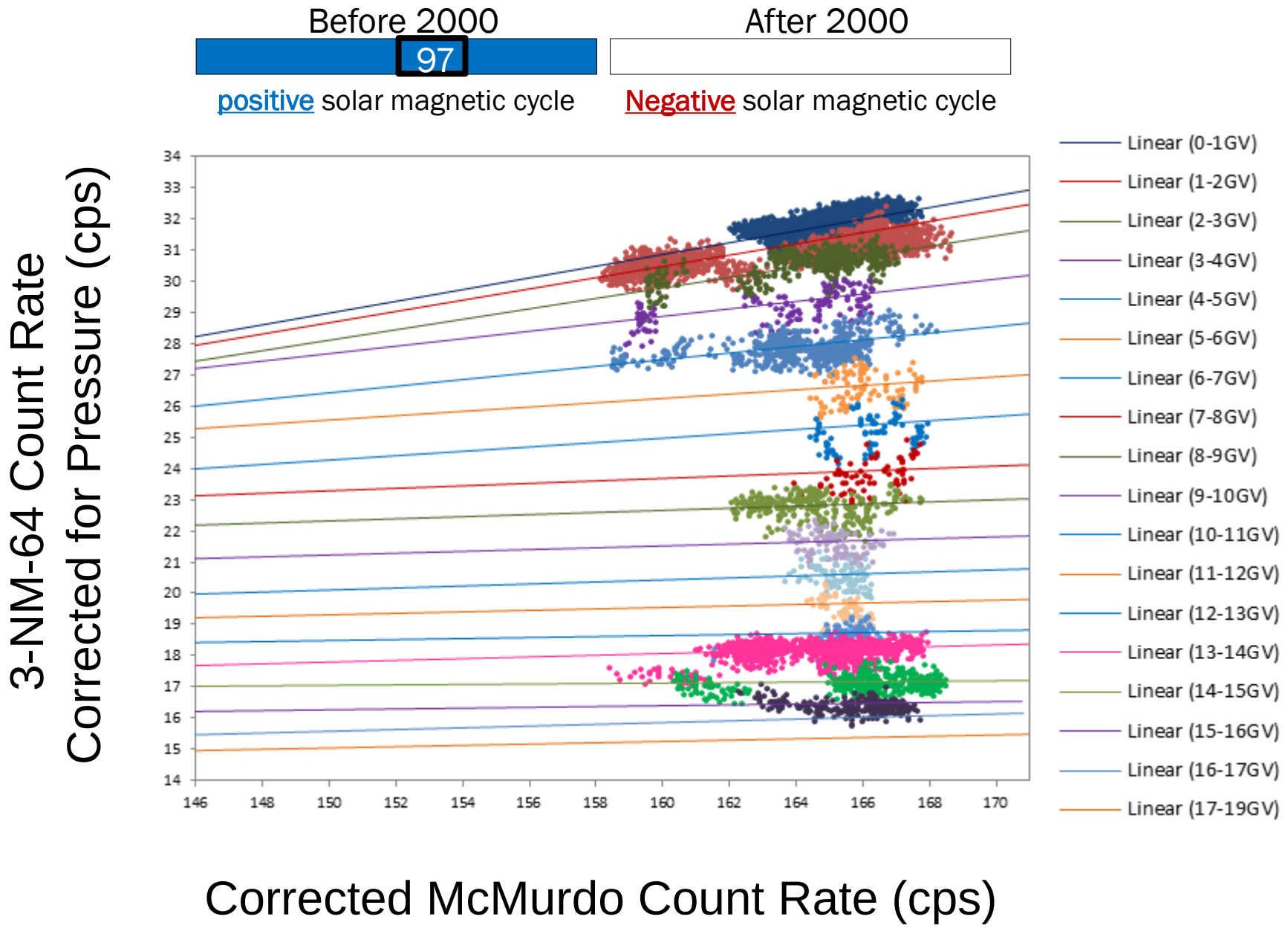
Before 2000
97
After 2000
positive solar magnetic cycle
Negative solar magnetic cycle
3-NM-64 Count Rate
Corrected for Pressure (cps)
34
33
32
31
30
29
28
27
26
25
24
23
22
21
20
19
18
17
16
15
14
146
148
150
152
154
156
158
160
162
164
166
168
170
Linear (0-1GV)
Linear (1-2GV)
Linear (2-3GV)
Linear (3-4GV)
Linear (4-5GV)
Linear (5-6GV)
Linear (6-7GV)
Linear (7-8GV)
Linear (8-9GV)
Linear (9-10GV)
Linear (10-11GV)
Linear (11-12GV)
Linear (12-13GV)
Linear (13-14GV)
Linear (14-15GV)
Linear (15-16GV)
Linear (16-17GV)
Linear (17-19GV)
Corrected McMurdo Count Rate (cps)

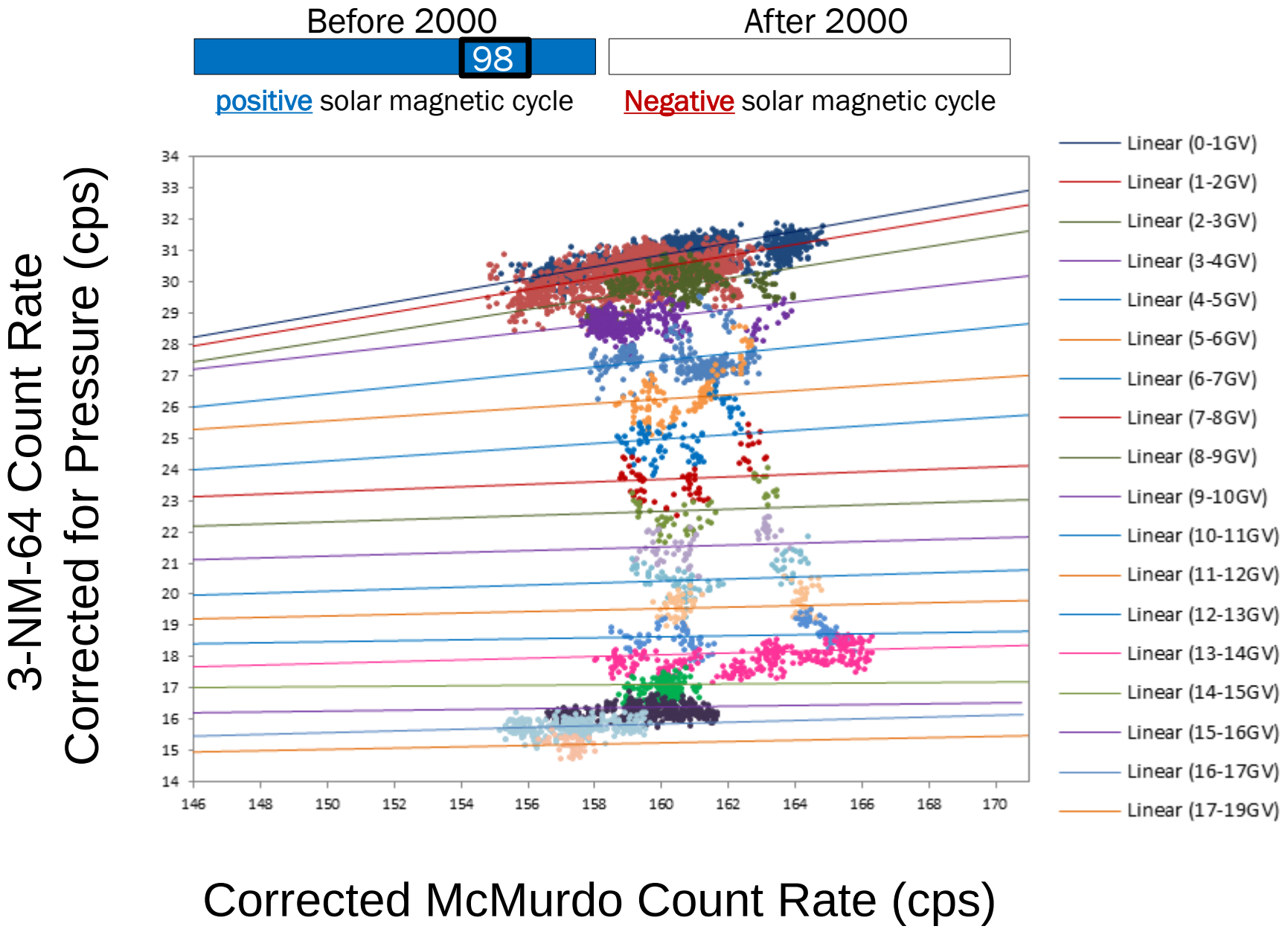
Before 2000
After 2000
98
positive solar magnetic cycle
Negative solar magnetic cycle
3-NM-64 Count Rate
Corrected for Pressure (cps)
Corrected McMurdo Count Rate (cps)
Linear (0-1GV)
Linear (1-2GV)
Linear (2-3GV)
Linear (3-4GV)
Linear (4-5GV)
Linear (5-6GV)
Linear (6-7GV)
Linear (7-8GV)
Linear (8-9GV)
Linear (9-10GV)
Linear (10-11GV)
Linear (11-12GV)
Linear (12-13GV)
Linear (13-14GV)
Linear (14-15GV)
Linear (15-16GV)
Linear (16-17GV)
Linear (17-19GV)

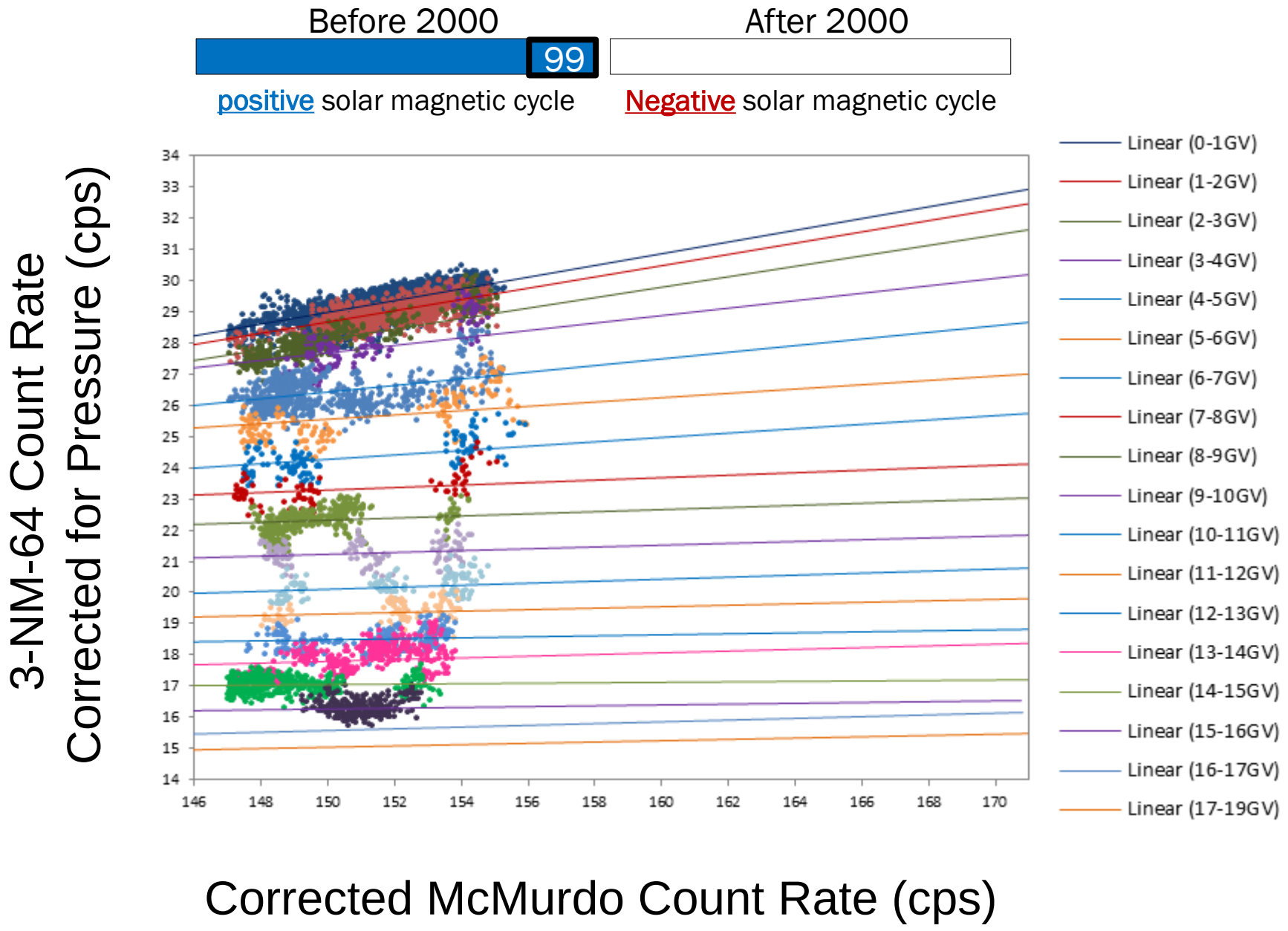
Before 2000
After 2000
99
positive solar magnetic cycle
Negative solar magnetic cycle
3-NM-64 Count Rate
Corrected for Pressure (cps)
Corrected McMurdo Count Rate (cps)
Linear (0-1GV)
Linear (1-2GV)
Linear (2-3GV)
Linear (3-4GV)
Linear (4-5GV)
Linear (5-6GV)
Linear (6-7GV)
Linear (7-8GV)
Linear (8-9GV)
Linear (9-10GV)
Linear (10-11GV)
Linear (11-12GV)
Linear (12-13GV)
Linear (13-14GV)
Linear (14-15GV)
Linear (15-16GV)
Linear (16-17GV)
Linear (17-19GV)

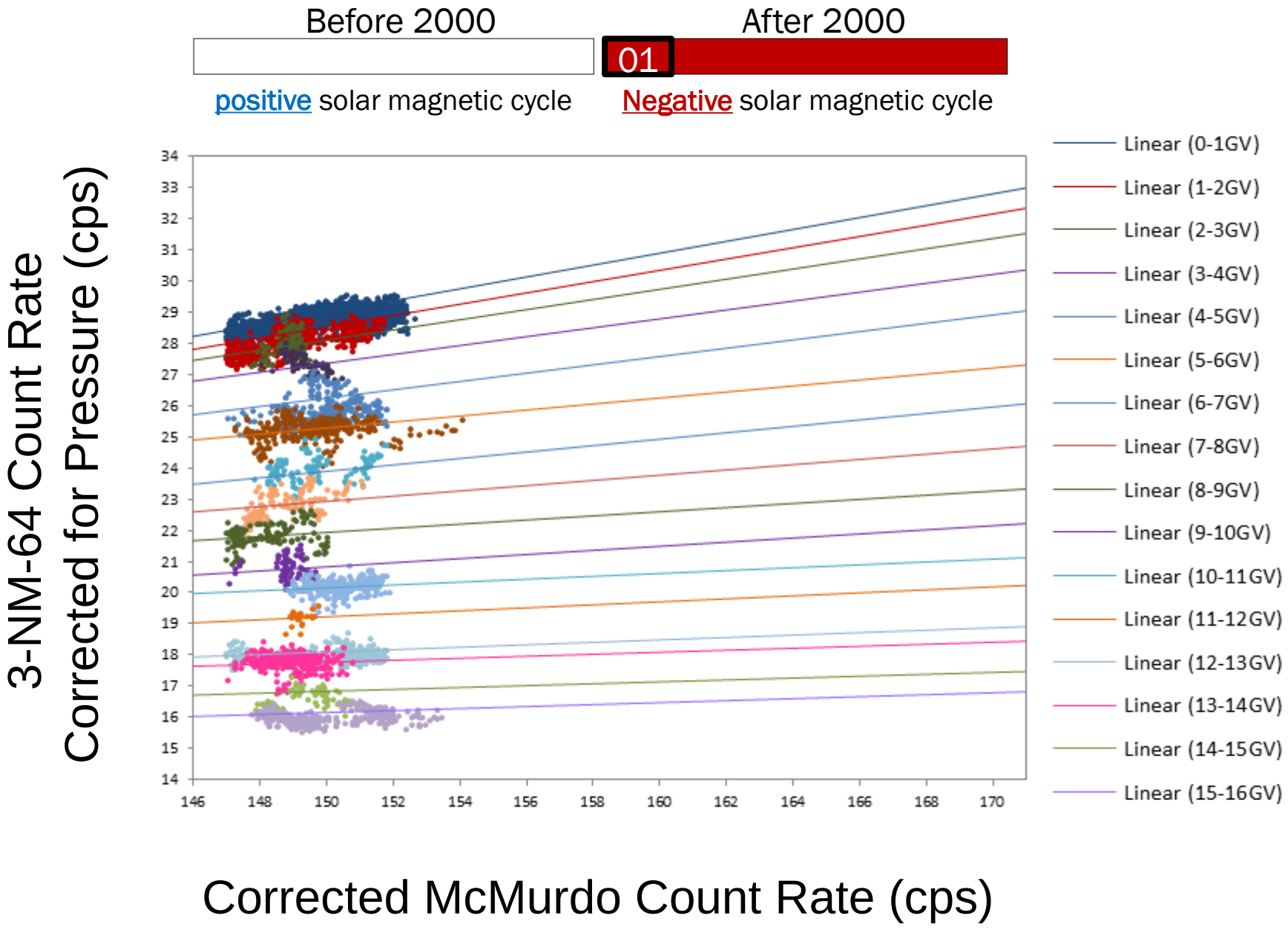
Before 2000
After 2000
01
positive solar magnetic cycle
Negative solar magnetic cycle
3-NM-64 Count Rate
Corrected for Pressure (cps)
Corrected McMurdo Count Rate (cps)
Linear (0-1GV)
Linear (1-2GV)
Linear (2-3GV)
Linear (3-4GV)
Linear (4-5GV)
Linear (5-6GV)
Linear (6-7GV)
Linear (7-8GV)
Linear (8-9GV)
Linear (9-10GV)
Linear (10-11GV)
Linear (11-12GV)
Linear (12-13GV)
Linear (13-14GV)
Linear (14-15GV)
Linear (15-16GV)

Before 2000 | After 2000

02

positive solar magnetic cycle | Negative solar magnetic cycle

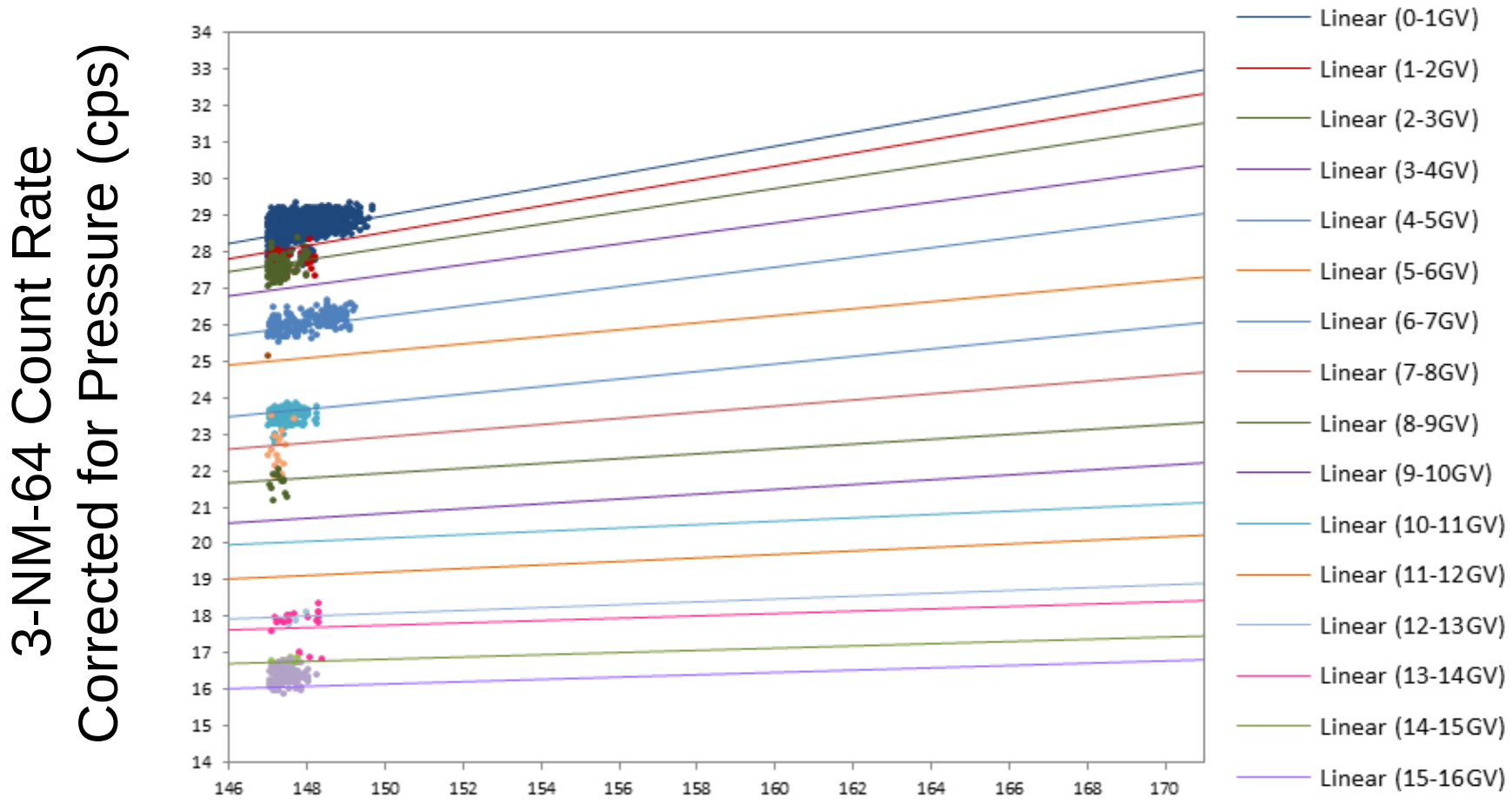

Corrected McMurdo Count Rate (cps)

Before 2000

After 2000

03

positive solar magnetic cycle

Negative solar magnetic cycle

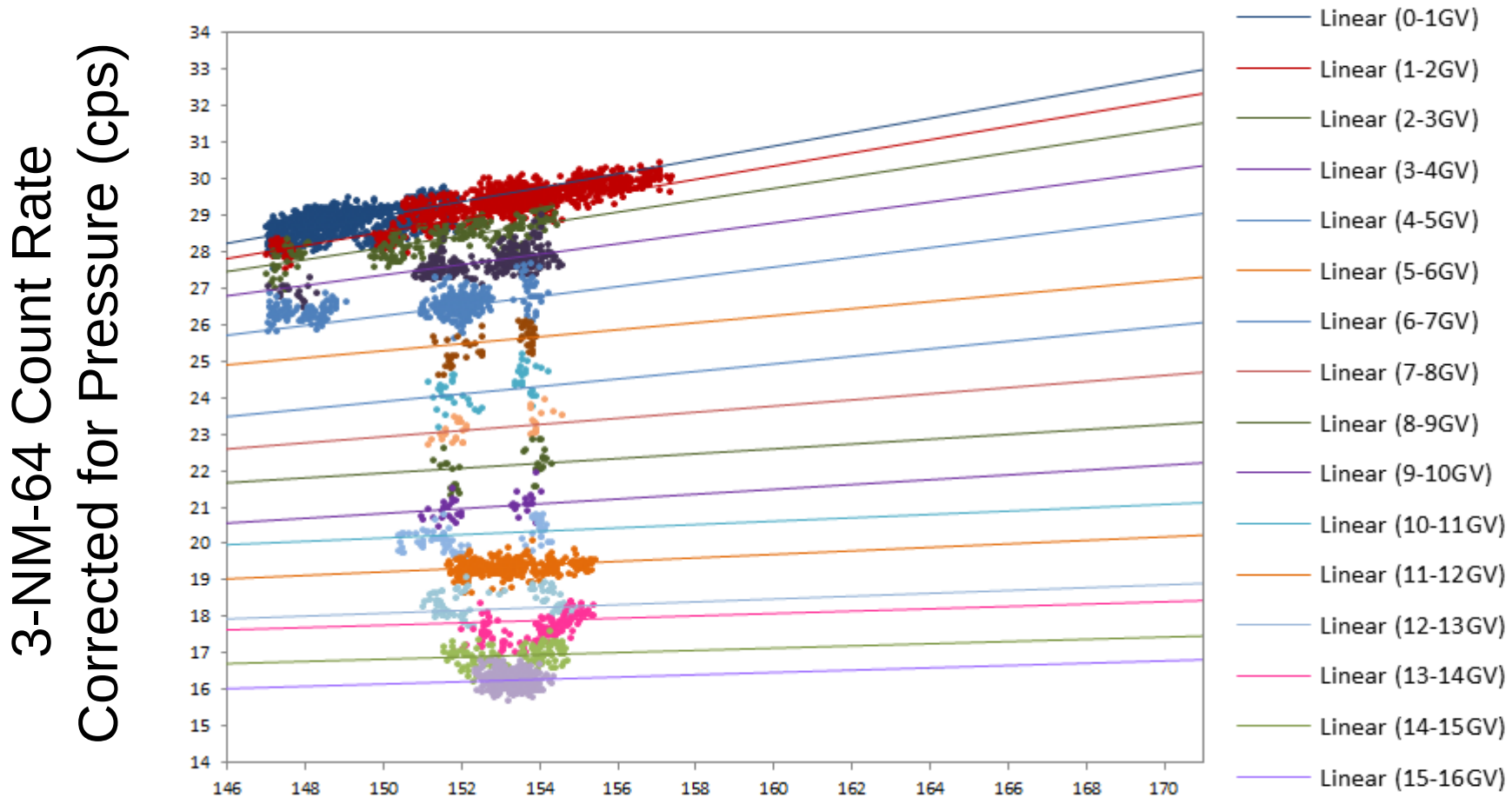

Corrected McMurdo Count Rate (cps)

Before 2000

After 2000

04

positive solar magnetic cycle

Negative solar magnetic cycle

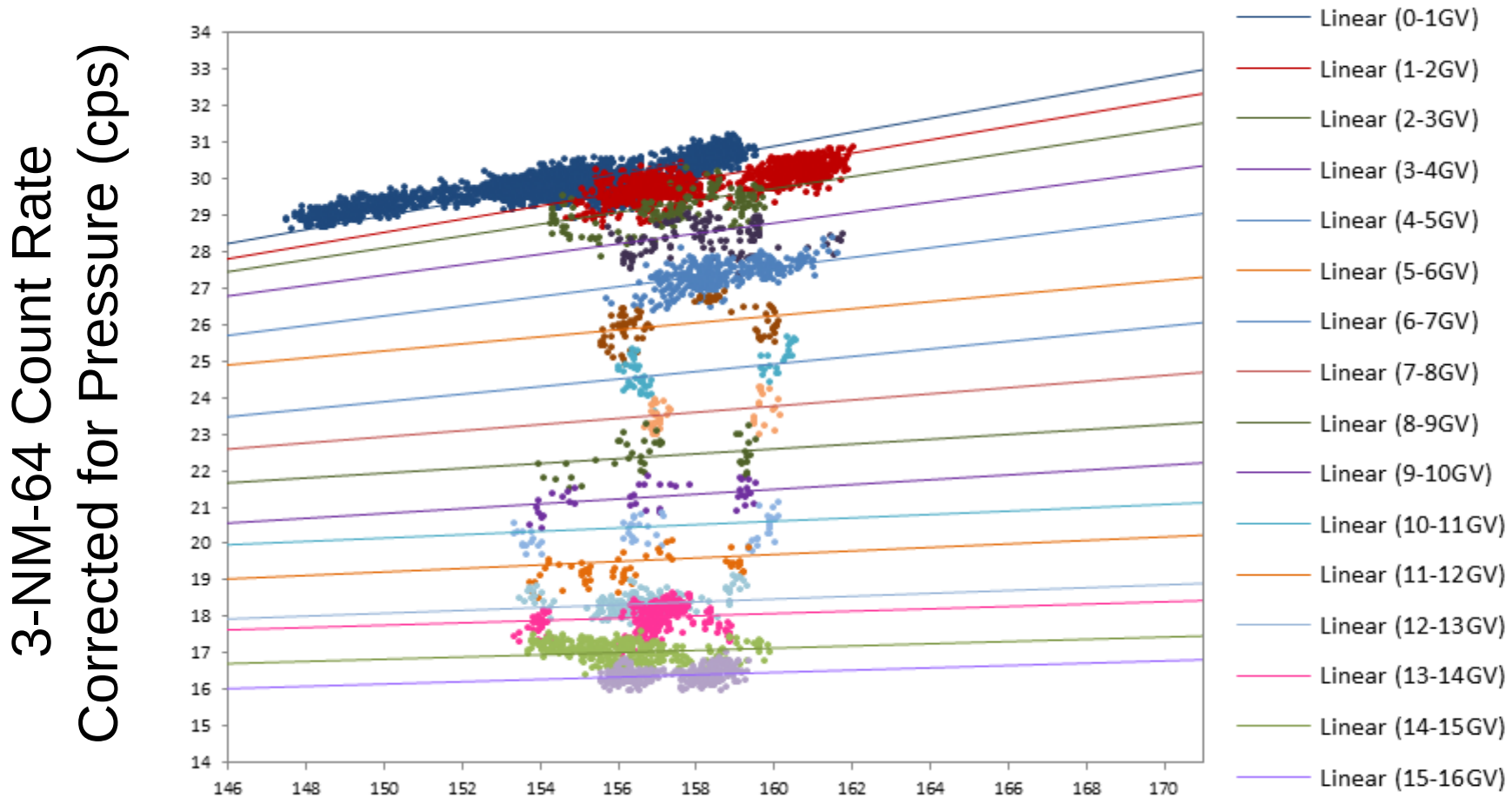

Corrected McMurdo Count Rate (cps)

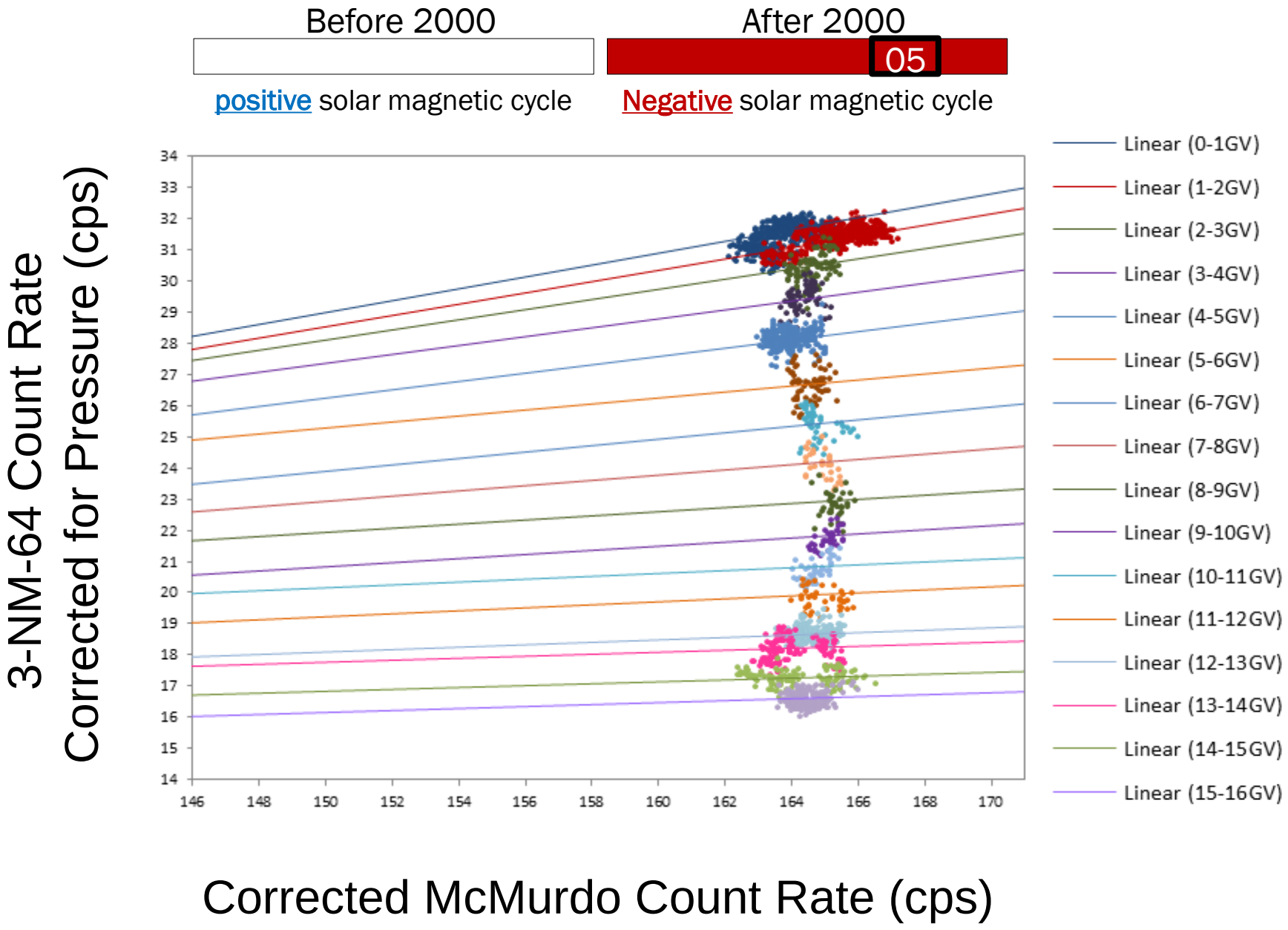
Before 2000
After 2000
05
positive solar magnetic cycle
Negative solar magnetic cycle
3-NM-64 Count Rate
Corrected for Pressure (cps)
34
33
32
31
30
29
28
27
26
25
24
23
22
21
20
19
18
17
16
15
14
146
148
150
152
154
156
158
160
162
164
166
168
170
Linear (0-1GV)
Linear (1-2GV)
Linear (2-3GV)
Linear (3-4GV)
Linear (4-5GV)
Linear (5-6GV)
Linear (6-7GV)
Linear (7-8GV)
Linear (8-9GV)
Linear (9-10GV)
Linear (10-11GV)
Linear (11-12GV)
Linear (12-13GV)
Linear (13-14GV)
Linear (14-15GV)
Linear (15-16GV)
Corrected McMurdo Count Rate (cps)

Before 2000

After 2000

06

positive solar magnetic cycle

Negative solar magnetic cycle

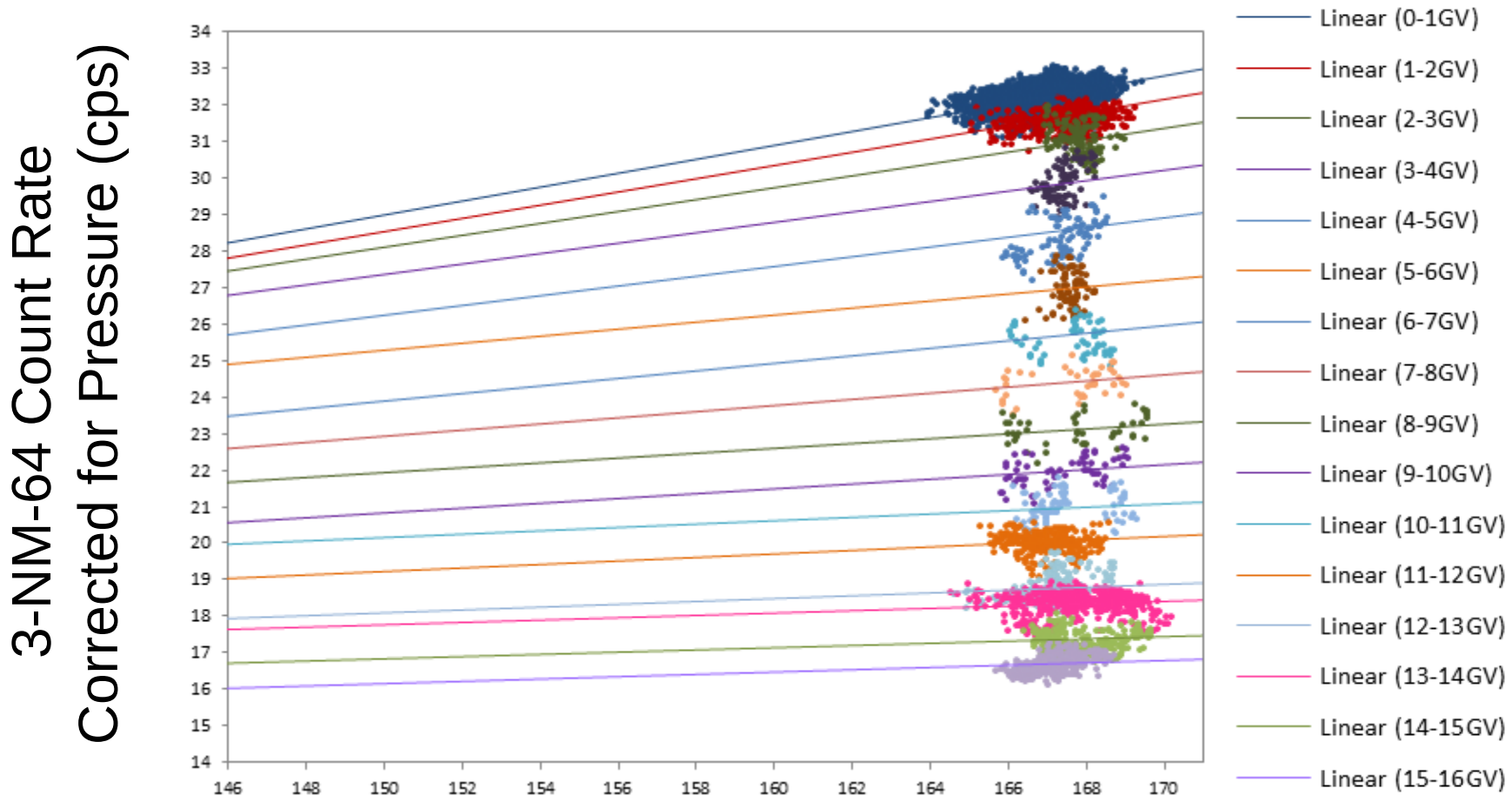

Corrected McMurdo Count Rate (cps)

Revisited this work
by
Miss Kledsai Pupakun

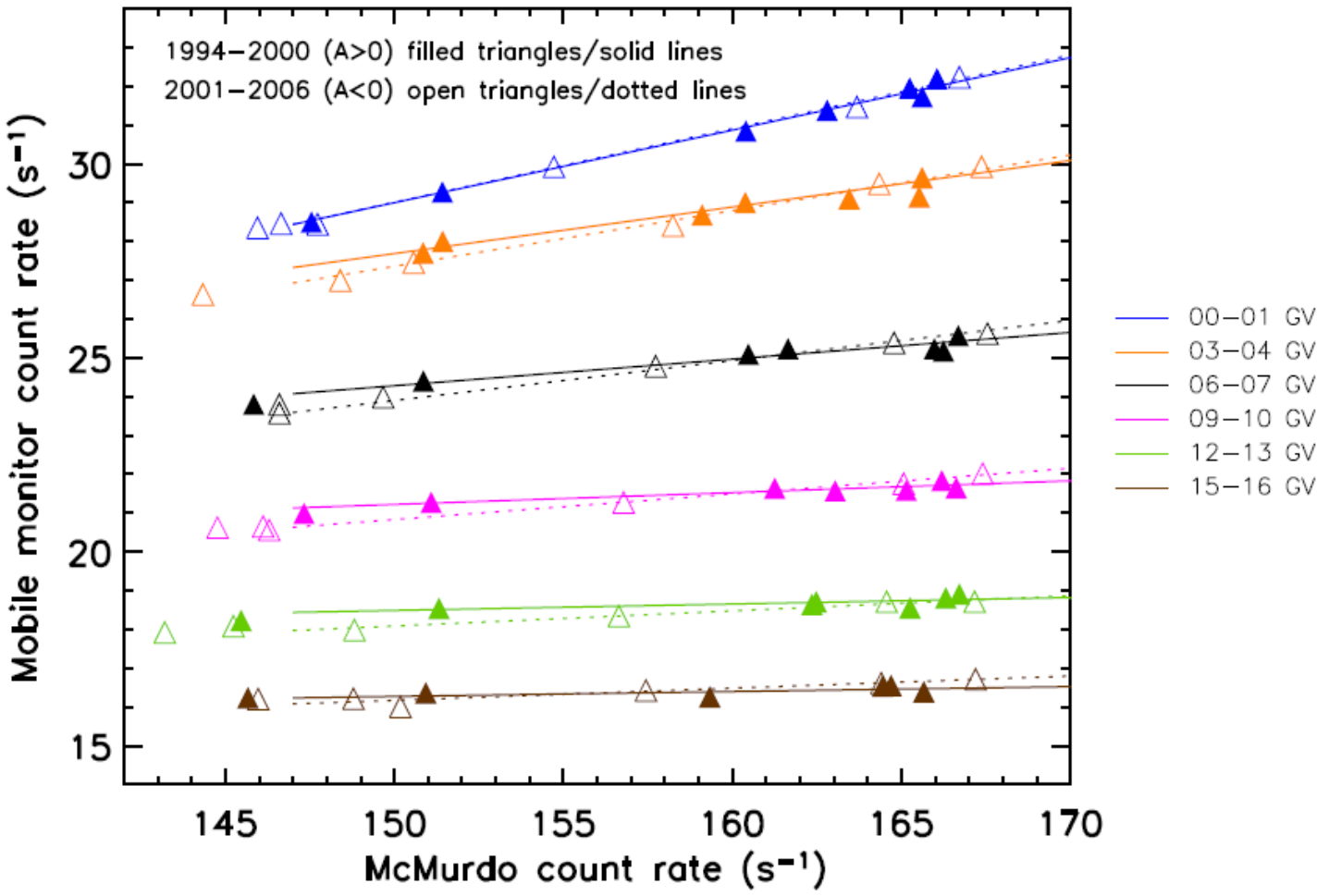

Figure 11 Alternative presentation of the averaged data using selected rigidity bins and superimposing the data for different solar magnetic polarities. A filled triangle is used to indicate positive ($A > 0$) solar magnetic polarity with solid lines showing the linear fits. Open triangles indicate data for negative ($A < 0$) solar magnetic polarity while the dotted lines are linear fits to these data. There are clear differences in cosmic ray modulation before and after the solar magnetic polarity reversal.

LATITUDE SURVEY: VOYAGE IN 2009 SURVEY YEAR

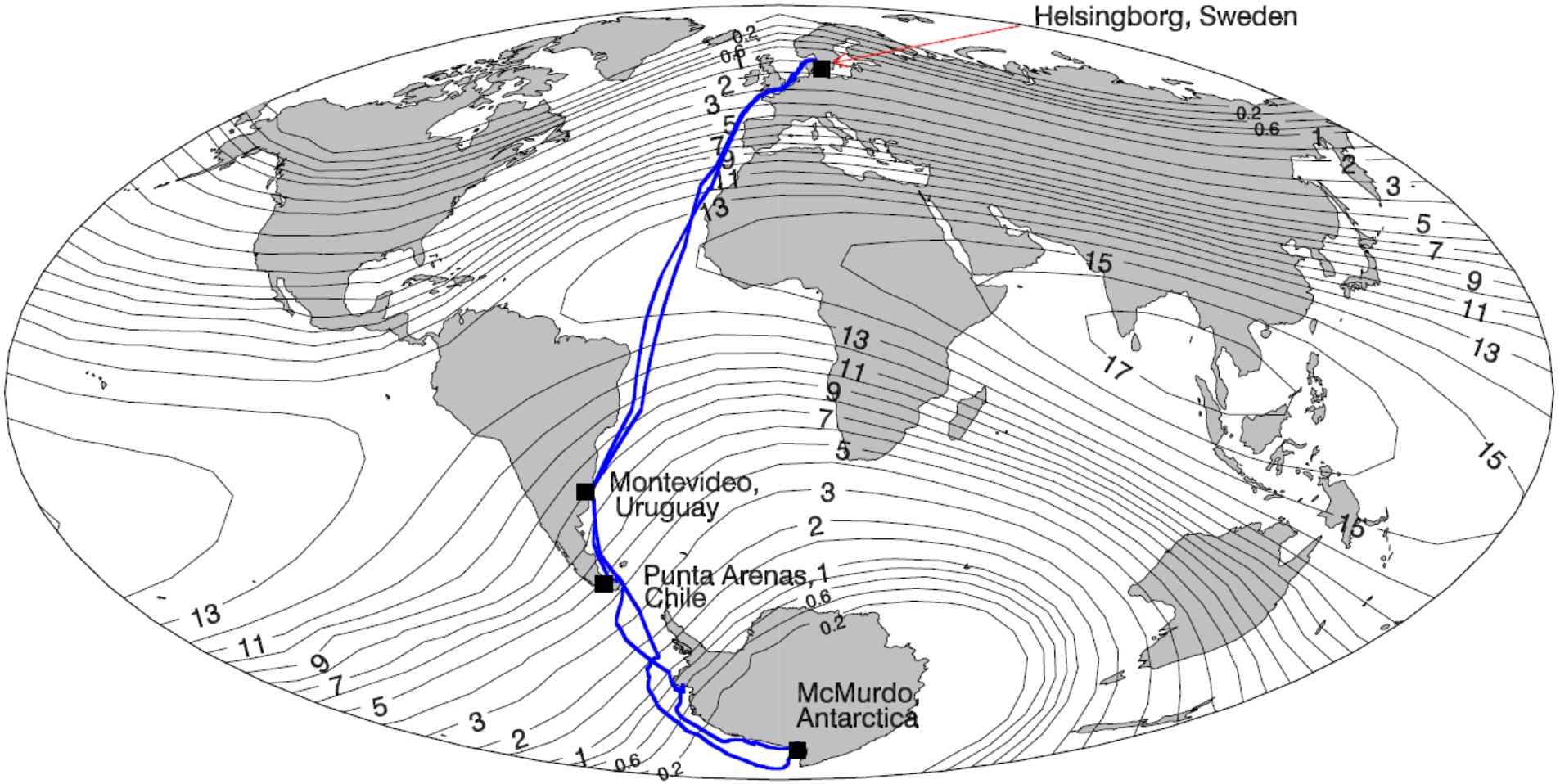

FIGURE 12 Route of the Oden for the 2009–2010 latitude survey, superimposed on contours of the 2010 effective vertical cutoff rigidity, calculated for April 08, 2010 at 12:00 UT. Numbers at each contour indicate the effective vertical cutoff rigidity in GV.

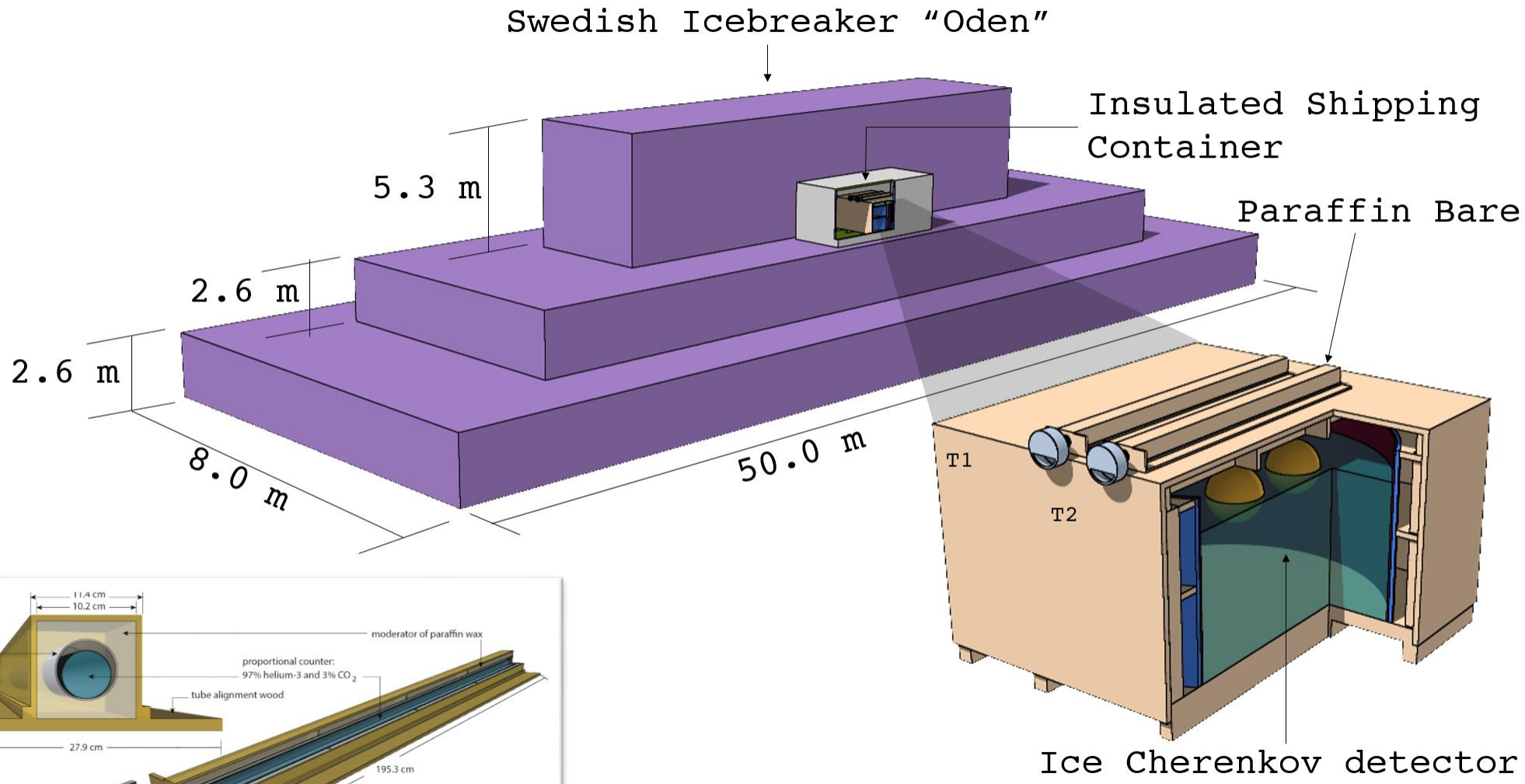

2 Paraffin Bares

FIGURE 13 Bare neutron detector & IceTop Tank
Courtesy *Pagwhan et al. and Tangjai et al.*

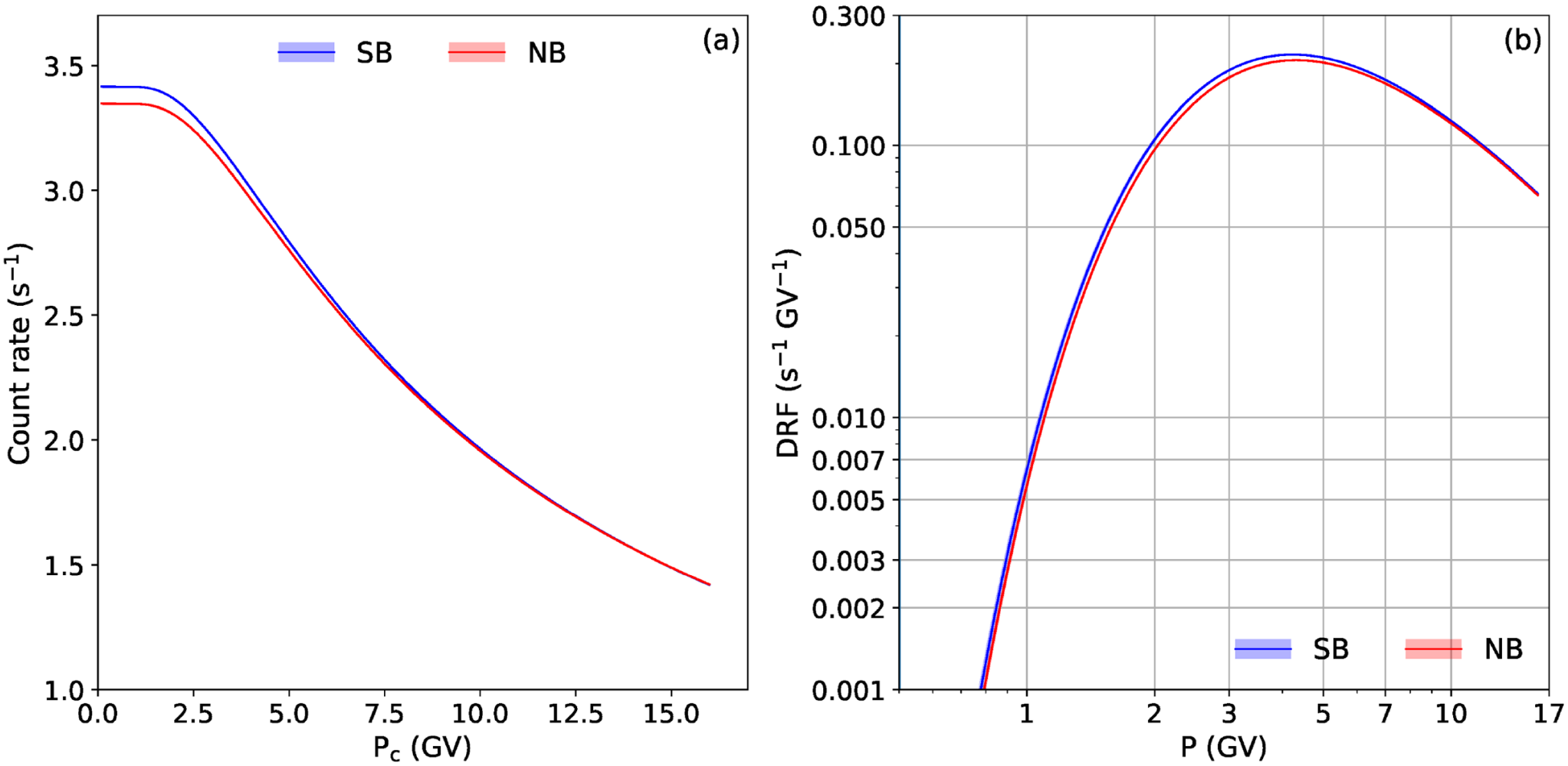

Figure 14 Comparison of (a) the Dorman functions and (b) the differential response functions for southbound and northbound survey intervals.

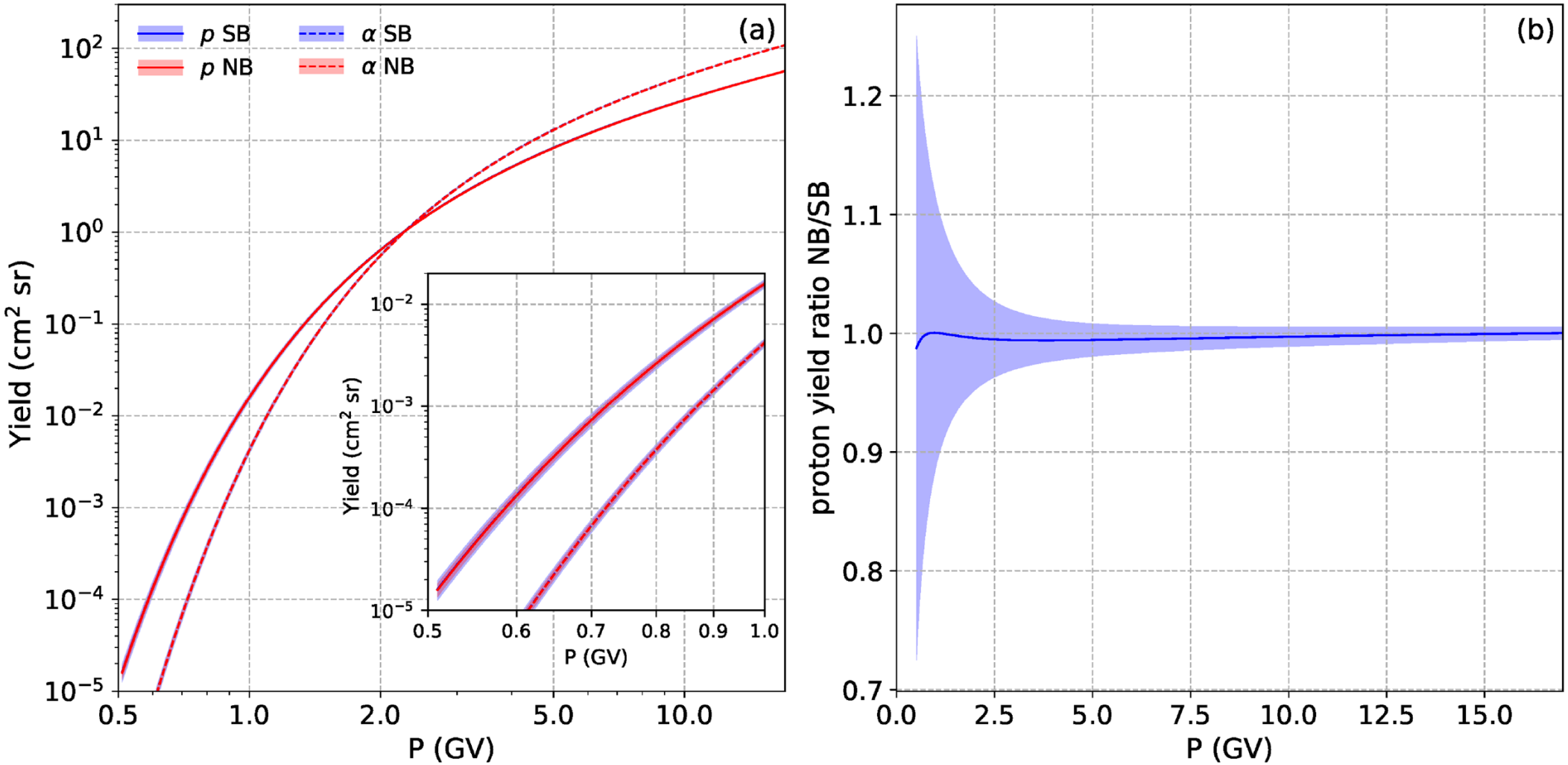

Figure 15 (a) Yield functions of the two bare neutron counters for protons and alphas derived from the 2009–2010 latitude survey and particle spectra at the top of the atmosphere. (b) Ratio of the southbound to the northbound proton yield functions.

LATITUDE SURVEY: VOYAGE IN 2018-2020 SURVEY YEAR

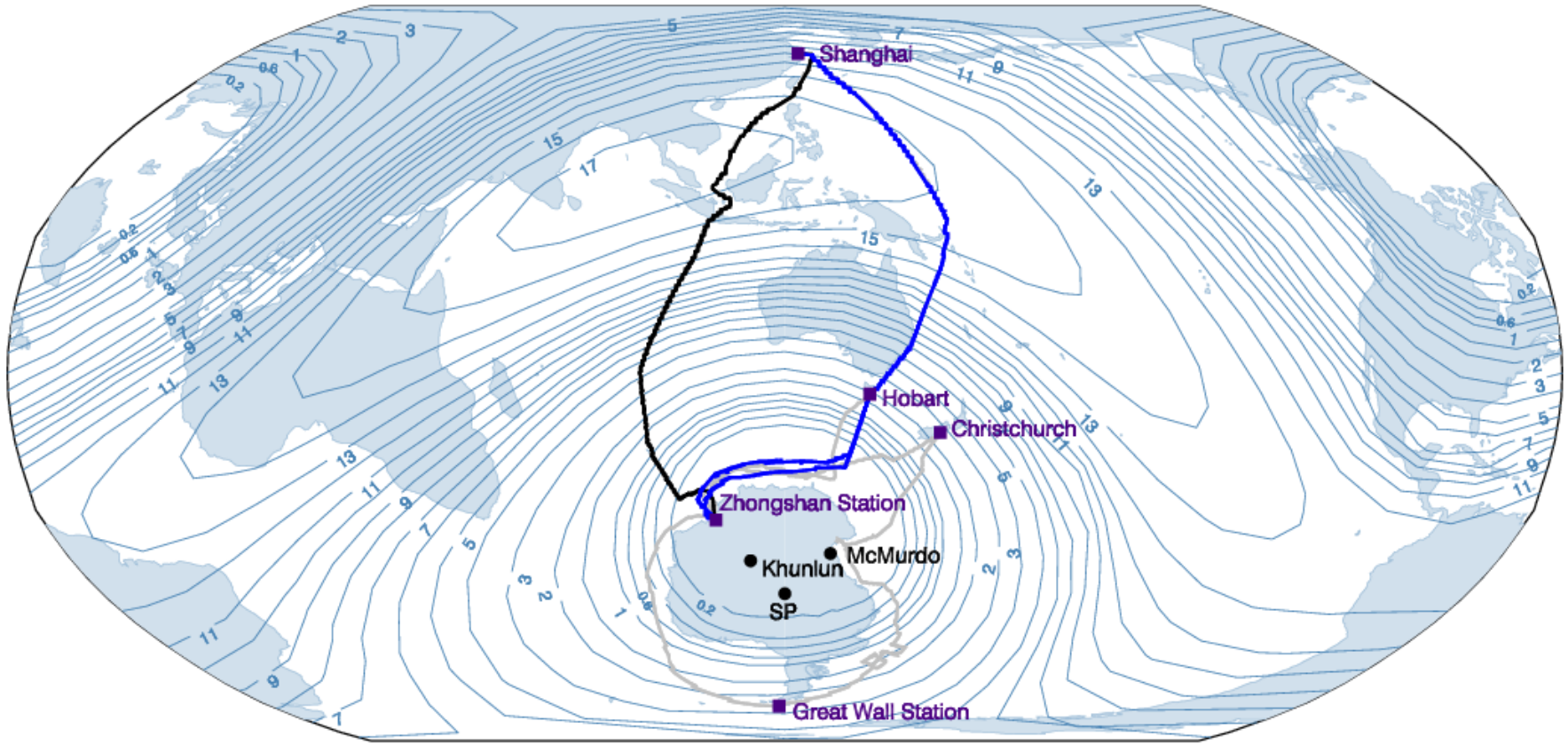

Chinare35-XueLong
Chinare35-Changvan
Chinare36

FIGURE 16 Route of the Oden for the 2019-2020 latitude survey, superimposed on contours of the 2018 effective vertical cutoff rigidity, calculated for May 01, 2018 at 12:00 UT. Numbers at each contour indicate the effective vertical cutoff rigidity in GV. Courtesy *Khampakdee et al.*


CCTV+

CHANGVAN NEUTRON DETECTORS

FIGURE 17 The placement of the 2NM64 and semi-leaded neutron detectors inside the Changvan
Courtesy *Khampakdee et al.*

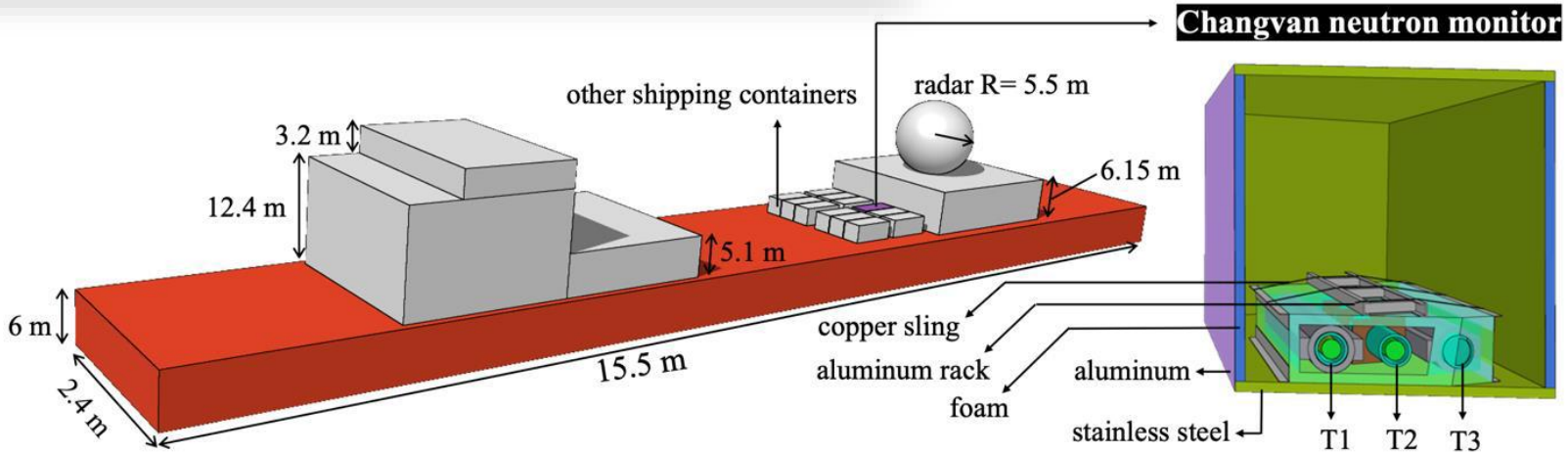

FIGURE 18 The geometry of the Changvan neutron monitor implemented in the FLUKA program. The dimensions and materials of some the main components are provided.
Courtesy *Fongsamut et al.*

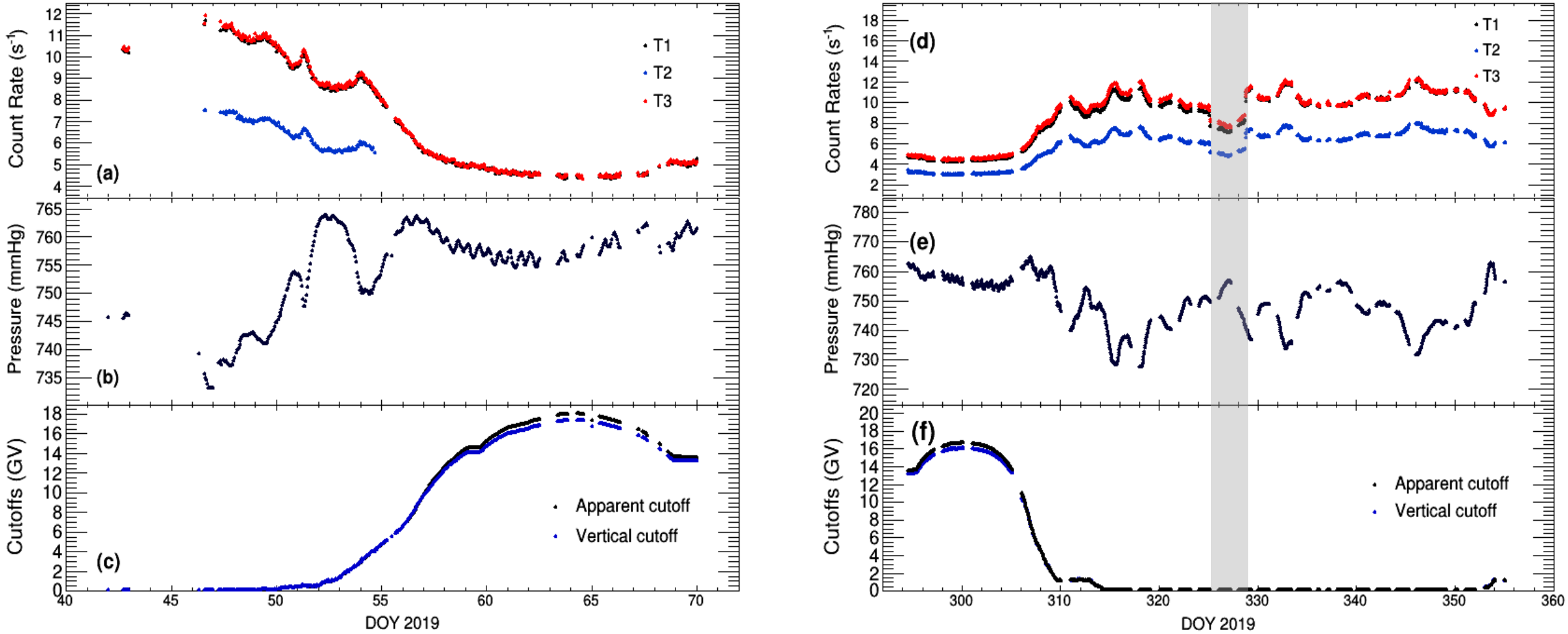

Figure 19 (a)-(c) Data set of the survey year 2019 and (d)-(f) of the survey year 2020, as a function of time. (a) and (d) Hourly averaged count rates for T1 (black), T2 (blue), and T3 (red). The vertical grey lines show the time period that causes the count rate to fluctuate by having other containers intervene. (b) and (e) The barometric pressure. (c) and (f) The geomagnetic cutoff rigidity, where the black line shows the apparent geomagnetic cutoff rigidity and the blue line shows the vertical effective cutoff rigidity. We will clearly see the difference between the two geomagnetic cutoffs at high cutoffs (low latitudes). Courtesy *Khampakdee et al.*

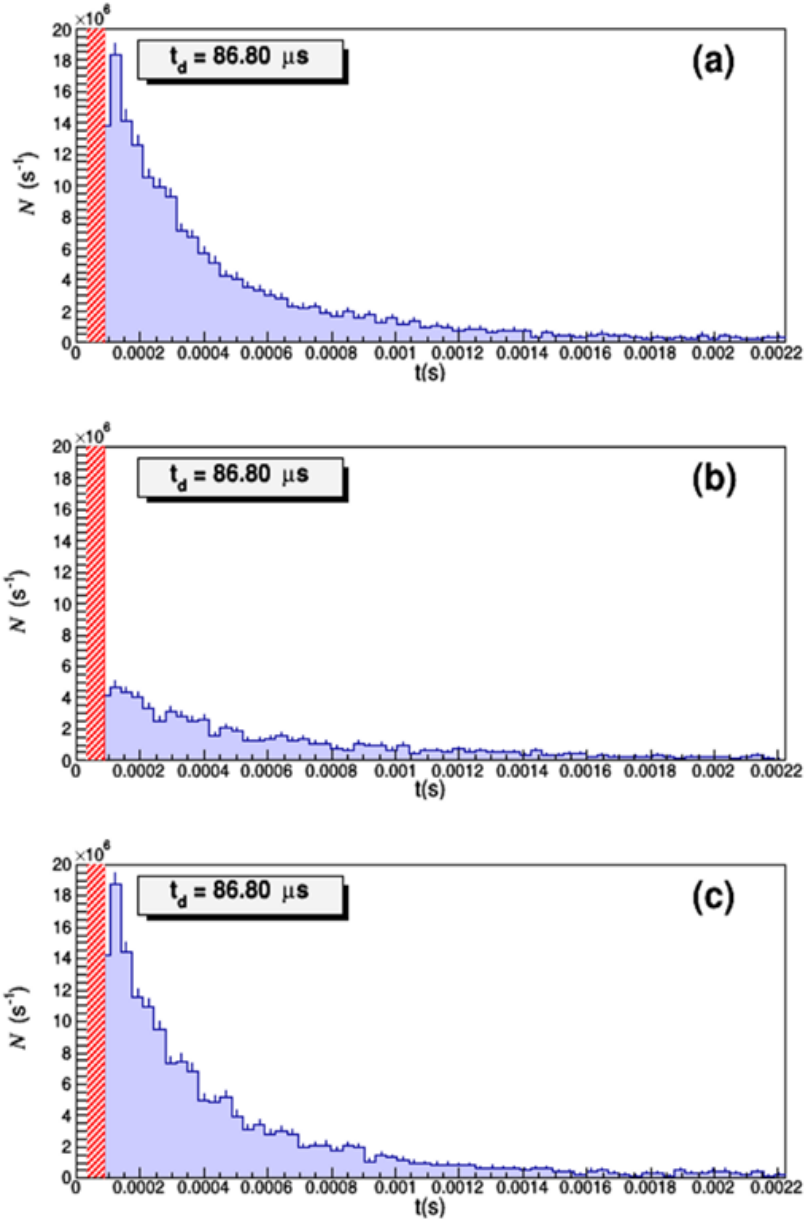

Figure 20 Frequency histograms of short time delays collected for each neutron counter tube during one hour (2nd hour of universal time (UT) on the 20 December 2019 of the survey year 2020): (a) tube 1, (b) tube 2, and (c) tube 3. The red vertical band shows the electronics dead time for each tube, about 87 μs. Statistical error bars are shown.

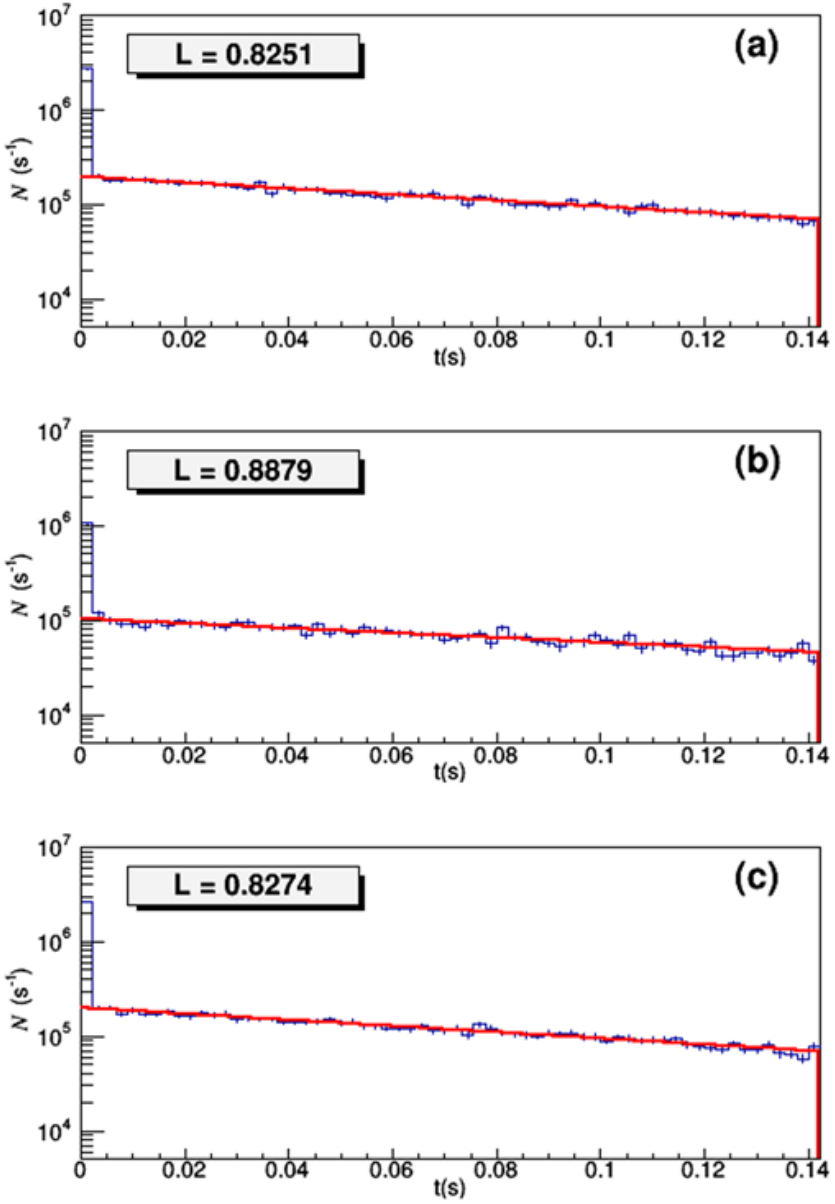

Figure 21 Example of analysis of long time delay histograms collected for each neutron counter tube during one hour (2nd hour UT on the 20th December 2019 of the survey year 2020) of (a) tube 1, (b) tube 2, and (c) tube 3. Error bars are shown.

Courtesy *Yakum et al.*

JANG BOGO AND MCMURDO STATION

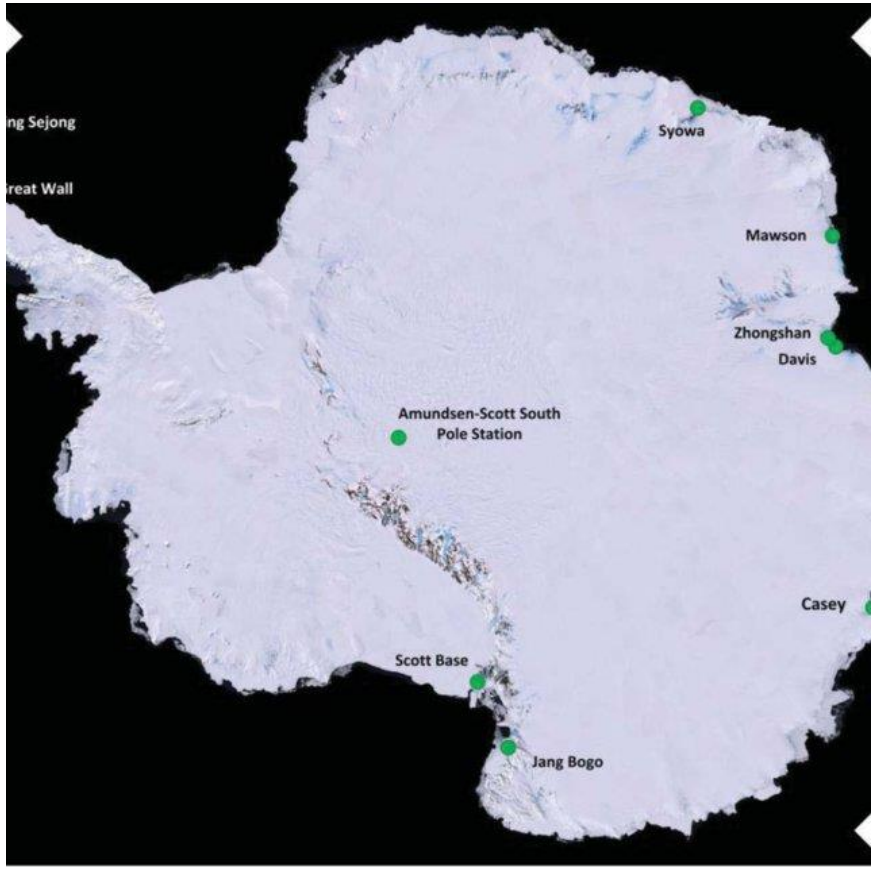

Station	Location		Altitude	Cutoff Rigidity
	Geographic	Geomagnetic		
Jang Bogo	74° 37.4′S 164° 13.7′E	77° 3′S 85° 18′W	29 m	< 0.2 GV
McMurdo	77° 51′S 166° 40′E	78° 58.8′S 72° 22.8′E	48 m	< 0.2 GV

Distance apart ~ 300 km

Similar Geomagnetic latitude, but different Geomagnetic longitude

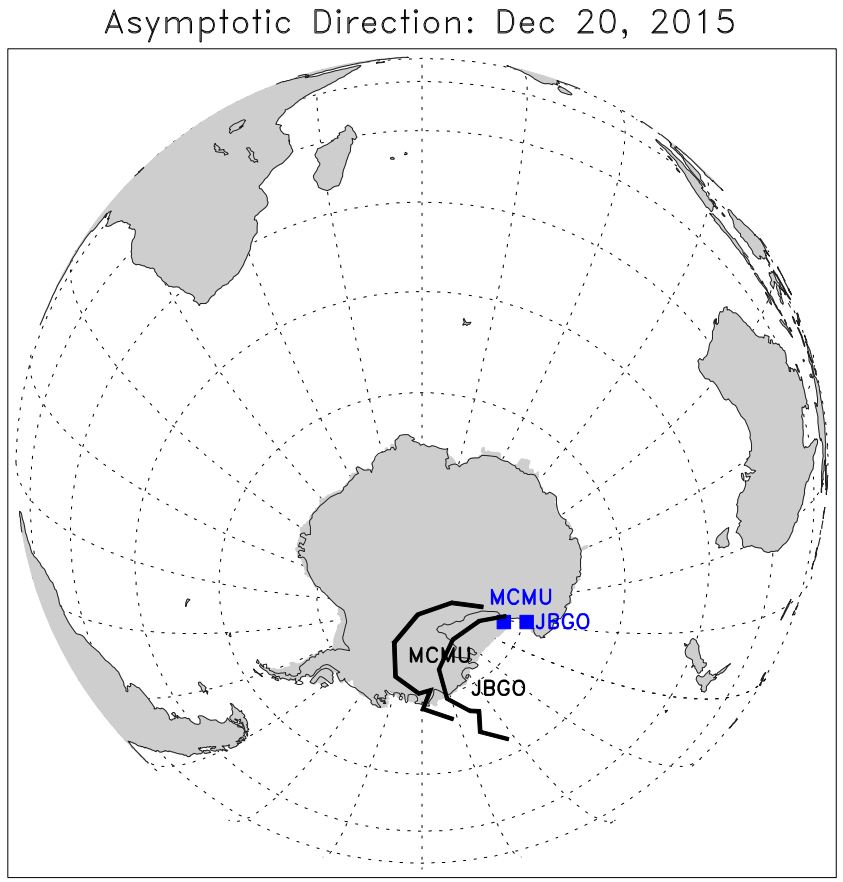

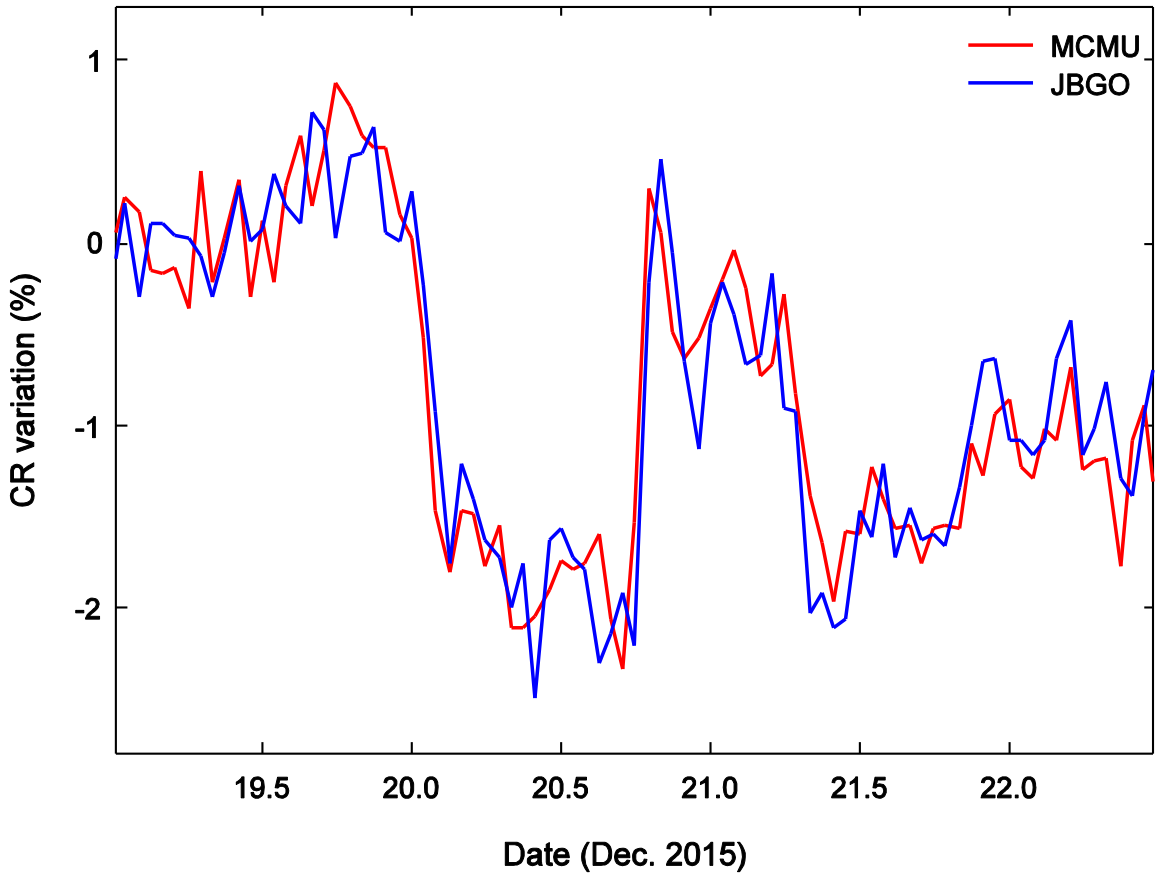

LEFT: Asymptotic directions on December 20, 2015 at 18:00 UT.
RIGHT: Small scale features as seen by Jang Bogo and McMurdo neutron monitors.

This work will be presented by Mr. Kittinan Jomprasert

OUTREACH

Web resources & Facebook Page

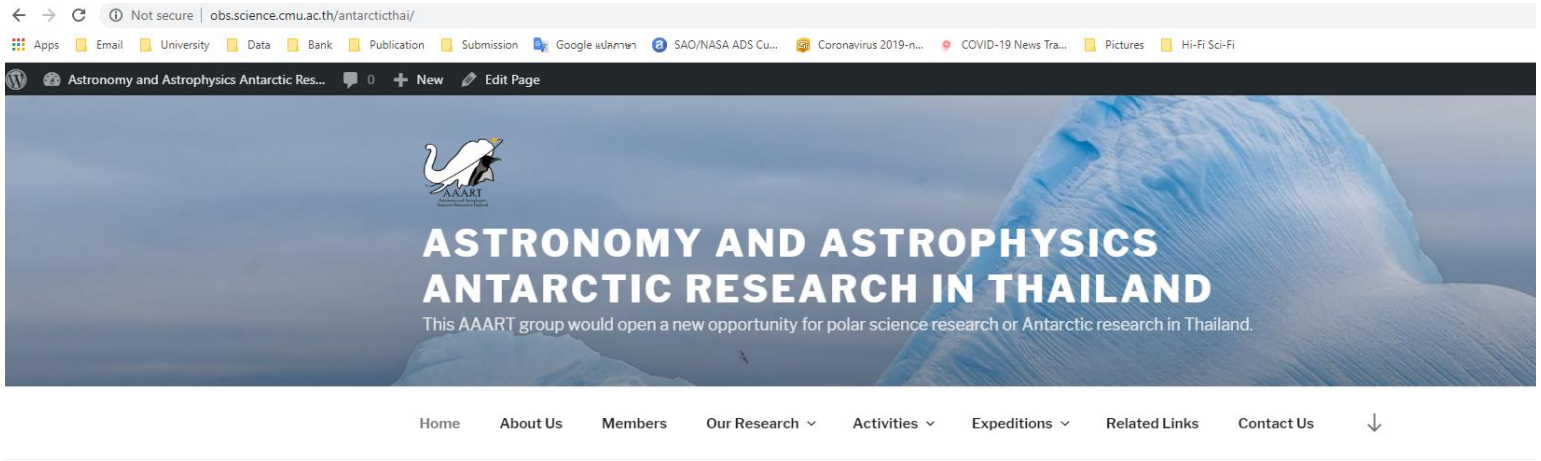

- Establish http://obs.science.cmu.ac.th/antarcticthai/ to provide information and present activities regarding my research
- Update Facebook Page that I have already been developed highlighting ongoing Astronomy and Astrophysics Research in Antarctica, especially projects with Thai involvement.

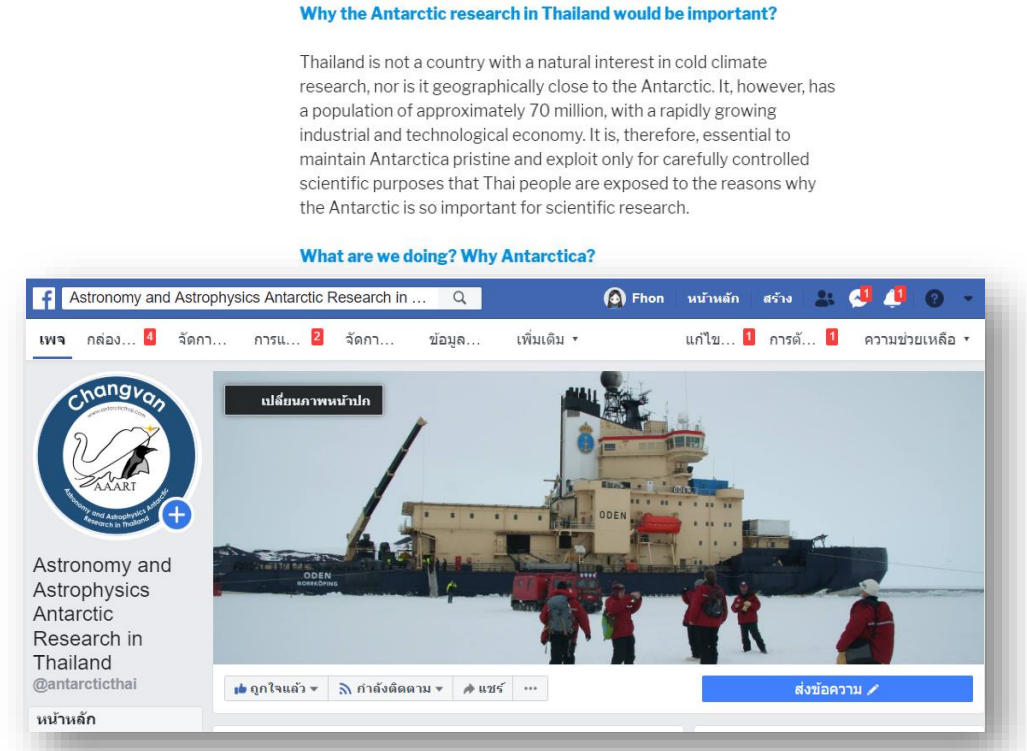

Thank You